# Quantitative Ventricular Fibrillation Metrics in a Biosignal Guided Cardiopulmonary Resuscitation Device for Cardiac Arrest and Their Translation to Clinical Data

by

Matthew Leo Sundermann

Bachelor of Engineering, Vanderbilt University, 2011

Submitted to the Graduate Faculty of

Swanson School of Engineering in partial fulfillment

of the requirements for the degree of

Doctor of Philosophy

University of Pittsburgh

2017

UNIVERSITY OF PITTSBURGH

SWANSON SCHOOL OF ENGINEERING

This dissertation was presented

by

Matthew Leo Sundermann

It was defended on

August 21, 2017

and approved by

William Federspiel PhD, Professor, Department of Bioengineering

Clifton Callaway MD, PhD, Professor, Department of Emergency Medicine

Patrick Loughlin, PhD, Professor, Department of Bioengineering

Dissertation Director: James Menegazzi, PhD, Professor, Department of Emergency Medicine, Department of Bioengineering

**Quantitative Ventricular Fibrillation Metrics in a Biosignal Guided Cardiopulmonary Resuscitation Device for Cardiac Arrest and Their Translation to Clinical Data**

Matthew Leo Sundermann, PhD

University of Pittsburgh, 2017

Out of hospital cardiac arrest is a major cause of mortality with an estimated yearly incidence of 350,000 in the United States alone. Cardiopulmonary resuscitation (CPR) is a treatment for cardiac arrest involving chest compressions and rescues breaths that can save lives but is limited by the fact that it currently treats all patients in a 'one size fits all' approach. This work describes an adaptive approach to chest compressions controlled by a mechanical device that receives biosignals from the patient it treats. The device is capable of adjusting its chest compression parameters such as rate and depth in response to the biosignals it receives. We focused on integrating the quantitative electrocardiogram (QECG) of the ventricular fibrillation signal, a biosignal shown to respond to increased perfusion of the myocardium during CPR, into a chest compression algorithm controlled by the adaptive chest compression device. QECG is readily available for cardiac arrest patients since ECG analysis is standard of care in cardiac arrest. In our first aim we developed the adaptive chest compression device and tested it in animal feasibility studies which demonstrated that it responded appropriately to the biosignals it received. Next, in a computational model of adaptive chest compressions, adjustments in chest compression depth yielded the largest increase in cardiac output in patients with simulated variable physiology. In follow-up animal studies, select QECG measures responded to changes in chest compression parameters which demonstrated the initial feasibility of QECG measures as a potential biosignal in this model. We found that the QECG measures of median slope, centroid frequency, and log of the absolute correlation responded to changes in chest compression rate in the early phase of chest

compressions. We found that in late phases of chest compressions the QECG measure median slope responded to chest compression rate changes and the QECG measure AMSA responded to chest compression duty cycle changes. Our second aim sought to retrospectively translate the findings in the first aim animal studies to human clinical data in the continuous chest compression trial of the Resuscitation Outcomes Consortium (ROC). The clinical trial provided us with ECG and compression data in covering thousands of cardiac arrest events. All QECG metrics in the clinical data set was predictive of shock outcome and chest compression rate along with chest compression bout duration were predictive of survival. However, when controlled for the presenting first rhythm status and demographic variables, only chest compression bout duration was predictive of survival. In addition to the predictive value of chest compression parameters and QECG measures, associations were found between varying chest compression parameters averaged across bouts of compressions with change in QECG values (dQECG) in the clinical data. Chest compression rate was found to be predictive of the dQECG metric median slope (dMS) and the dQECG metric (dAMSA). Dosed compression rate was found to be predictive of the dQECG metric dMS as well. dCF responded to changes in chest compression duty cycle. These findings provide a foundation for delivering adaptive chest compressions with the potential of improving survival outcomes to cardiac arrest.

## TABLE OF CONTENTS

## LIST OF TABLES

## LIST OF FIGURES

# PREFACE

Acknowledgements: This work would not have been possible without the help of many people. My advisor, Dr. James J. Menegazzi along with the rest of the committee, Dr. Clifton W. Callaway, Dr. William J. Federspiel, and Dr. Patrick J. Loughlin, provided insightful feedback and guidance throughout the studies and writing process. Dr. David Salcido provided invaluable help and guidance with Matlab coding, statistics, and data organization. Allison C. Koller provided help in case reviews and data searches. I would like to thank all of them for their insight and support as well as the support of all my friends and family throughout graduate school.

# 1.0 INTRODUCTION

## 1.1 CARDIAC ARREST

Out-of-hospital cardiac arrest (OHCA) is a leading cause of mortality in the industrialized world[1]. OHCA is characterized as an abrupt cessation of mechanical activity of the heart leading to the loss of blood perfusion to vital organs which sustain life. OHCA, when left untreated, leads to sudden cardiac death (SCD). Successful treatment of OHCA necessarily involves cardiopulmonary resuscitation (CPR).

CPR combines both rescue breaths to provide oxygenation and ventilation and chest compressions that function to circulate blood and perfuse vital organs. CPR is performed with the primary purpose of circulating blood until electrical defibrillation is available. To an extent, chest compressions 'prime' the heart with perfusion so that it will be more responsive to a defibrillation attempt. Successful defibrillation terminates cardiac arrest and can be performed in both the out-of-hospital and in-hospital settings.

### 1.1.1 Cardiac Arrest Etiology

OHCA has a variety of etiologies. These etiologies can be categorized into medical or non-medical. A majority of OHCA cases have a presumed cardiac (medical) etiology (55-78%)[2-5].

Medical etiologies of OHCA are most often attributed to coronary artery disease[6]. OHCA is initiated from life threatening arrhythmias such as ventricular fibrillation (VF), asystole, (AS), ventricular tachycardia (VT), or pulseless electrical activity (PEA).

Non-medical causes of OHCA include trauma, obstructive pulmonary disease, drug abuse, or unknown causes. One study that looked at 1360 OHCA found that 25% were determined to be initiated by a non-cardiac etiology[4].

### 1.1.2 Incidence and Outcomes

Surviving a cardiac arrest is difficult and the approach to treatment is clinically challenging. Despite aggressive efforts to both raise awareness of OHCA and teach CPR to the public, survival rates from OHCA are dismal[1]. The latest statistics from the American Heart Association (AHA) report that survival to hospital discharge from OHCA with any first recorded rhythm was 10.6% for all ages. Factors that improve the likelihood of survival include younger age, whether the cardiac arrest was witnessed by a bystander, whether bystander CPR was performed, whether the cardiac arrest was in public, and whether the first rhythm observed in the cardiac arrest was a rhythm capable of being defibrillated. Survival odds also appear to increase when a non-shockable rhythm is converted to a shockable rhythm[7].

### 1.1.3 Stages of Cardiac Arrest

Drastic physiologic changes occur within the body during the course of cardiac arrest. These changes can be described as a time sensitive model, split into three phases that include

electrical, circulatory, and metabolic[8]. The three stage model, has developed into a treatment paradigm, where each stage would be more responsive to select resuscitation treatments. The model established an approach to cardiac arrest where select interventions that are timed to coordinate with changing physiology would provide the most benefit to the patient.

In the electrical phase, commonly defined as the first four minutes of cardiac arrest, defibrillation is viewed as the most critical treatment in reversing lethal arrhythmias[8]. Chest compressions and rescue breaths are necessary during this first phase, however electrical defibrillation is paramount in reversing arrhythmia as there is still adequate energy stores in the myocardium to facilitate successful defibrillation. The importance of early defibrillation is realized in a study that showed prompt defibrillation in OHCA yielded a hospital discharge rate of 29.3% when compared to patients in whom defibrillation was delayed by 2 minutes or more from onset of VF. The delayed comparison group had a hospital discharge rate of 22.2% [9].

In the circulatory phase of cardiac arrest, the myocardium has been further starved of oxygen, and its optimal viability for cardioversion. This period is commonly defined as the 4th to 10th minute after onset of cardiac arrest[8]. During the circulatory phase of cardiac arrest, chest compressions remain of paramount importance to keep the myocardium perfused so that the window for successful defibrillation remains intact.

In the metabolic phase of cardiac arrest, the myocardium has been starved of oxygen for longer than 10 minutes[8]. Continued perfusion generated through chest compressions is now required to prime the heart after the optimal window for defibrillation has passed. Chest compressions remain vital during the metabolic phase, but often other treatment options are required at this point such as drug delivery and extracorporeal membrane oxygenation[10].

## 1.2 CARDIOPULMONARY RESUSCITATION

Cardiopulmonary Resuscitation (CPR), first described in detail in the 1960s, is a proven treatment for OHCA and has shown strong evidence to improve survival odds when performed correctly and with limited delay[11-14]. Chest compressions during CPR are delivered through a rhythmic, downward force and can be given to patients manually or with mechanical devices. This motion encompasses various parameters that define CPR including rate of compression, depth of compression, compression duty cycle, and CPR fraction.

Chest compressions are delivered as an applied force to the sternum of the patient. This cyclic movement can be generalized to a kinematic relationship between the downward force of the chest compression, whether delivered by a provider's hands or a medical device, and the volumetric rate of blood flow leaving the heart. Efforts have been made in the past by other research groups and organizations to standardize the reporting of CPR metrics[15]. Diligence has been made in the work described in this dissertation to adhere to these standards.

### 1.2.1 CPR Mechanism

Chest compressions, when defined by variables such as rate, depth, and duty cycle have a tendency to be highly variable when delivered by medical providers and bystanders[16, 17]. Large clinical trials have measured chest compression parameters and subsequently paired them with clinical outcomes [18, 19]. Common chest compression parameters include chest compression depth, chest compression rate, and chest compression duty cycle. These three parameters are

shown and defined visually in Figure 1. In Figure 1 the sinusoidal waveform representative of continuous chest compressions is quantified using a graphical representation.

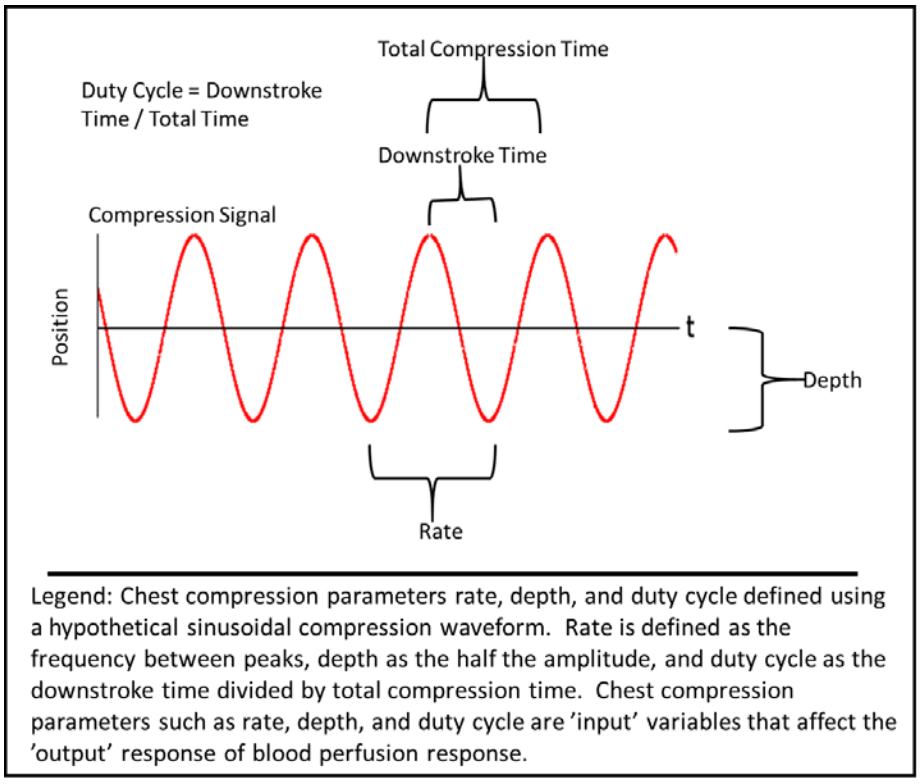


Legend: Chest compression parameters rate, depth, and duty cycle defined using a hypothetical sinusoidal compression waveform. Rate is defined as the frequency between peaks, depth as the half the amplitude, and duty cycle as the downstroke time divided by total compression time. Chest compression parameters such as rate, depth, and duty cycle are 'input' variables that affect the 'output' response of blood perfusion response.

**Figure 1: Chest compression parameters defined on sample waveform**

There are two primary theories that explain the mechanism of CPR. The two mechanisms include the cardiac pump model and the thoracic pressure model. In the cardiac pump model chest compressions during the downward motion squeeze the heart between the sternum and spinal column causing the ejection of blood [20]. This applied pressure is the contributing force for forward movement of blood.

In the thoracic pressure model, a rise in the intrathoracic pressure generated by the 'release' of a chest compression creates a pressure differential necessary for blood to fill the heart. In the thoracic model intrathoracic pressure is transmitted unequally to the peripheral arterial and venous tree. This generates what is described as a peripheral arteriovenous pressure gradient that is the

pressure difference responsible for the generation of blood flow[21]. This description of the CPR mechanism has been further confirmed in animal studies that have observed echocardiography and pressure gradients in animal and human studies[22, 23].

A further study by Paradis et al., determined that the intrathoracic pressure and cardiac pump models are not mutually exclusive[24]. An even more recent study has shown that hemodynamics during CPR may not be governed by a specific model, but a complex interaction of forward and backward flow within the thoracic space[25].

Many factors in the delivery or timing of CPR may affect its potential to produce positive outcomes for patients such as chest compression depth, chest compression rate, and chest compression duty cycle.

### 1.2.2 Chest Compression Depth

The depth of the chest compressions contributes as a factor to the cardiac pump model of CPR. Depth has long been a target parameter to optimize during CPR, with a targeted depth of 2 inches for adults set by the American heart association (AHA) as an evidence-based guideline[1].

Chest compression depth in the out-of-hospital setting when studied in large clinical trials including the Resuscitation Outcomes Consortium (ROC) have been found to be variable. In this trial, increasing chest compression depth was directly correlated with resuscitation outcomes when adjusting for case and process characteristics[26]. In other studies deeper chest compressions were associated with an increased probability of survival and favorable functional outcome[18, 27].

The survival dependence of chest compression depth at a population level from analyses conducted by Stiel et al. is shown in Figure 2 above letter A. The findings summarized in this figure demonstrate that the probability of survival from cardiac arrest increases linearly for mid-

range chest compression depths studied in the trial. The linear increase in benefit however was not seen for chest compression depths at the high and low end of chest compression depths observed in this study.

The effect of insufficient compression depth also has a deleterious effect on defibrillation success. In one study a higher mean compression depth during the 30 seconds immediately preceding a defibrillation increased the likelihood for a successful shock[28].

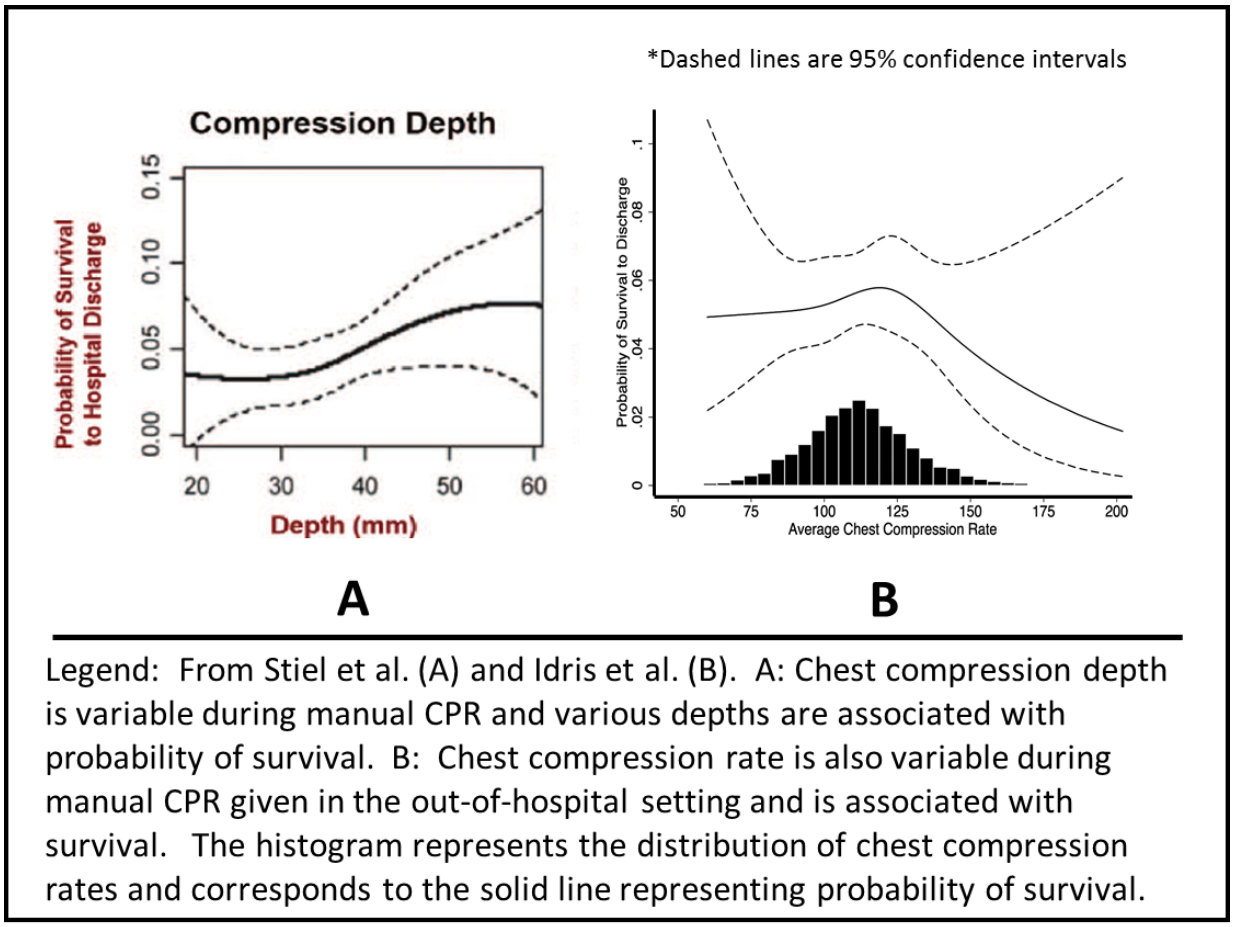


Legend: From Stiel et al. (A) and Idris et al. (B). A: Chest compression depth is variable during manual CPR and various depths are associated with probability of survival. B: Chest compression rate is also variable during manual CPR given in the out-of-hospital setting and is associated with survival. The histogram represents the distribution of chest compression rates and corresponds to the solid line representing probability of survival.

**Figure 2: Survival Dependence on chest compression depth and rate in OHCA**

### 1.2.3 Chest Compression Rate

Chest compression rate plays an important role in generating blood perfusion during CPR and has been studied extensively in the delivery of CPR. Too fast of a rate may not allow for adequate venous return of blood to the heart during CPR if there is reduced filling time caused by a fast chest compression rate. Moreover a faster rate is associated with a reduction in sufficient depth[29]. If the compression rate is too slow, cardiac output is compromised as less volume of blood is ejected from the heart over time.

When assessing the chest compression rates in manikins one study found that a chest compression rate between 100 and 120 compressions per minute did not compromise other chest compression parameters such as chest compression depth and chest compression duty cycle[30]. Another group found that chest compression rate was associated with return of spontaneous circulation (ROSC) but not survival to hospital discharge[31]. A further study found that after adjustment for chest compression fraction and chest compression depth, chest compression rates between 100 and 120 compressions per minute were associated with the greatest likelihood for survival to hospital discharge[19]. The survival dependence of chest compression rate at a population level from Idris et al. is shown in Figure 2 above letter B. This figure summarizes the findings in the study and demonstrates that there is a strong negative Higher chest compression rates have also been found to increase the likelihood for ROSC[32].

### 1.2.4 Chest Compression Duty Cycle

Duty cycle plays an important role in the perfusion and movement of blood during CPR. Duty cycle of a chest compression is defined as the proportion of the time spent compressing the

chest in one chest compression cycle (start of one compression to start of next compression). Some studies suggest that by increasing duty cycle or increasing the duration of the chest compression downstroke, more effective chest compressions would be generated because of the increased refilling time of the thorax[33]. This reasoning speaks to the thoracic mechanism of generating filling pressures as well as enhancing the downstroke ejection phase explained by the cardiac pump mechanism.

Although some initial studies using animal data found that a 30% duty cycle optimized blood flow, AHA guidelines recommend a 50% duty cycle for OHCA CPR treatment, largely based on animal data[1, 33]. This guideline has been found to be largely unmet according to a CPR analysis that found the median duty cycle in a sample of 164 patients to be 38.8%[34].

Duty cycle has also been studied in the context of incomplete chest wall decompression. This is a significant area of research study as the phenomenon of incomplete chest wall decompression is often a result of 'leaning' by the CPR provider and/or fatigue. Leaning during a compression occurs when the provider fails to completely remove compressive force after the upstroke of compression. As the provider fatigues throughout the duration of CPR leaning becomes more prevalent resulting in incomplete chest recoil and CPR quality is compromised[35].

### 1.2.5 Chest Compression Fraction

Chest compression fraction (CCF) refers to the fraction of time during a cardiac arrest that chest compressions are given. In an observational cohort of the ROC trial, one study found that an increase in chest compression fraction was independently predictive of survival. This effect however was only studied in VF/VT as the presenting rhythm subset[36]. In a further analysis of non-VF patients the survival effect was not as strong.[37]

The effect of pauses in chest compressions on perfusion pressure can be visualized in Figure 3. Any brief pause in perfusion will decrease blood perfusion to the brain, worsen ischemia, and result in a period of inadequate perfusion during the time chest compressions have begun to resume.

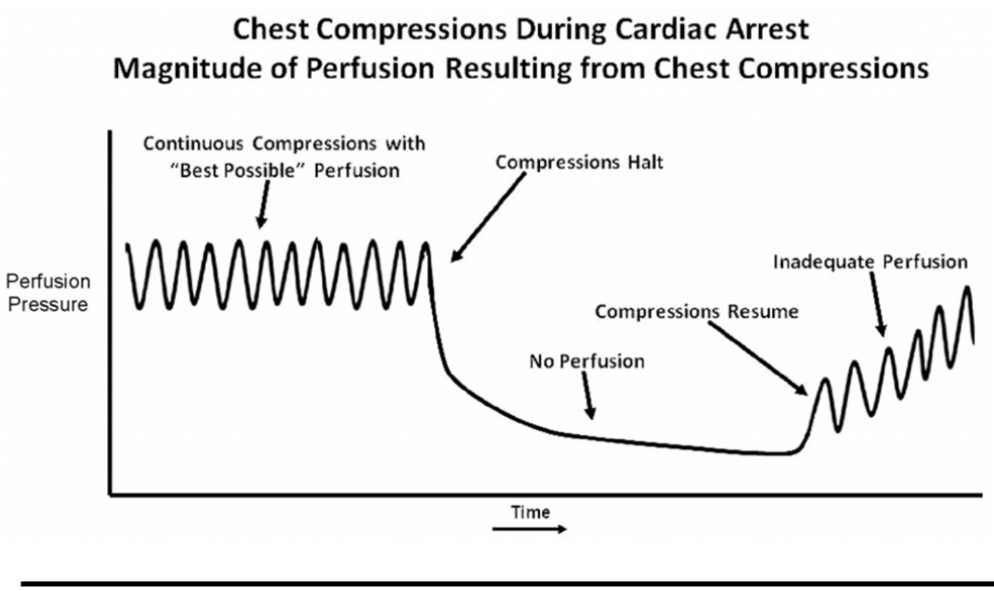


Legend: From Paradis et al. During chest compression interruptions during CPR, perfusion pressure to the heart and other organs is lost, and takes time to reach baseline pressures after chest compressions are restarted. Variable such as chest compression interruptions or chest compression fraction, as well as chest compression rate, depth, and duty cycle, play an important role in adequate perfusion during CPR.

**Figure 3: Pauses in chest compression affects perfusion pressure**

## 1.3 CARDIAC ARREST OUTCOMES AND BIOSIGNALS

### 1.3.1 Cardiac Arrest Outcomes

Outcomes from cardiac arrest range from short term, return of spontaneous circulation (ROSC) and changes in blood pressure, to long term, survival to hospital discharge and neurological outcome at hospital discharge. Long term survival follow-up has been used as well ranging from days to years.

ROSC is viewed as a positive outcome of CPR. Successful achievement of ROSC in the cardiac arrest patient, as well as animal models of cardiac arrest is indicative of a beneficial response to CPR. Evidence of ROSC, especially when reviewing cardiac arrest signal data such as the electrocardiogram (ECG) retrospectively, is difficult to definitively confirm. Higher coronary perfusion pressure (CPP) and 'dose' of elevated CPP over the course of cardiac arrest, are predictive of ROSC[38].

The definition of ROSC by most standards not only requires ECG indicative of a beating heart, but requires a palpable pulse. The presence of pulseless electrical activity (PEA), a lethal arrhythmia that sometimes resembles healthy ECG, may confound the ability to confirm ROSC. This is due to the fact that without physical palpation of an artery or connection to a blood pressure monitor, a PEA rhythm may appear to be pulsatile when it is actually in fact pulseless. End-tidal carbon dioxide levels ($EtCO_2$) measured through the endotracheal tube is used in distinguishing true PEA from a pulsatile rhythm.

Survival is the most desirable outcome measurement or cardiac arrest however even after surviving a cardiac arrest, quality of life is often accompanied with neurologic injury[12]. Survival to hospital discharge even when taken as a positive outcome may not capture the overall medical

condition of the patient. Detailed assessments of the neurologic status of the patient post-hospital discharge such as the Modified Rankin Scale (MRS) further help elucidate treatment effects and outcomes of OHCA[12].

### 1.3.2 Biosignals During Cardiac Arrest

Unlike short or long term outcomes, biosignals provide real-time feedback of the effects of CPR. Biosignals generated from the patient during cardiac arrest are direct responses to the CPR being delivered. Biosignals that have shown evidence to be feasible in monitoring perfusion in cardiac arrest include end-tidal carbon dioxide levels ($EtCO_2$), pulse oximetry, and invasive pressure measurements[38-41]. Although this feedback is not immediate, it is most often in the time-scale of seconds, allowing any resuscitation intervention to be titrated to change in biosignals.

Biosignals in the context of cardiac arrest are physiologic responses that the body generates in response to CPR. Translating the hemodynamics that are generated from the applied force in a chest compression into discernable biosignals that measure CPR effectiveness, is difficult[25]. Some biosignals characterize the ECG during cardiac arrest[42]. These metrics are called quantitative electrocardiogram signals (QECG).

### 1.3.3 Electrocardiogram in Cardiac Arrest

The ECG is a measure of the electrical activity of the heart. The ECG is recorded through electrodes and represents the superposition of the sum of electrical fields across the myocardium. In healthy individuals, the ECG is driven by pacemaker cells in the sinoatrial node of the heart.

Cardiac cells then experience a progression of depolarization events that trigger the atria and ventricles to contract.

In cardiac arrest, the ECG waveform is generally categorized into four distinct rhythms, ventricular fibrillation (VF), ventricular tachycardia (VT), asystole (AS), or pulseless electrical activity. VF and VT have the potential to be defibrillated, while AS and PEA do not. A prospective observational trial of more than 400 hospitals that involved over 50,000 patients from 1999 to 2005 found that that the shockable rhythms of VF and VT had a prevalence of 24% compared to 37% PEA and 39% AS[14]. Similar findings were observed in other studies as well [7, 43]. As would be expected, studies have shown that having a shockable rhythm at any point during OHCA is favorable for patient outcomes[7].

### 1.3.4 QECG Metrics as a Biosignal

The VF waveform has morphologic characteristics that can be quantified. These quantifiable characteristics make up QECG biosignals mentioned in the previous section. QECG involves components of the frequency and amplitude distribution of VF, as well as non-linear characterizations. QECG metrics are well described in the literature for their ability to predict shock success[44]. Amplitude methods, when compared to frequency methods, have a limitation in their ability to drive resuscitation in that they are more susceptible to movement artifact, recording devices, body habitus, and electrode placement[44].

VF waveforms exhibit predictable changes over the course of cardiac arrest. The signal characteristics of the VF and VT waveform are a reflection of the energy status of the myocardium, specifically the presence of high energy phosphates such as ATP[45]. During ischemia of the myocardium in untreated cardiac arrest, the organization of the VF waveform deteriorates from

course, low frequency characteristics, to fine, high frequency characteristics. This change in VF waveform from ‘course to fine’ in untreated cardiac arrest reflects the ion imbalance across the cell membrane. These changes can be seen in Figure 4, taken from a review paper by Callaway and Menegazzi, and demonstrates the time sensitive response of QECG values [44]. In Figure 4, the left column shows the VF ECG at various time points after initiation of cardiac arrest

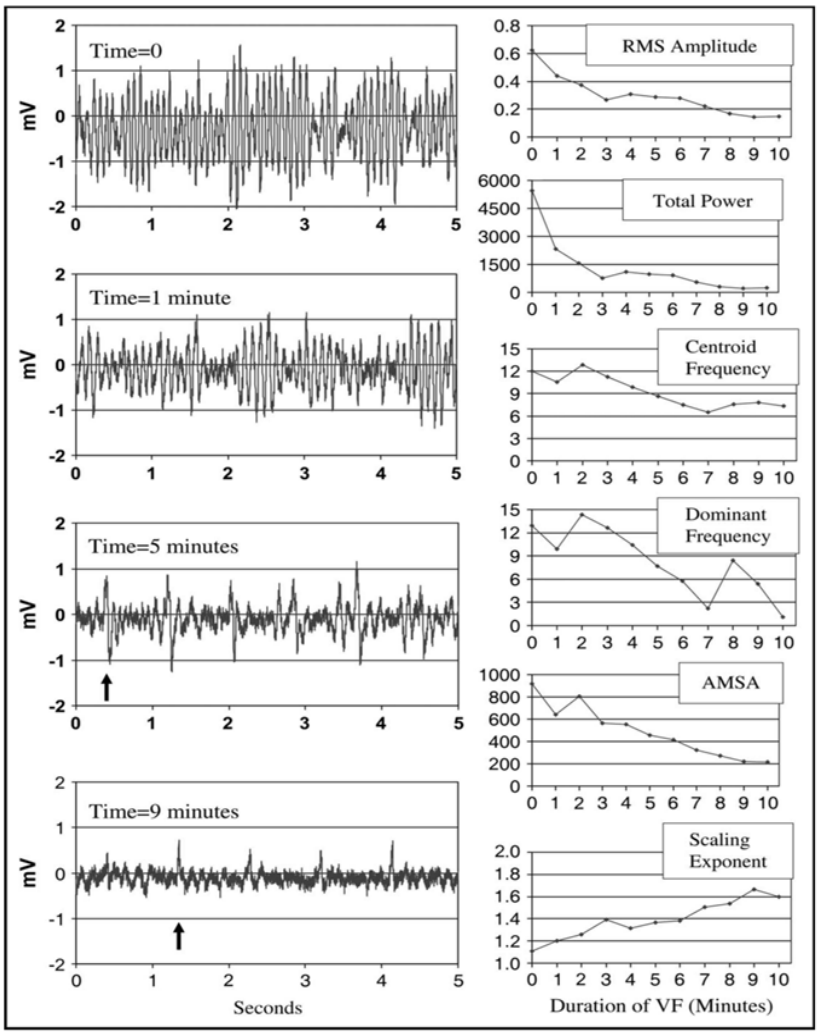


Legend: QECG behavior of VF during untreated cardiac arrest from Menegazzi et al. The left column shows VF in the ECG at initiation of cardiac arrest (Time = 0) to nine minutes after VF initiation (Time = 9 minutes). The right column shows various QECG metrics as they track with increasing time post cardiac arrest initiation.

**Figure 4: QECG response to untreated cardiac arrest**

Research has shown that this deterioration could possibly be due to energy failure, acidosis local hyperkalemia, progressive development of chaotic turbulence, conduction blocks, and changes in restitution potential during ischemia[46-49].

QECG metrics were first used in the application of shock prediction. Multiple studies have confirmed that quantifying the components of the VF waveform prior to a defibrillation attempt can predict the likelihood of a successful defibrillation. Early studies examined amplitude based QECG metrics, however amplitude based metrics had been found to be susceptible to electrode placement and were initially determined to be untrustworthy in evaluating the status of the myocardium[44]. The focus of VF waveform analysis was then placed on frequency component analysis.

Other studies have found that QECG metrics are better predictors of successful defibrillation in a prolonged model of cardiac arrest when compared to shorter duration arrests giving credence that shock prediction by QECG is a dynamic process[50]. In shock resistant VF, AMSA and ECG slope are highly predictive of shock success[51].

One study found that the amplitude QECG measures were the best at shock success prediction, outperforming frequency and nonlinear based QECG metrics[52]. This was a study that observed 3,828 defibrillations from 1,617 patients and found that combining multiple metrics together, did not improve the detection accuracy for successful defibrillation.

### 1.3.5 Common QECG Metrics

Common QECG metrics characterize both the frequency components and the amplitude components of the VF waveform. Additional metrics incorporate non-linear components of the VF waveform. The QECG metrics used in this dissertation include amplitude spectrum area

(AMSA), median slope (MS), centroid frequency (CF), log of the absolute correlation (LAC), and detrended fluctuation analysis (DFA).

#### 1.3.5.1 AMSA

Amplitude spectrum area is a metric that quantifies the frequency components of the VF waveform. AMSA is calculated as the sum of contributing frequencies weighted by the absolute values of the Fourier transform of the signal. Multiple studies have confirmed its ability to predict the outcome of defibrillation in the cardiac arrest patient[53-55]. The equation used for AMSA is shown in Figure 5.

AMSA (Amplitude Spectrum Area)

$$AMSA = \sum_{i=4}^{i=48} A_i * F_i$$

Legend: Equation for AMSA. AMSA is the summed values of the amplitude multiplied by its respective frequency ranging from 4 to 48 Hz.

**Figure 5: Equation for AMSA**

#### 1.3.5.2 Median Slope

Median slope is an amplitude measure of the VF waveform, taken as the median of successive ECG voltage values, and has been used to predict shock success. MS is commonly included with other amplitude measures such as mean slope. The equation for median slope is shown in Figure 6.

MS (Median Slope)

$$Median\ Slope = median(ecg_i - ecg_{i-1})$$

Legend: Equation for median slope. Median slope is calculated as the median of successive ecg voltage values where $ecg_i$ is the ecg voltage value within the ecg discrete time series. The difference between each successive voltage value is calculated, and the median of all the differences is taken as the Median Slope

**Figure 6: Equation for median slope**

#### 1.3.5.3 Centroid Frequency

CF gives insight into the frequency composition of VF and is the frequency coordinate of the center of the spectral mass. CF is calculated as the mean of all contributing frequencies of VF weighted by the power at each frequency[42, 56]. The equation for centroid frequency is shown in Figure 7.

Centroid Frequency

$$CF = \frac{\sum_{i=1}^{n} (f_i \cdot p_i)}{\sum_{i=1}^{n} p_i}$$

Legend: Equation for centroid frequency where $f_i$ is the ith frequency component of the frequency distribution and $p_i$ is the power at $f_i$. CF is therefore the frequency coordinate of the center of the spectral mass.

**Figure 7: Equation for centroid frequency**

### 1.3.5.4 Logarithm of Absolute Correlation

Logarithm of the Absolute Correlation (LAC) is described as a measurement of the 'roughness' of the VF waveform and seeks to quantify the periodicity and self-similarity of VF. It has been used in the study of shock prediction in OHCA as it less affected by lower sampling rates common in defibrillator monitors when compared to more complex non-parametric QECG measures such as the scaling exponent[57]. The equation for LAC is shown in Figure 8.

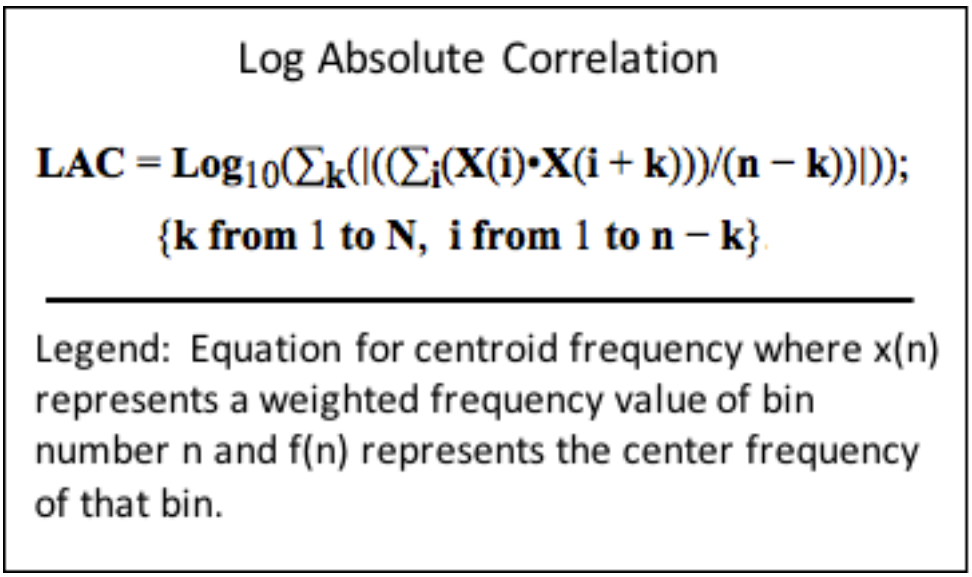


**Figure 8: Equation for LAC**

### 1.3.5.5 Detrended Fluctuation Analysis

Non-linear measures of QECG include the metric DFA. DFA is a measure of randomness of the VF signal and has been shown in studies to predict defibrillation success[58]. One limitation of computational intensive calculations such as DFA is that they are sensitive to filtering and noise common in patient monitors in the out-of-hospital setting. The equation for DFA is shown in Figure 9.

Detrended Fluctuation Analysis

$$F = \sqrt{\frac{1}{N}\sum_{t=1}^{N}(X_t - Y_t)^2}$$

Legend: Equation for detrended fluctuation analysis described by Lin et al. F represents the root mean square deviation from the trend where $X_t$ represents the cumulative sum of the mean value of the time series and $Y_t$ represents the piecewise sequence of straight line fits.

**Figure 9: Equation for DFA**

#### 1.3.5.6 Models with Multiple QECG Metrics

It has often been thought that combining multiple frequency based metrics may produce a stronger predictive value for defibrillation success, and that the nuance gained from a single metric, such as AMSA could be broadened with the addition of other frequency metrics. Neurater et al. attempted to improve the predictive capability through neural networks composed of single predictive features and were unable to increase sensitivity or specificity[59]. This study however was conducted on a sample of only 197 recordings, much smaller than the work presented here. Multiple QECG metrics and their ability to predict shock outcome was also demonstrated in other studies of defibrillation outcomes[52, 60].

## 1.4 QECG RESPONSE TO CPR

QECG metrics have the potential to not only play a role in the timing of shock attempts, but also play a role in the guidance of chest compressions. Chest compressions have a direct effect on myocardial perfusion, which consequently drives QECG changes and shock viability. In an animal study, Salcido and colleagues demonstrated that QECG is responsive to deterioration of myocardial perfusion during untreated VF as well as reperfusion during cardiopulmonary bypass. During untreated VF, the QECG values change in a direction that is indicative of poor perfusion of the myocardium; these values recover once perfusion is reestablished[10, 61].

This phenomenon is observed in Figure 10 from a study performed by Salcido and colleagues.[10] In this study cardiac arrest was induced at time =0 and left untreated for either 15, 10, 25, or 30 minutes. At the end of untreated ischemia reperfusion was provided to the animal through the use of extracorporeal membrane oxygenation (ECMO) to simulate optimal delivery of perfusion through chest compressions. When ECMO was initiated the median slope QECG metric recovered to near baseline levels in the 15 and 20 minute groups but struggled to recover in the longer ischemia groups of 25 and 30 minutes. These data demonstrate that recovery of QECG metrics is not only based on quality reperfusion but also the time duration of ischemia before reperfusion is initiated.

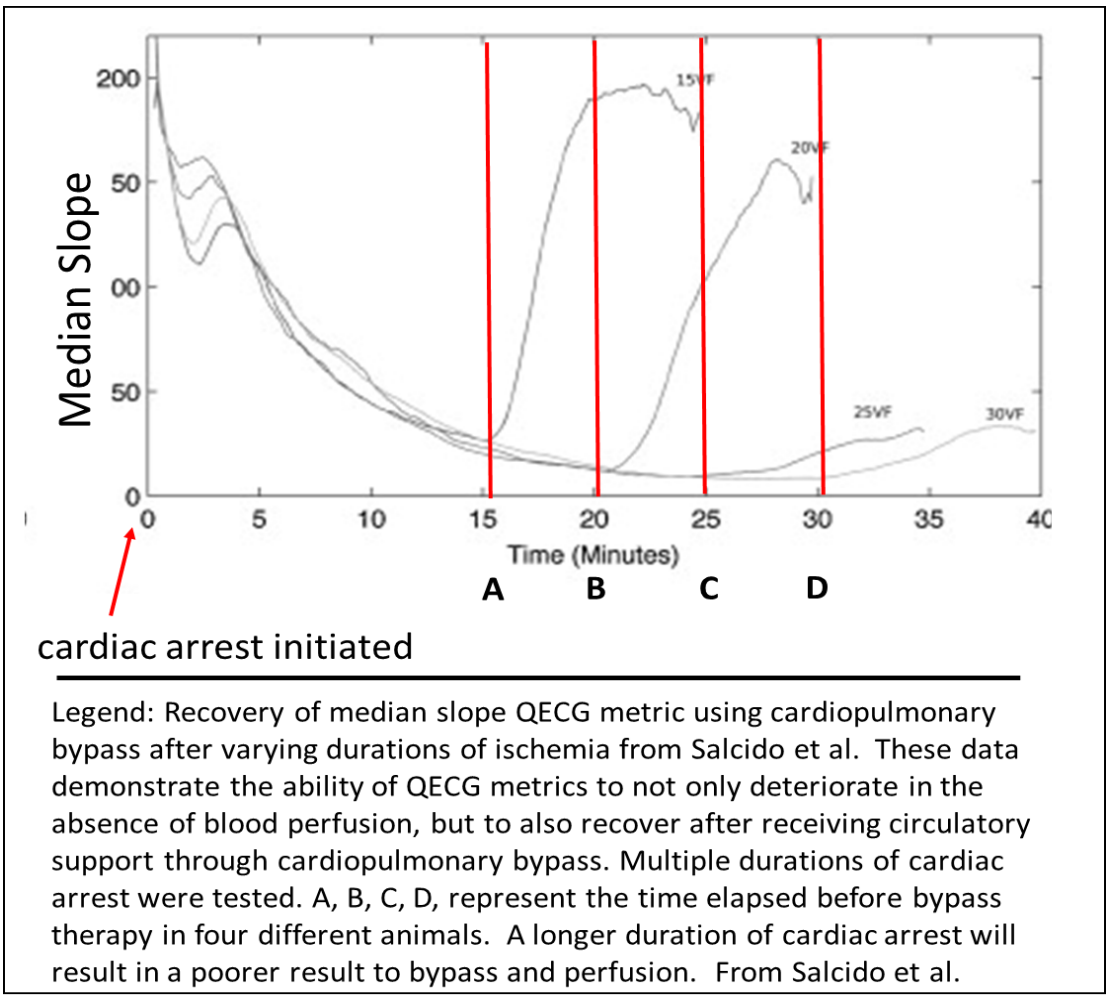


Legend: Recovery of median slope QECG metric using cardiopulmonary bypass after varying durations of ischemia from Salcido et al. These data demonstrate the ability of QECG metrics to not only deteriorate in the absence of blood perfusion, but to also recover after receiving circulatory support through cardiopulmonary bypass. Multiple durations of cardiac arrest were tested. A, B, C, D, represent the time elapsed before bypass therapy in four different animals. A longer duration of cardiac arrest will result in a poorer result to bypass and perfusion. From Salcido et al.

**Figure 10: QECG response to ischemia and perfusion**

Invasive pressure measurements such as coronary perfusion pressure and mean arterial pressure have been the most desirable metric for measuring the effectiveness of chest compressions. However, these invasive metrics are unavailable in the out-of-hospital setting. In contrast, all cardiac arrest patients are instrumented with ECG leads per standard of care for cardiac arrest. This noninvasive approach of quantifying the ECG signal is more feasible than an invasive pressure measurement requiring extensive training, a sterile environment, and time to instrument the patient for measurement. The advantage of using QECG metrics for not only defibrillation

guidance, but chest compression feedback is that chest compression feedback based on QECG could increase survival odds in addition to successful defibrillation odds.

A study by Indik et al. provides evidence that AMSA and slope of the ECG were predictive of shock success in a cardiac arrest model of prolonged VF[50]. This study provides further evidence that timing, of both chest compressions and defibrillation, is of importance in the delivery of chest compressions.

There are two obvious limitations to the QECG approach to drive defibrillation decisions and monitor resuscitation efforts. To quantify ECG accurately, the signal collection process needs to be artifact-free. Chest compressions that are part of CPR and likely ongoing during QECG analysis produce artifact. Movement of the patient by medical providers may also cause artifact to occur in the ECG signal. This artifact can be mitigated through certain techniques, however it is still an issue for real-time QECG analysis[62-64]. The other limitation is that the ECG rhythm must be VF for QECG analysis. VF occurs in cardiac arrest in only about a fourth of all cases.

The work described in this dissertation seeks to further link the relationships between the way chest compressions are delivered to the QECG biosignals that are generated from treatment.

## 1.5 GOAL DIRECTED CPR

Cardiac arrest patients have varying chest anatomy, body mass index (BMI), and underlying etiology. A tailored therapeutic response to the individual patient would therefore be beneficial to the OHCA patient. CPR that changes and adapts to meet certain physiologic goals, have long been theorized to improve organ perfusion and subsequently improve outcomes. The adoption of mechanical chest compression devices for OHCA in the past decade provides an

opportunity to deliver chest compressions with precision. Precision delivered chest compressions, driven by a computer capable of making data driven decisions, have the potential to optimize blood flow.

In animal models, hemodynamic, goal directed CPR, driven by invasive pressure measurements, has been shown to improve short term survival, and has been validated in both asphyxial and pediatric swine models[65-67]. It has also been shown to improve cerebral perfusion and brain tissue oxygenation[68]. There has also been a link established between $EtC0_2$ levels and CPR quality in both in-hospital and out-of-hospital settings. The swine model of resuscitation used in these experiments, in addition to the work described in this dissertation, has been commonly used as a translatable model for human cardiac arrest[69]

In further human studies, an association was found between physiologic monitoring of CPR quality and patient outcomes when clinicians monitor either $ETCO_2$ or diastolic blood pressure during CPR. The rates of ROSC improved in the physiologic monitoring group[70]. However, when studying associations between physiologic monitoring and survival, only $ETC0_2$, when titrated to be kept at above a threshold greater than 10mmHg, was significantly associated with survival. This study further validates the need for a multimodal approach to physiologic monitoring during CPR.

There are many questions that must be addressed when designing a chest compression device capable of receiving physiologic feedback from a cardiac arrest patient, and subsequently adapting its chest compression response to that feedback. The work described in this dissertation seeks to further connect the way CPR is delivered to QECG response and outcomes. Establishing these connections gives further credence to adaptive CPR that could be tailored to the patient, etiology, or phase of cardiac arrest.

## 1.6 SIGNIFICANCE AND AIMS

Cardiac arrest is lethal and survival rates are low. CPR, the main treatment intervention for cardiac arrest, is performed as a 'one size fits all' approach. The chest compression component of CPR can be described by parameters such as rate and depth. Biosignals received from the patient during CPR are a reflection of the perfusion status of the patient, and can be used as a surrogate for CPR effectiveness. There are gaps in knowledge in how biosignals respond to changes in chest compression parameters, and no technology exists that completes the feedback loop between changes in chest compression parameters, blood flow, and measured biosignals.

Aim 1 of the work described here covers the development of a mechanical chest compression device along with subsequent feasibility tests. Further animal tests sought to link the QECG biosignal to chest compression parameters in a controlled cardiac arrest model. It was hypothesized such an adaptive compression device is feasible, and that certain QECG signals respond to specific changes in chest compression parameters.

Aim 2 of the work seeks to investigate relationships between chest compression parameters and QECG in retrospective human clinical data, where measured outcomes such as survival and return of spontaneous circulation are available. It was hypothesized that certain QECG metrics measured in the clinical data would be responsive to changes in chest compression data.

Both aims of the work described in this dissertation seek to answer three primary questions in how to complete a 'closed feedback loop' of chest compressions being guided by biosignsls. These primary questions include which biosignals to measure, be it a type of QECG or other signal, which chest compression parameter to adjust such as chest compression rate, chest compression depth, or chest compression duty cycle, and finally how much and when to adjust the chest

compression parameter. Findings from this work seek to fill the knowledge gaps that exist in developing an adaptive approach to chest compressions in cardiac arrest.

# 2.0 AIM 1 – VALIDATION OF ADAPTIVE CPR DEVICE

Aim 1 of this dissertation includes sections that describe the initial feasibility studies conducted using the adaptive chest compression device which utilizes physiologic feedback. Parts of text and figures in sections 2.1-2.3 are derived from the publication 'Feasibility of Biosignal-guided Chest Compression During Cardiopulmonary Resuscitation: A Proof of Concept' in *Academic Emergency Medicine[71]*. The primary hypothesis of this feasibility study was that such an adaptive chest compression device could be built, and that it would respond appropriately to biosignals.

Aim 1 also describes a computational model that applies an adaptive approach to chest compressions in a simulated population of variable physiology. The adaptive approach adjusts chest compression rate, depth, and duty cycle in response to calculated cardiac ouput values generated by the model. We hypothesized that individual chest compression parameters would be more influential than other chest compression parameters in affecting the simulated cardiac output generated by the model.

Lastly, Aim 1 includes animal experiments where the adaptive chest compression device adjusts specific chest compression parameters while holding all other chest compression parameters constant. The purpose of these experiments was to observe how QECG metrics responded to these chest compression parameter changes in controlled setting of an animal model.

## 2.1 DEVELOPMENT OF CPR DEVICE

Our first task was to engineer and construct an adaptable chest compression device capable of receiving biosignals and responding to them according to an algorithm. We built a custom, electromechanically controlled, signal-guided chest compression device. This system included three principal components: a computer central processing unit (CPU)-coupled linear actuator responsible for piston movement, a signal acquisition unit that collected biosignals, and a main control computer that coordinated feedback signals and commands between the actuator and biosignal acquisition unit (Powerlab 16/30 Model ML880, AD Instruments) recording at 1000 Hz. Chest compressions were delivered by the actuator piston (UltraMotion, Inc., Cutchogue, NY; and Moog, Inc., Elma, NY). Guidance signals were then transmitted to MATLAB (Mathworks, Inc.) through a custom cross-platform memory sharing script provided by AD Instruments. The layout of this design is shown in Figure 11. Using experience from previous swine models, the signal-guided chest compression device was limited to a maximum depth of 2 inches and a maximum rate of 130 compressions/minute. This was accomplished by programming the actuator piston to never accept input from the acquisition device that instructed the device to compress at depths greater than 2 inches or at a rate greater than 130 compressions per minute.

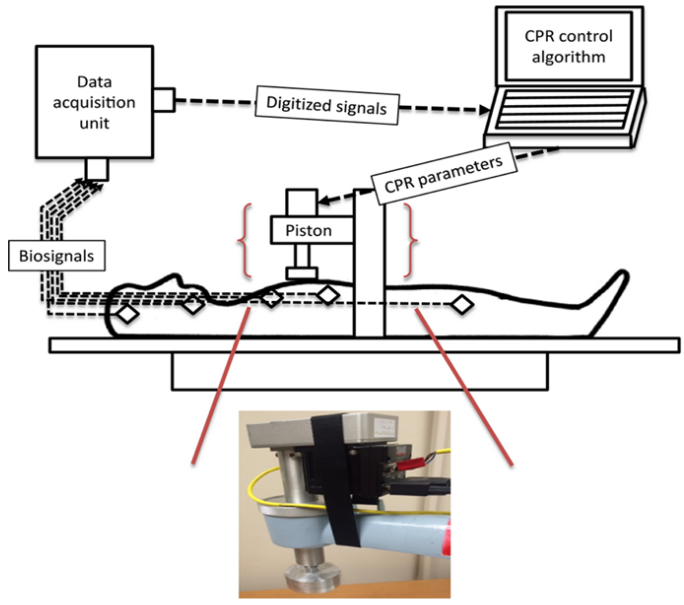


Legend: Design of our closed loop chest compression device that incorporates physiologic feedback. A picture of the piston and compressor is shown. Biosignals are acquired from the patient, received by the computer's control algorithm. Relevant changes are sent to the piston by the computer

**Figure 11: Design of adaptive chest compression device**

The signal-guided chest compression device was programmed to make adjustments independent of the user. Adjustments to depth and rate would be made only when a preset physiologic "threshold" was not met during any given chest compression pause, and CPR parameters were changed until the threshold was reached or until the maximum rate and depth were reached. Figure 11 displays an outline of the prototype device in its projection as a closed feedback loop. Figure 12 is a photograph of the prototype device.

Biosignals from the patient that guide the adaptation of the device are transmitted to MATLAB (Mathworks, Inc.) through a custom memory sharing script that was provided by AD Instruments. The layout of this design is shown in Figure 11 including one of the first iterations of

the piston design. Further iterations of the piston included a suction cup attached to the lower portion and interfacing with the chest that aided in active decompression during the upstroke movement. Active decompression has been shown to increase cardiac output and improve survival in some studies[72, 73].

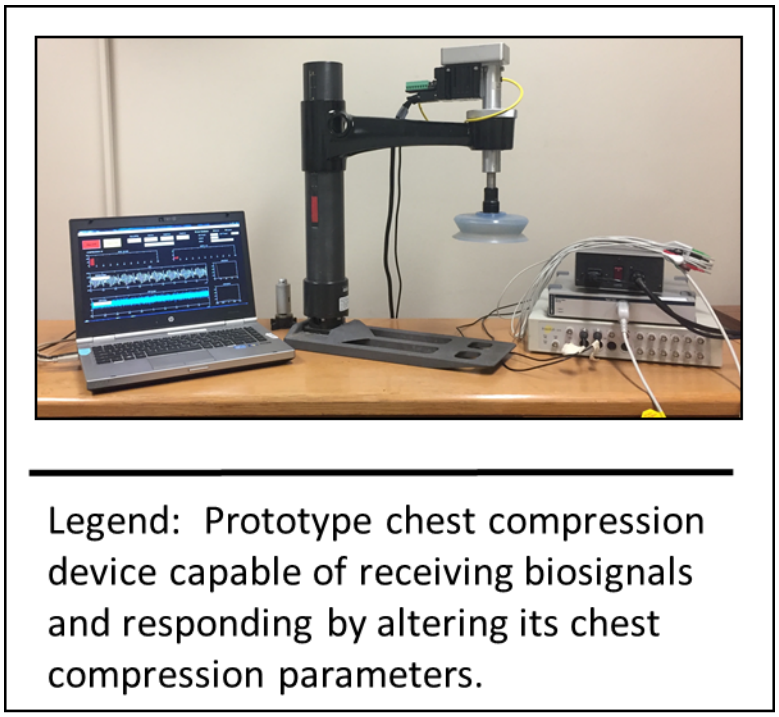

Legend: Prototype chest compression device capable of receiving biosignals and responding by altering its chest compression parameters.

**Figure 12: Photograph of adaptive chest compression device**

A graphical user interface was created through MATLAB that allowed for control of chest compression rate, depth, and duty cycle. The user interface also allowed for easy programming of chest compression algorithms.

Limits to the chest compression settings and algorithms were programmed to not exceed certain values to guard against too extreme depths and rates that could cause harm to the patient/animal. For example, compressions that are too deep could cause rib fracture. Chest compression parameters in the device are limited to a maximum depth of 2 inches and a maximum rate of 130 compressions/minute.

The signal-guided chest compression device was programmed to make adjustments independent of the user. Adjustments to depth and rate would be made only when a preset physiologic "threshold" had not been reached during any given chest compression pause. Chest compression parameters were changed until the threshold was reached or until the maximum rate and depth were reached.

## 2.2 ANIMAL MODEL OF CARDIAC ARREST

All animal studies done in this work were performed using a swine model of cardiac arrest that has been IACUC approved.

In the feasibility study, female mixed-breed domestic swine (*Sus scrofa*) were prepared in a standardized fashion. The animals had a mean mass of 24.1kg and were sedated (Ketamine [10mg/kg]/ Xylazine [4mg/kg]), anesthetized (Fentanyl [50mcg/kg loading dose / 50 mcg/kg/hr infusion]) and paralyzed (Vecuronium [4mg bolus/2mg additional boluses as needed]). Following endotracheal intubation, the animals were mechanically ventilated (Ohmeda 7000) with room air. Central arterial and venous pressure monitoring were measured by using a femoral cut-down technique and inserting Millar catheters (Millar Instruments, Houston, TX) to the aorta and right atrium. ECG was recorded and sampled at 1000Hz (Dual Bio AMP FE 135, AD Instruments, Colorado Springs, CO).

## 2.3 INITIAL FEASIBILITY STUDY

The aim of the first feasibility test was to show that the custom-built CPR device could respond to biosignals in an appropriate way and independent of the user. We hypothesized that the chest compression device would react appropriately to the biosignals it received.

### 2.3.1 Feasibility Experiment Protocol

The biosignals we investigated in this initial feasibility study were central arterial pressure (CAP) and median slope (MS), a QECG metric. These biosignals were monitored during 3-second chest compression pauses every 30 seconds throughout the resuscitation in an effort to reduce signal artifact from the chest compressions. CAP was calculated as the mean central aortic pressure over a 3-second window of a continuous 1000-Hz sample. MS was calculated as the median of the collective sample to sample differences taken from a down-sampled, 250-Hz 3-second window of VF smoothed with a 10-point moving average filter.

The primary outcome we assessed was “appropriate response” of the signal-guided chest compression device to biosignals above and below our biosignal threshold. We defined “appropriate response” as adherence to a 'threshold' algorithm.

The "threshold' algorithm was defined as the device making rate or depth adjustments in response to being below a defined biosignal threshold (MS threshold or CAP threshold). The biosignal threshold was arbitrarily set to an optimal level, based on previous swine studies, and treated as a target that the device would aim to achieve. If both the MS or CAP biosignals were below their respective thresholds, the device would make incremental chest compression adjustments. In this model, both rate and depth were adjusted simultaneously at increments shown

in Table 1. The biosignals were analyzed every 30 seconds. If either one of the MS or CAP biosignals were above its respective threshold, the chest compression parameters would stop adjusting and be held constant by the adjustment algorithm. Table 1 displays example algorithm parameters that the chest compression device followed for one animal experiment.

The general experimental timeline for the initial feasibility study is displayed in Figure 13. VF was induced with a 3-second 100 mA transthoracic shock and left untreated for 6 minutes to simulate an OHCA. After 6 minutes following the induction of cardiac arrest, chest compressions were initiated using the biosignal chest compression system with 3-second pauses every 30 seconds for rhythm analysis. If either a biosignal threshold was met (MS or CAP), or if the chest

**Table 1: Example algorithm for feedback CPR**

| CPR Parameter | Value |
|---|---|
| Initial Depth | 1.2 inches |
| Initial Rate | 100 cpm |
| Depth Increment | .25 inches |
| Rate Increment | 5 cpm |
| MS Threshold | 45 |
| CAP Threshold | 50 mmHg |
| Analysis Interval | 30 seconds |

Legend: Example chest compression parameters for one animal in the feasibility study of adaptive chest compressions. Initial rate and depth are set at the start of compressions and then adjusted

compression parameters of rate and depth had reached their maximum limit, a rescue shock (150J, Zoll M-Series, Zoll, Chelmsford, MA) was attempted in the subsequent 30 seconds. In the event of a failed rescue shock, no further shocks were attempted. Six animals were used in feasibility test.

The target biosignal threshold was adjusted each experiment in reference to the baseline animal biosignal observed during the baseline measurements as well as historical data we had observed in past swine models. Chest compression depth and chest compression rate changes were made simultaneously. The duty cycle of the chest compression was held constant and not adjusted. Figure 13 displays the protocol visually for animals after either a biosignal threshold was met, 14 minutes had elapsed, or ROSC (return of spontaneous circulation) was achieved.

If ROSC was achieved after defibrillation, the swine were monitored briefly. While still under general anesthesia, surviving animals were euthanized with a rapid IV infusion of 40 mEq of potassium chloride.

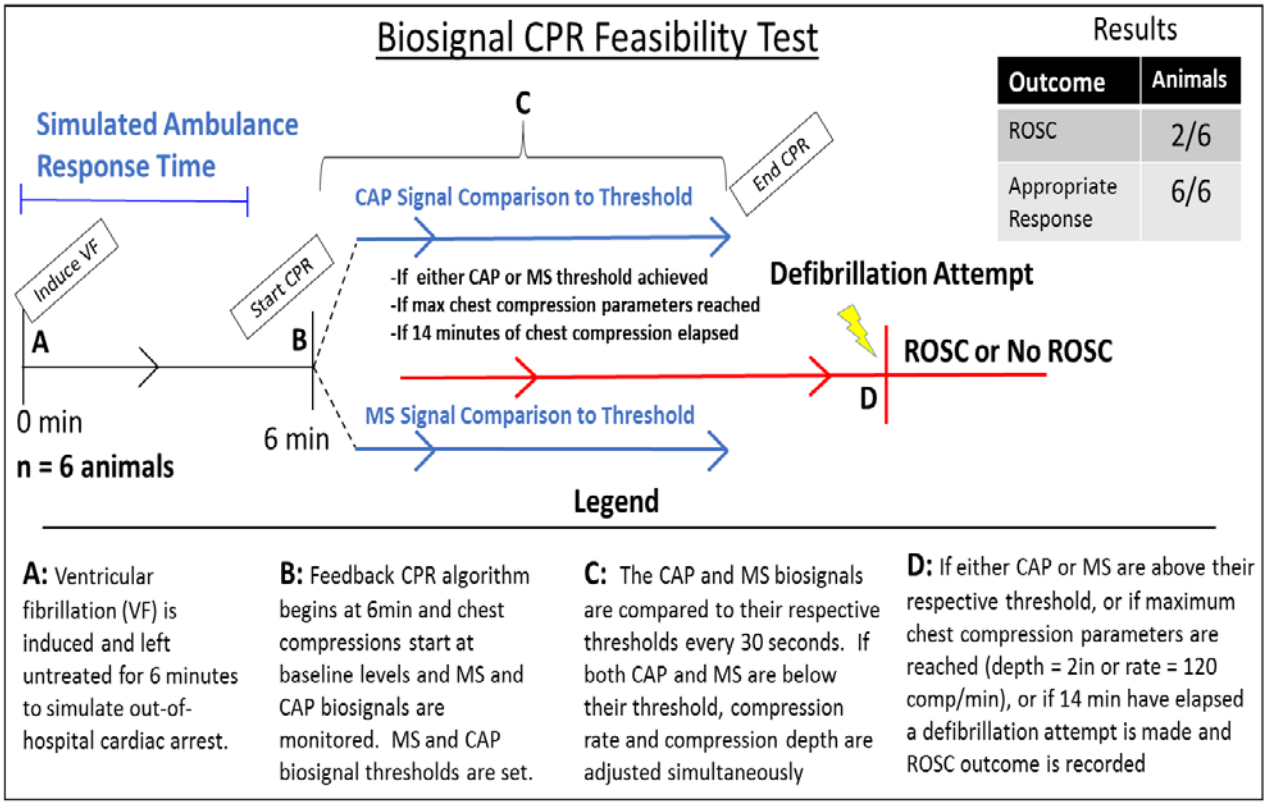


**Figure 13: Outline of feasibility study**

### 2.3.2 Feasibility Study Results

Our custom device responded appropriately to biosignals by changing its rate and depth. All animals exhibited positive improvements in their biosignals. The animals that did not reach either of the two biosignal thresholds had their chest compression parameters adjusted until they reached the maximum parameter level (depth = 2 inches, rate = 130 compression/min).

In the six animal trials conducted, defibrillation was attempted on five animals and two animals achieved ROSC. A summary of the results can be seen in Table 2. Four out of six animals achieved the maximum final rate of 130 compressions per minute and all animals achieved the maximum final depth of 2 inches.

**Table 2: Results from feasibility experiment**

| Experiment | Device Responded Appropriately to Biosignals | MS Baseline / MS Threshold / Threshold Achieved? | CAP Baseline / CAP Threshold / Threshold Achieved? | ROSC? | Final Rate | Final Depth |
|---|---|---|---|---|---|---|
| 1 | Yes | 17 / 30 / No | 25 / 40 / Yes | No | 130 | 2 |
| 2 | Yes | 24 / 40 / Yes | 20 / 50 / No | Yes | 130 | 2 |
| 3 | Yes | 17 /35 / No | 33 / 50 / Yes | Yes | 120 | 2 |
| 4 | Yes | 23 / 35 / Yes | 35 / 50 / No | No | 130 | 2 |
| 5 | Yes | 20 / 45 / No | 24 / 50 / No | No | 125 | 2 |
| 6 | Yes | 41 / 45 / Yes | 28 / 50 / No | No | 130 | 2 |

Legend: Results from the feasibility experiment. Six animals were tested with various CAP and MS biosignal thresholds. All animals responded appropriately to changing biosignals defined as the device correctly adjusting its rate and depth when both measured biosignals were below their respective thresholds, and then ceasing adjustments as soon as one of the two biosignals thresholds were reached. Two of the six animals in the study achieved ROSC. The final rate in each number was variable and the final depth was 2 inches for all animals

Figure 14 shows an example experiment for an animal that reached the MS biosignal threshold and was successfully defibrillated. Figure 15 shows a separate animal that reached the CAP biosignal threshold and was not successfully defibrillated.

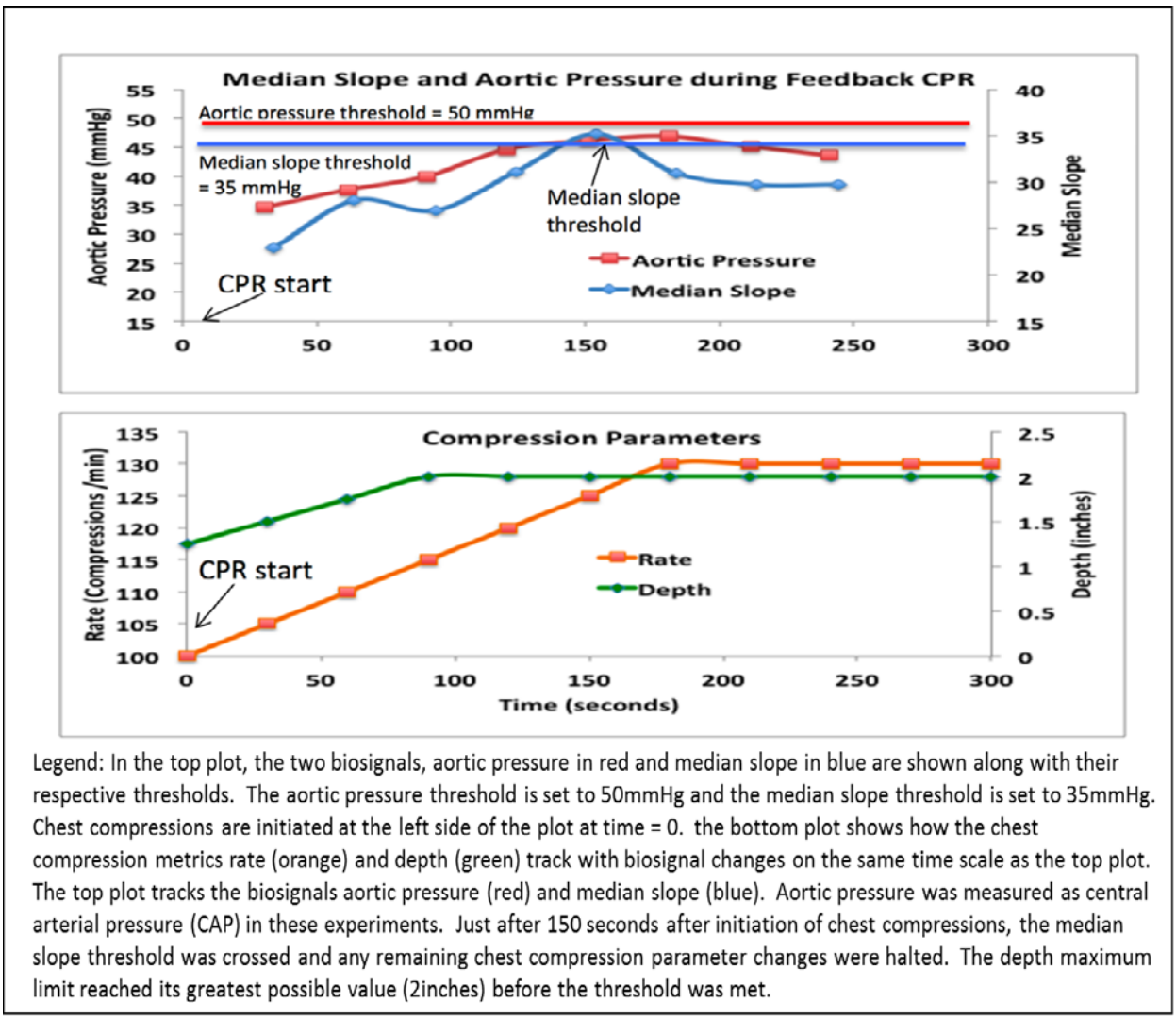


Legend: In the top plot, the two biosignals, aortic pressure in red and median slope in blue are shown along with their respective thresholds. The aortic pressure threshold is set to 50mmHg and the median slope threshold is set to 35mmHg. Chest compressions are initiated at the left side of the plot at time = 0. the bottom plot shows how the chest compression metrics rate (orange) and depth (green) track with biosignal changes on the same time scale as the top plot. The top plot tracks the biosignals aortic pressure (red) and median slope (blue). Aortic pressure was measured as central arterial pressure (CAP) in these experiments. Just after 150 seconds after initiation of chest compressions, the median slope threshold was crossed and any remaining chest compression parameter changes were halted. The depth maximum limit reached its greatest possible value (2inches) before the threshold was met.

**Figure 14: Example feasibility experiment**

During the course of the resuscitation, three of the six animals improved their biosignals to reach the MS threshold, while two of the six animals reached the CAP threshold. The maximum depth of 2 inches was met in all experiments. In Figure 14 and Figure 15, the top plot tracks the change in biosignals (CAP in red and MS in blue), while the lower plot tracks the changes in chest compression parameters the device implemented before the biosignal threshold was met. The

device appropriately ceased making chest compression adjustments as soon as one of the two biosignal thresholds were met.

The MS threshold was achieved in three out of six animals while the CAP threshold was achieved in two out of six animals. The device responded appropriately in all animals, that is it continued making adjustments when biosignal thresholds were not met and correctly halted chest compression adjustments once one of the two biosignal thresholds was met.

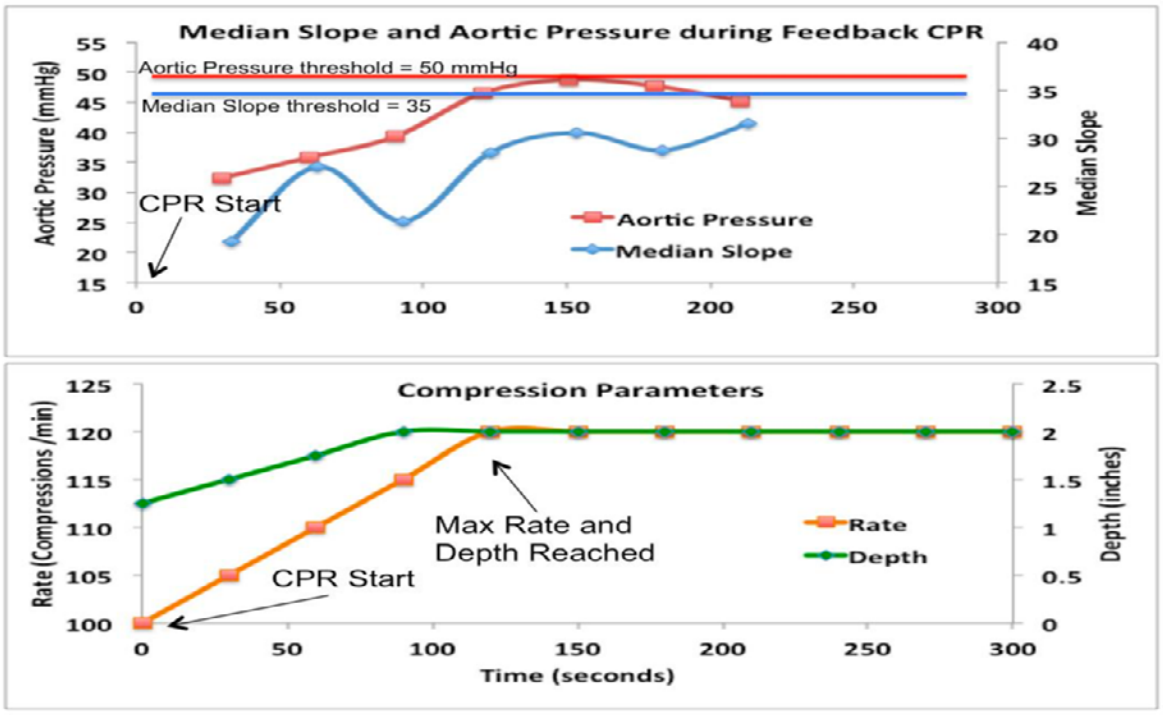


Legend: In the top plot, the two biosignals, aortic pressure in red and median slope in blue are shown along with their respective thresholds. The aortic pressure threshold is set to 50mmHg and the median slope threshold is set to 35mmHg. Chest compressions are initiated at the left side of the plot at time = 0. the bottom plot shows how the chest compression metrics rate (orange) and depth (green) track with biosignal changes on the same time scale as the top plot. The top plot tracks the biosignals aortic pressure (red) and median slope (blue). Aortic pressure was measured as central arterial pressure (CAP) in these experiments. Chest compression depth reached its maximum value at 2 inches at 90 seconds. The aortic pressure threshold was met at time = 120 seconds, and the rate adjustments subsequently stopped adjusting at a final rate of 120/min.

**Figure 15: Example feasibility experiment**

### 2.3.3 Feasibility Study Discussion and Limitations

The treatment of cardiac arrest remains a “black box” in terms of providing optimized care for patients. The variable nature of patients necessitates an adaptive approach to CPR. Mechanical chest compression devices, when coupled to a smart CPU capable of receiving biosignal input, are adaptable to the variable nature of patients.

Our approach very much depends on how accurately our adaptive device is able to acquire and interpret biosignals and in turn relate those biosignals to the quality of perfusion generated by the chest compressions. In a prehospital setting, however, it would be required that these biosignals are noninvasively measured. Biosignal metrics used in our study such as MS QECG are noninvasive and readily available and are derived from the ECG, which is ubiquitously recorded in ambulances for every cardiac arrest patient. A link could therefore be established between existing defibrillator monitors and a biosignal-driven CPR device.

Our findings provide preliminary evidence that a beneficial increase in perfusion may be achieved in cardiac arrest patients by linking the delivery of CPR to invasive and noninvasive biosignals. With more optimal CPR given to patients, patient survival outcomes could be improved. While we have focused on using the biosignals to modify the chest compressions provided by a mechanical CPR device, this feedback could likely also be given to EMS personnel providing manual compressions.

Limitations include translating these findings from a controlled animal lab setting to humans as well as QECG only being available for analysis in VF cardiac arrests. We also acknowledge that the threshold settings need to be further studied to understand what a reasonable positive increase in biosignals would be expected in a successful adaptive approach.

## 2.4 CPR IN A COMPUTATIONAL MODEL

After the initial feasibility of feedback driven chest compressions was established in an animal model described in the previous section, further gaps in knowledge remained that encompassed which chest compression parameter would have the greatest effect on measurable biosignals. To explore this issue more in depth, a computational analysis was conducted to test changes in chest compression in a simulated patient population that had variable chest sizes and physiology. In this computational model cardiac output was used as the measured biosignal. The simulation would adjust chest compression parameters to optimize the cardiac output biosignal. This computational model tested the theory that 'one size fits all' may not be optimal, especially when dealing with a variable population.

We hypothesized that an adaptive approach in a computational model involving chest compression parameter adjustments would yield greater cardiac outputs at the end of the simulation's iterations. It was also hypothesized that chest compression depth adjustments would have the greatest effect on final cardiac output in the adaptive model based on previous anecdotal observations in our animal lab.

Simple computational models have long been used to simulate pressure, volume, and flow relationships in the circulatory system. A computational model provides the ultimate controlled setting to study hemodynamics. To simulate the basic conditions of a feedback CPR approach in patients with variable physiology, we collaborated with Dr. Charles Babbs at Purdue University, an expert in computational models of CPR. Dr. Babbs has developed computational models for various methods of chest compression techniques.[74-76] The purpose of using this collaborative model was to establish a basic foundation of various hemodynamic responses to varying chest compression rate, depth, and duty cycle in patient models of varying body sizes.

### 2.4.1 Model Design

The model used for chest compression in this study included 5 compartments: a chest pump connected in series with supraphrenic and subphrenic aortic segments and corresponding upper and lower body caval segments. There are input and output valves in the chest pump component of the model. Chest compressions in the model create thoracic pressure and was linearly related

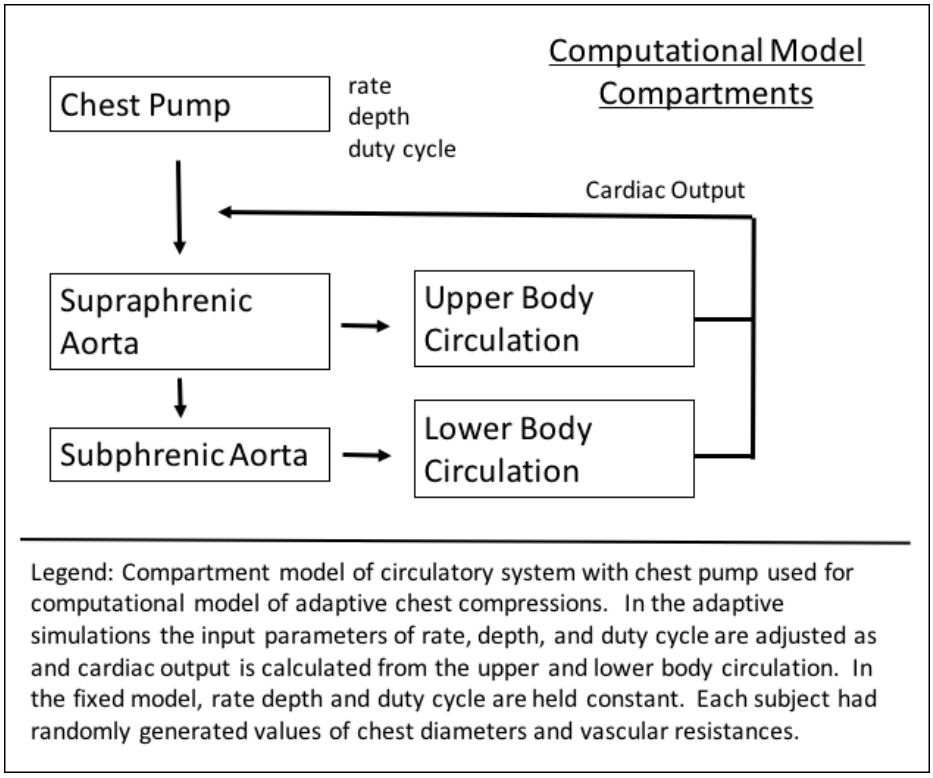


Legend: Compartment model of circulatory system with chest pump used for computational model of adaptive chest compressions. In the adaptive simulations the input parameters of rate, depth, and duty cycle are adjusted as and cardiac output is calculated from the upper and lower body circulation. In the fixed model, rate depth and duty cycle are held constant. Each subject had randomly generated values of chest diameters and vascular resistances.

**Figure 16: Computational chest compression model**

to the ratio of chest compression amplitude to chest diameter. The outline of this model simplified to compartments can be seen in Figure 16.

100 simulated patients were used in the simulation where each patient was randomly assigned a body weight ranging from 40 to 110 kg. The mean body weight in the simulated patient population was set to 70 kg and the standard deviation of body weight was set to 15 kg. To simulate

an average patient of a particular body size, vascular compliances were scaled in proportion to body weight, chest diameter is scaled in proportion to the 1/3 power of body weight, and vascular resistances were scaled in proportion to the negative 2/3 power of body weight. Vascular resistance in this chest compression model can be thought of as the resistance to forward blood flow due to the 'chest pump' component of the system. Cardiac output is then calculated as the difference in pressures across component compartments divided by the resistance. A sample calculation is shown in Figure 17. Microsoft Visual Basic Version 6.0 (Redmond, WA) was used for computational analysis.

Chest diameters used in the simulation is taken as the absolute distance between the chest and back similar to the anterior-posterior (AP) diameter used in reference for current AHA defined chest compression guidelines.[1] These average values are then multiplied by a

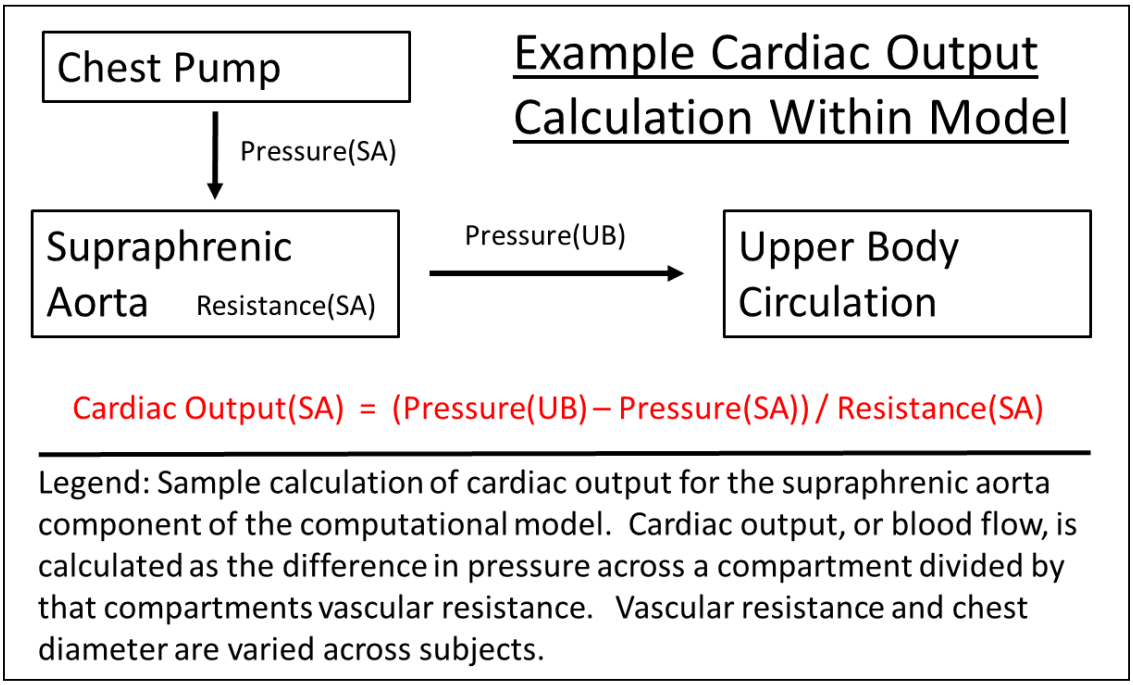


**Figure 17: Example cardiac output calculation**

Gaussian random variable with a mean of 1.0 and a standard deviation of 0.1 to represent a particular randomly selected patient. These physiologic variables were generated randomly to simulate the variable population of cardiac arrest patients. There were a total of 100 subjects simulated and each subject went through an iteration of standard chest compressions that were not adjusted as well as an iteration of adaptive chest compressions that were adjusted based on the cardiac output.

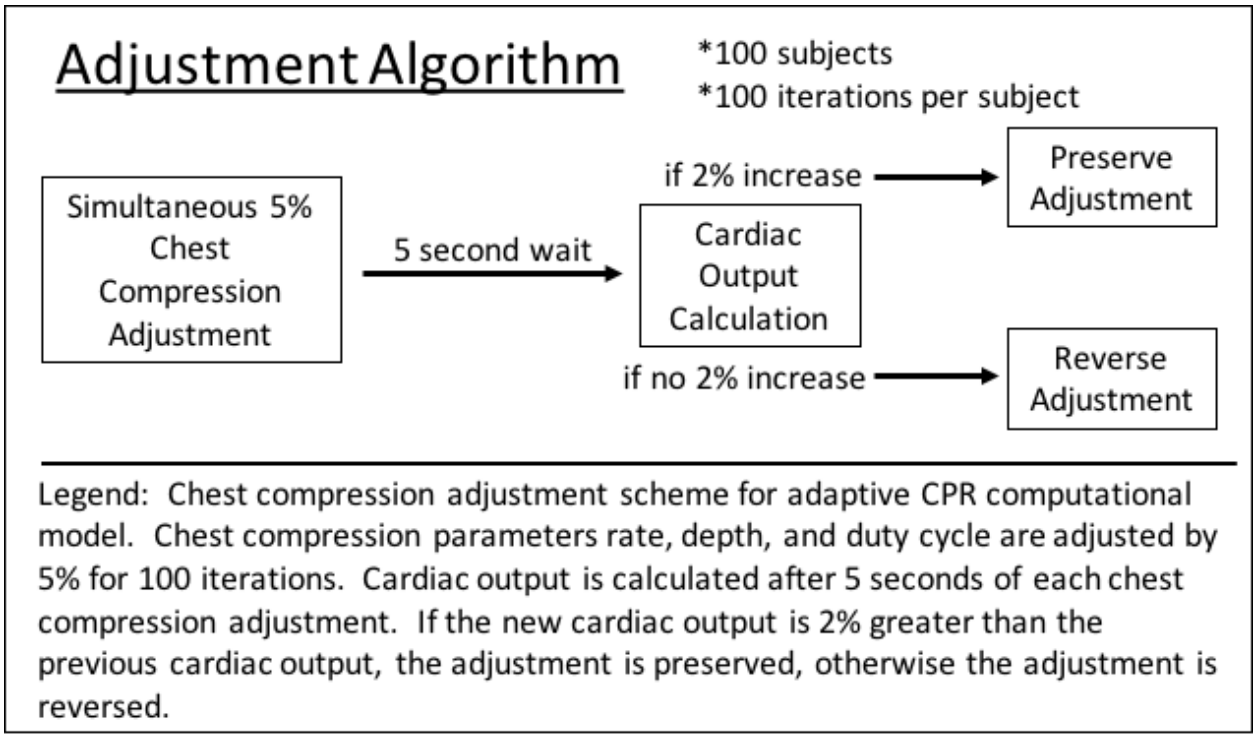


**Figure 18: Adjustment algorithm**

Chest compression adjustments in the adaptive model were performed according to the following guidelines. First, cardiac output is computed for standard chest compression (100/ min, 5 cm depth, duty cycle 50%) in the randomly selected patient model. Then the three chest compression variables (rate, depth, and duty cycle) are adjusted simultaneously using computer simulated evolution. Each chest compression variable was randomly increased or decreased by

5% after the cardiac output was determined for a 5 second test run of CPR. If the new computed cardiac output was 2% or better than the previous computed cardiac output value, the chest compression adjustment was preserved. Otherwise the chest compression adjustment is reversed. This process was repeated for 100 iterations to obtain an individually adjusted chest compression technique. A realistic hard limit on chest compression depth of 50% of chest diameter was imposed. This limit was set to meet the clinical reality that chest compressions deeper than 50% of the chest diameter would be deleterious to the patient. This adjustment algorithm is shown in Figure 18.

### 2.4.2 Model Results

A histogram of final cardiac output values was generated for the first 100 patients of the model and can be seen in Figure 9. In Figure 14 CO is the final output of the adaptive chest compression model divided by the cardiac output of the standard 'fixed' chest compression model in the same simulated subject to create a cardiac output ratio for each reflecting the effect of the adaptive model on cardiac output compared to the standard model of cardiac output. The histogram shows that the adaptive chest compression simulation improved final cardiac output by a nearly 3-fold increase. This represents a near 3-fold increase in the forward blood flow when

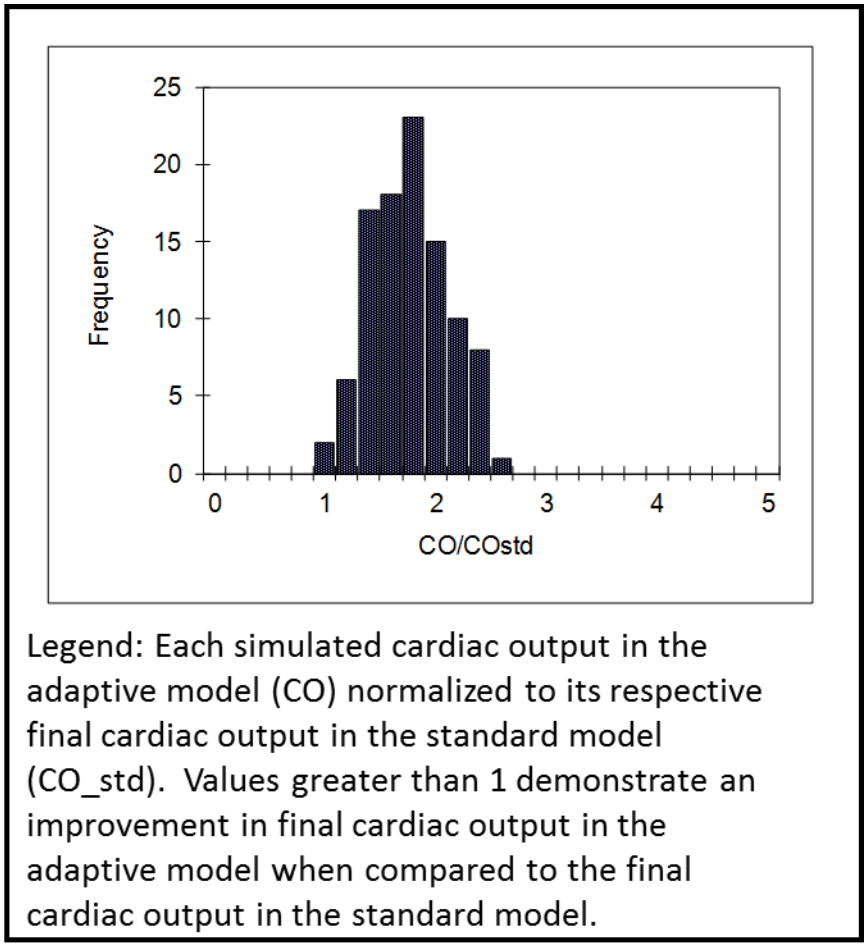


**Figure 19: Final cardiac output in adaptive model normalized to fixed model**

compared to a standard chest compression approach. Standard CPR works well in models with very thin chests front to back, but not so well in others.

After the end of all 100 simulations The final values of chest compression parameters shows that the increased amount of output is largely due to increased chest compression depth, rather than rate or duty cycle changes. Rates remained at 100/min and duty cycles remained at 50%. The mean final ratio of the adaptive model final cardiac output to the standard model final cardiac output was 1.77. The final mean chest compression depth value was .48 inches in the adaptive model and the final mean chest compression rate value was 100 compressions per minute.

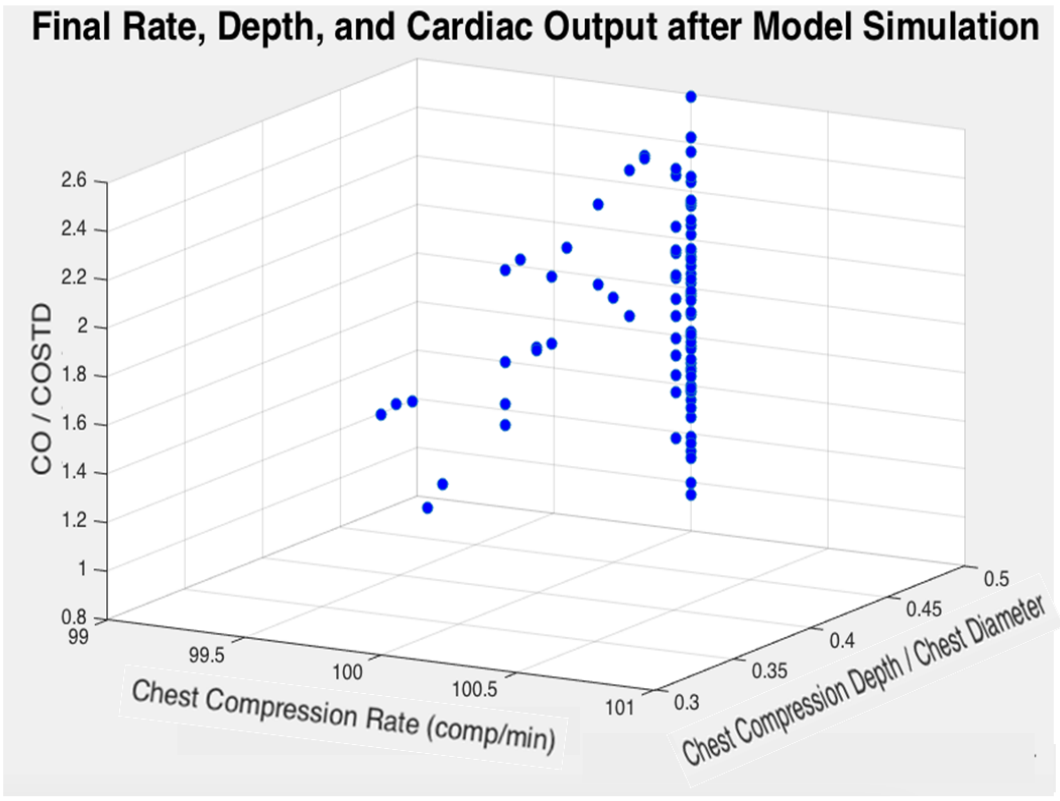


Legend: After full iteration of the adaptive simulation model, each simulated individual's final rate (compressions/min), final depth (as a proportion of chest diameter), and final cardiac output (normalized to final cardiac output during the standard simulation model) are shown in the plot. A hard limit of depth was set to 50% of the chest diameter. A final rate was 100 compressions per minute in all individuals.

**Figure 20: Final cardiac output, final rate, and final depth**

A 3D plot of the final rate and depth values by simulated individual in the adaptive model along with its respective final normalized cardiac output, can be seen in Figure 20.

This computational analysis shows that in simulation, improving blood flow due to chest compressions depends on increasing chest compression depth. This observation was found in the adaptive computational model in the setting of random variation in the resistive properties of the systemic circulation as well as variation in chest diameter across patients.

This model is limited by its simplicity in modeling complex physiologic phenomena, but provides the early basis that physiologic variability matters in an adaptive approach to chest compressions in CPR. The model is also limited in that chest compressions are given as a rectangular pulse waveform which may not reflect chest compression waveforms given in a real life clinical setting that may have rounded edges compression waveforms.

An additional factor worth considering in the computational model concerns whether the chest compression adjustment used in this model would be the optimal adaptive approach to cardiac output feedback driven chest compressions. The use of 5% adjustments in chest compression values reacting to at least 2% changes in cardiac output was chosen only based on the fact that these values seemed clinically reasonable. Five seconds was chosen as the amount of time after an adjustment to make a cardiac output calculation. Further work in computational models and animal models would be required before determining the optimal chest compression adjustment approach.

## 2.5 QECG IN RESPONSE TO VARYING CPR IN AN ANIMAL MODEL

To further examine the effect of varying chest compression rate, depth, and duty cycle on biosignals, a second animal study was conducted. This animal study was an important follow-up to the findings generated by the simulation data and initial feasibility study. However, unlike the simulation which used cardiac output as the biosignal, this second animal trial focused on QECG as the biosignal. Invasive measurements such as cardiac output are not available in the out-of-hospital setting and this animal study was conducted in an attempt to monitor a noninvasive biosignal in the context of changing chest compression parameters. QECG is a readily available non-invasive biosignal for OHCA patients.

The hypothesis of this second animal study was that in a controlled environment QECG metrics would respond to changes in chest compression rate, chest compression depth, or chest compression duty cycle. From the results in the computational model, it was hypothesized that chest compression depth would have the most significant effect. These studies sought to provide answers to the first two questions posed in the significance and aims discussion in Section 1.6 concerning which chest compression to adjust and which biosignals to monitor in an adaptive model of chest compression delivery.

### 2.5.1 Animal Model Methods

In this study, 12 mixed-breed domestic swine were sedated, anesthetized and paralyzed, followed by endotracheal intubation and mechanical ventilation. Animals were instrumented with a battery of physiological sensors, including multi-lead ECG, recorded continuously with a high-

fidelity data acquisition unit at 1000Hz. VF was induced with a 3-second 100mA transthoracic shock.

After 7 minutes of untreated VF, animals were randomized to receive continuous CPR with our custom-built robotic device. Animals were grouped using 1 of 6 pre-programmed, cross-over 2-phase CPR schemes. These schemes are shown visually in Figure 12. Each scheme varied 1 parameter in 5 x 1-minute intervals while holding other parameters unchanged. There were 2 phases of the 5 x 1 minute intervals, hence the crossover design to obtain as much data per animal as possible. This experimental setup is shown in Figure 21, 22, and 23.

Each grouping contains one chest compression variable that changes once a minute which is either chest compression rate, chest compression depth, or chest compression duty cycle. All parameter changes cycle in sequence and include values of 'low', 'medium', 'high', and 'very high'. These values are shown in Table 3.

We hypothesized that a linear response in QECG would result in the parameters studied due to the fact that the ranges included in chest compression parameters did not include 'extreme' values. For example, the range of chest compression values used was from 60 cpm to 120 cpm. A range that may have elicited a non-linear response would be 10cpm to 200cpm where the extreme values of chest compression parameters, such as compression given at 200cpm, would have disrupted any linear increase in response observed in the range of 60cpm to 120cpm.

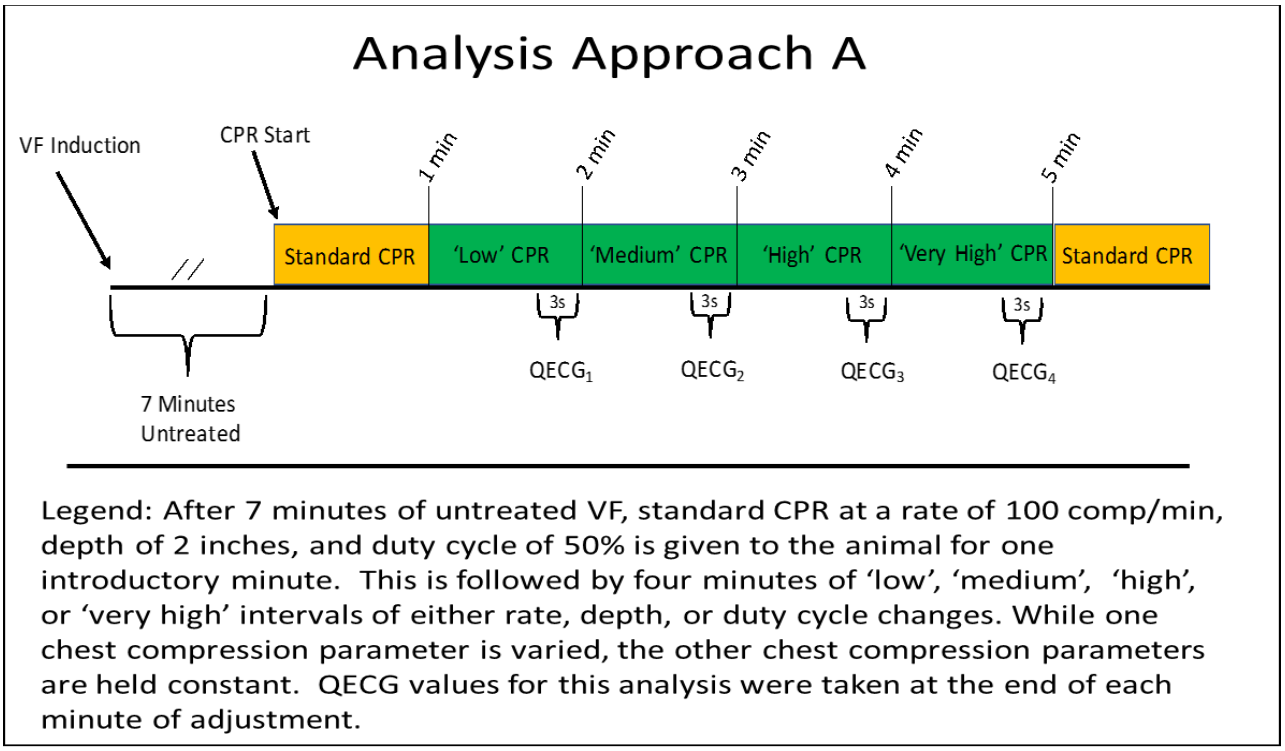


**Figure 21: Analysis Approach A**

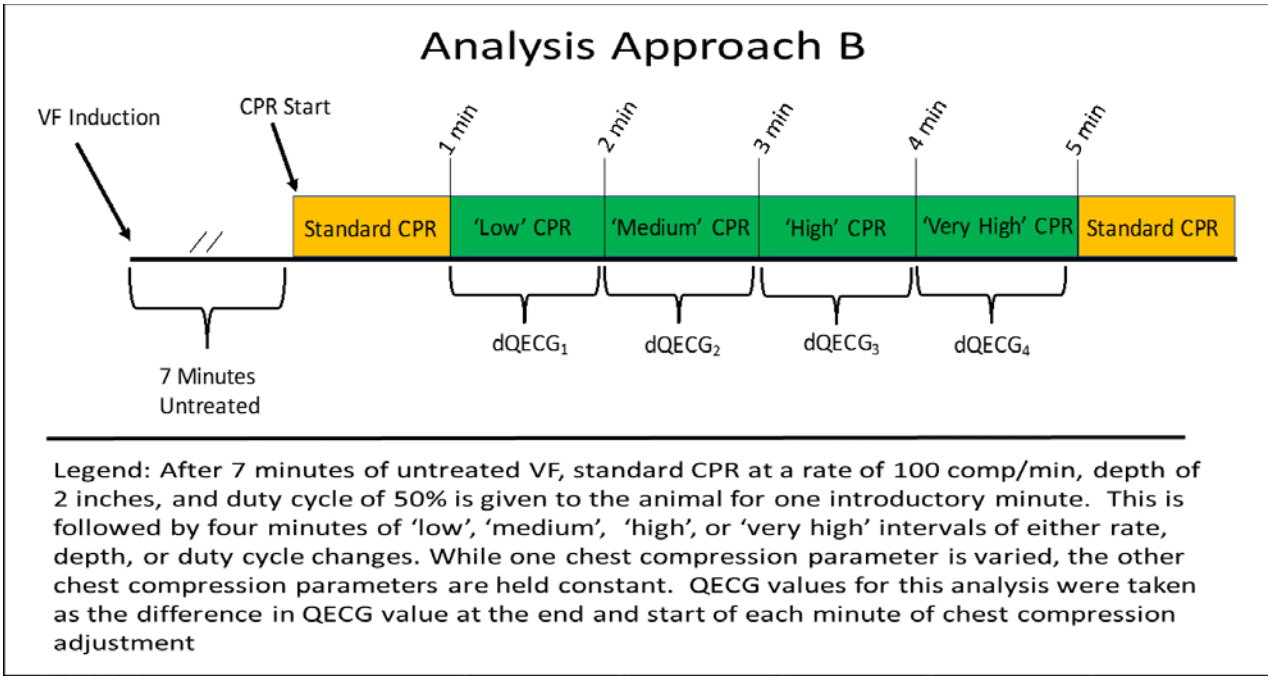


**Figure 22: Analysis Approach B**

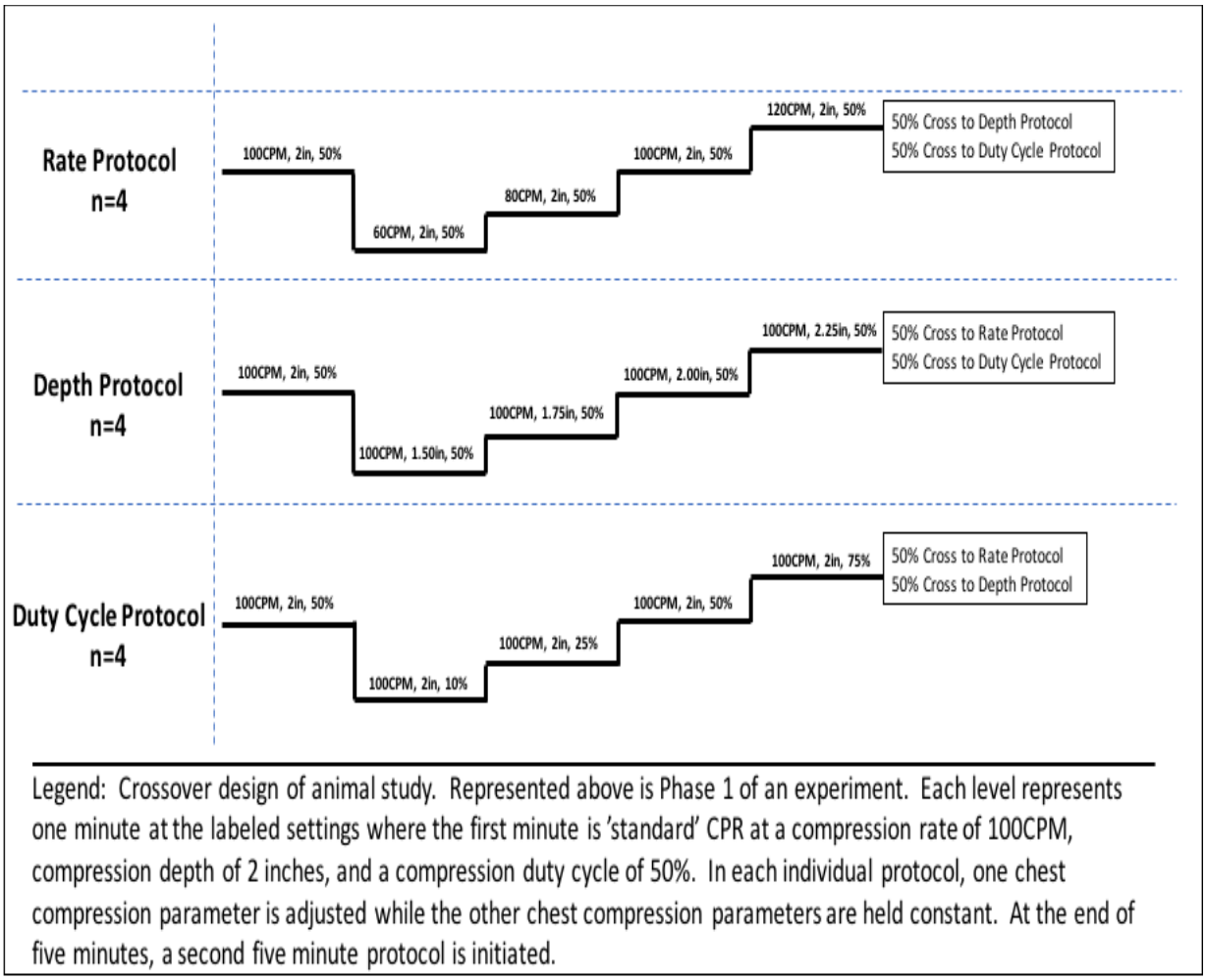


Legend: Crossover design of animal study. Represented above is Phase 1 of an experiment. Each level represents one minute at the labeled settings where the first minute is 'standard' CPR at a compression rate of 100CPM, compression depth of 2 inches, and a compression duty cycle of 50%. In each individual protocol, one chest compression parameter is adjusted while the other chest compression parameters are held constant. At the end of five minutes, a second five minute protocol is initiated.

**Figure 23: Crossover design of animal experiment**

| Depth Change Group | | | |
|---|---|---|---|
| | Depth | Rate | Duty Cycle |
| Minute 2 | 1.5 | 100 | 50 |
| Minute 3 | 1.75 | 100 | 50 |
| Minute 4 | 2 | 100 | 50 |
| Minute 5 | 2.25 | 100 | 50 |

| Rate Change Group | | | |
|---|---|---|---|
| | Depth | Rate | Duty Cycle |
| Minute 2 | 2 | 60 | 50 |
| Minute 3 | 2 | 80 | 50 |
| Minute 4 | 2 | 100 | 50 |
| Minute 5 | 2 | 120 | 50 |

| Duty Cycle Change Group | | | |
|---|---|---|---|
| | Depth | Rate | Duty Cycle |
| Minute 2 | 2 | 100 | 10 |
| Minute 3 | 2 | 100 | 25 |
| Minute 4 | 2 | 100 | 50 |
| Minute 5 | 2 | 100 | 75 |

Legend: Chest compression parameter values for each group in Phase 1. Cycles were repeated again for minutes 7-10 as part of Phase 2 in a crossover design. In each group, one parameter was varied, while the other 2 were held constant.

**Figure 24: Chest compression group classification**

Chest compression adjustments were made every minute, with a baseline of one minute of 'standard' CPR parameters before each adjustment phase. QECG characteristics (AMSA, MS, CF, LAC, and DFA) were calculated at the end of each 1-minute interval and compared against rate, depth and DC in both phase 1 and phase 2.

Change in QECG across adjustment minute was also calculated and compared to each chest compression parameter. Figures 10 and Figure 11 explain further this experimental setup. That is, both the QECG values at minute's end, and change over minute were taken.

Phase 1 and Phase 2 analyses were performed separately. Phase 2 results were inherently limited by what had occurred in phase 1, but were analyzed nonetheless to extract as much information as possible from each animal. The QECG values used in these animal studies were AMSA, MS, CF, LAC, and DFA. Their equations used for their calculation are shown in Figures 5-9 described in the introduction of this work. The frequency distribution calculated in centroid frequency equation was found using a fast fourier transform in MATLAB. The technique for the DFA calculation involved calculating the F term in Figure 9 in a technique outlined by Lin et al. and used in our Matlab code[58].

To test for relationships between the QECG and chest compression parameters, simple linear regression analysis was performed. We believe that this was the most appropriate test as past clinical evidence has shown that survival has a somewhat linear dependence on rate and depth for rates up to 120/min and depths just past 2 inches. It was assumed that since this linear relationship held for survival, a similar effect would be shown for QECG. There has been less evidence for these associations in duty cycle studies.

The timing of the QECG calculations were calculated using two separate methods. The first method involved calculating the QECG value using the last 3 seconds of every minute where a chest compression parameter was changed. The second method involved calculating the change in QECG over the minute using the change in QECG in the first and last 3 second interval.

### 2.5.2 Animal Model Results

Linear regression analysis was performed for both phase 1 and phase 2 of the crossover experimental design. $R^2$ values for each linear fit in phase 1 along with their associated p values are shown in tables 3 and 4 respectively. These tables represent phase 1 changes with the 'end of minute' technique used (Analysis Approach A). Plots shown in the following section are linear regression tests that contained significant results (yellow box). All plots that contained only insignificant results can be found in Appendix A. Error bars in all graphs are standard deviation.

**Table 3: R squared values in phase 1 at minute end**

| Simple Linear Regreesion R2 Value - Phase 1 | | | | | |
|---|---|---|---|---|---|
| QECG (at Minute End) | AMSA | MS | CF | LAC | DFA |
| Depth Changes | 0.336 | 0.118 | 0.521 | 0.164 | 0.063 |
| Rate Changes | 0.681 | 0.930 | 0.936 | 0.960 | 0.045 |
| Duty Cycle Changes | 0.243 | 0.739 | 0.579 | 0.258 | 0.043 |

**Table 4: P values in Phase 1, QECG values taken at minute end**

| Simple Linear Regression P Value - Phase 1 | | | | | |
|---|---|---|---|---|---|
| QECG (at Minute End) | AMSA | MS | CF | LAC | DFA |
| Depth Changes | 0.420 | 0.656 | 0.278 | 0.595 | 0.593 |
| Rate Changes | 0.175 | 0.036 | 0.033 | 0.020 | 0.394 |
| Duty Cycle Changes | 0.507 | 0.141 | 0.239 | 0.492 | 0.919 |

The QECG metrics median slope (MS), centroid frequency (CF), and log absolute correlation (LAC) had significant linear responses to rate changes when using Analysis Approach A during the Phase 1 section of the experiment. Plots of these responses are shown in Figures 25,

26, and 27. Plots with a yellow box represent significant linear responses. Plots for the non-significant QECG responses in AMSA and DFA are shown in Appendix B. Depth changes and duty cycle changes did not produce a significant linear response in any QECG metric.

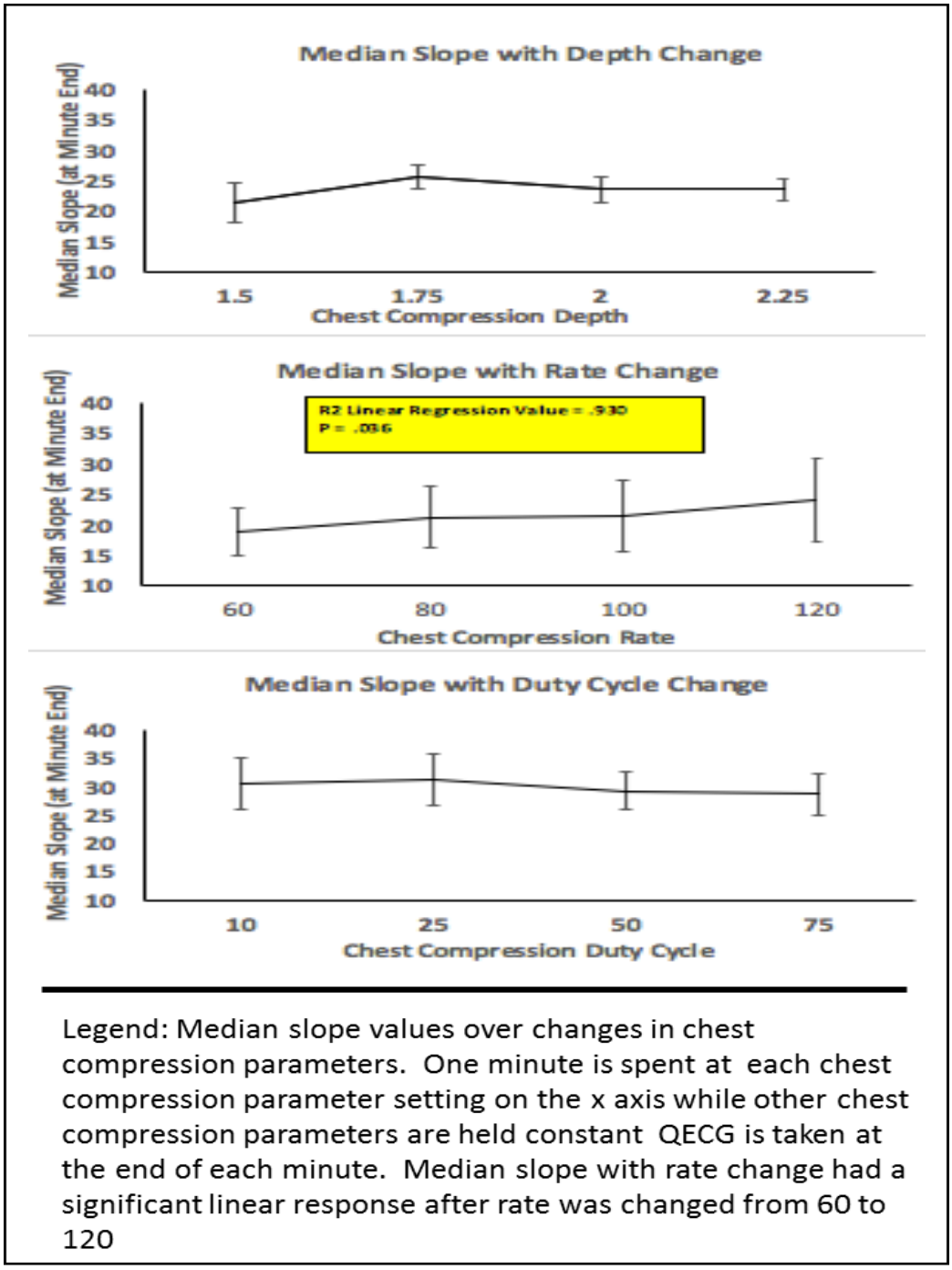


**Figure 25: Median slope response to CC changes in Phase 1 (Analysis Approach A)**

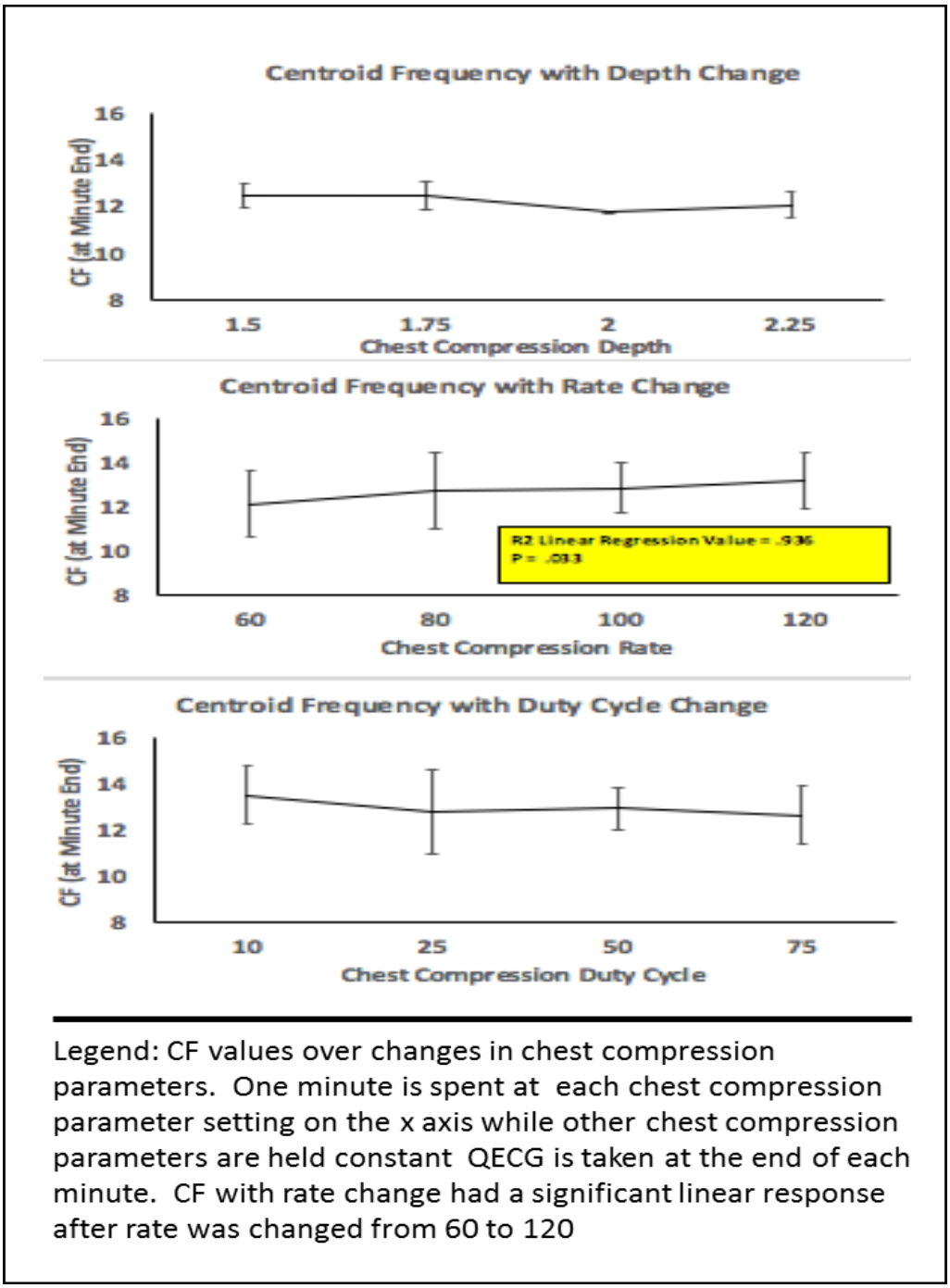


**Figure 26: CF response to CC changes in phase 1 (Analysis Approach A)**

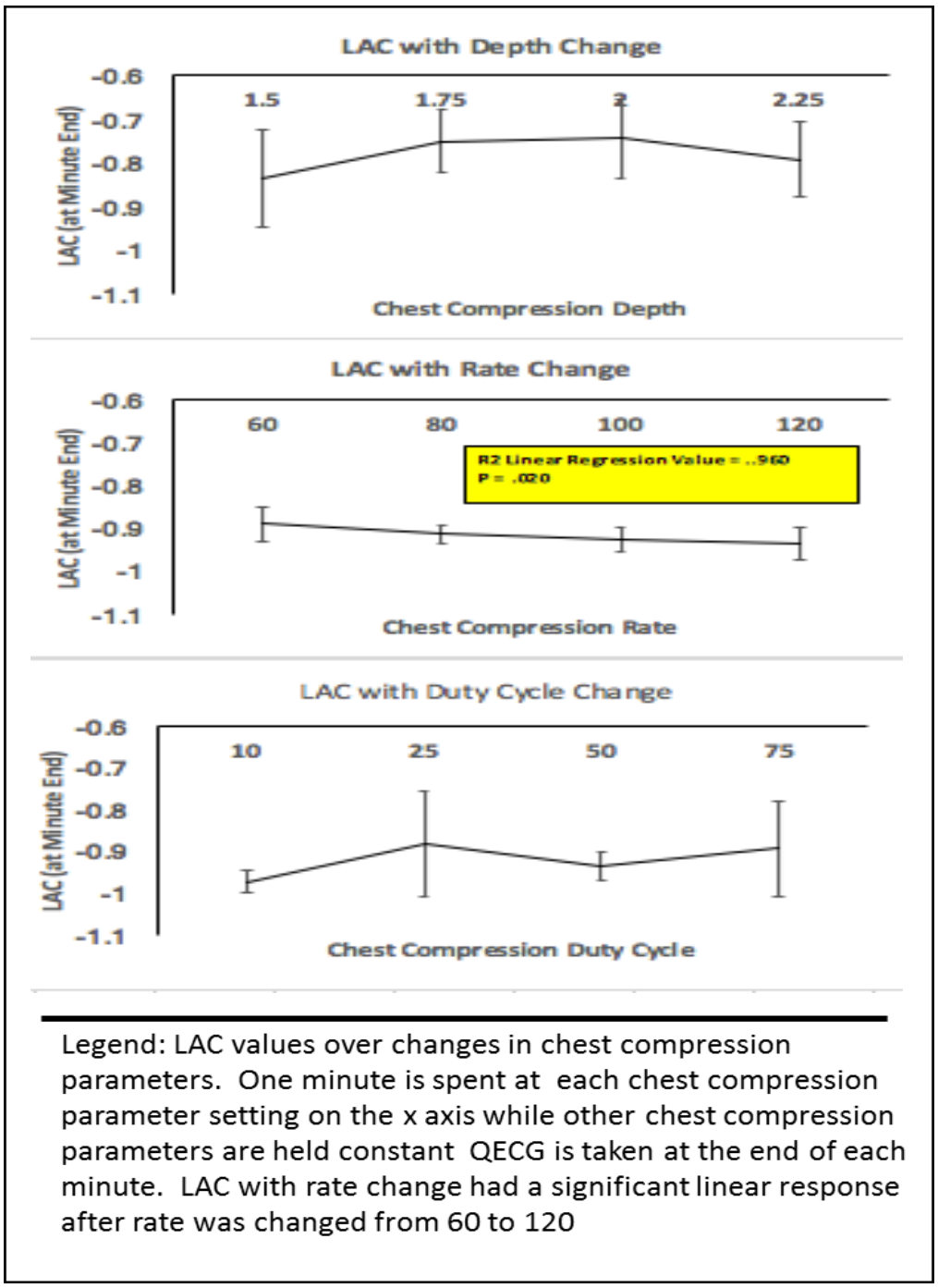


**Figure 27: LAC response to CC changes in Phase 1 (Analysis Approach A)**

In the analysis looking at the change in QECG over minute (Analysis Approach B), no linear regression was significant. The $R^2$ values, p values are shown in Table 5 and Table 6 respectively. The figures for these non-significant results are shown in Appendix B.

**Table 5: R squared values in phase 1, QECG values taken as change over minute**

| Simple Linear Regression P value | | | | | |
|---|---|---|---|---|---|
| dQECG (over minute) | AMSA | MS | CF | LAC | DFA |
| Depth Changes | 0.529 | 0.511 | 0.175 | 0.104 | 0.931 |
| Rate Changes | 0.476 | 0.900 | 0.628 | 0.526 | 0.680 |
| Duty Cycle Changes | 0.516 | 0.485 | 0.899 | 0.459 | 0.998 |

**Table 6: P values in phase 1, QECG taken as change over minute**

| Simple Linear Regreesion R2 Value - Phase 1 | | | | | |
|---|---|---|---|---|---|
| dQECG (over minute) | AMSA | MS | CF | LAC | DFA |
| Depth Changes | 0.222 | 0.239 | 0.680 | 0.803 | 0.129 |
| Rate Changes | 0.275 | 0.010 | 0.139 | 0.225 | 0.039 |
| Duty Cycle Changes | 0.234 | 0.265 | 0.010 | 0.293 | 0.081 |

To summarize the Phase 1 findings, MS, CF, and LAC had significant linear responses when assessing the QECG values at the end of each change in rate (Analysis Approach A). After assessing Phase 1 through the use of change in QECG value over minute (Analysis Approach B), no significant linear response was observed.

The same analysis approach applied to Phase 1 was applied to Phase 2. Phase 2 results are shown for both QECG values taken at minute end (Analysis Approach A) and change over minute (Analysis Approach B).

Analysis Approach A $R^2$ values and p values are shown in Table 7 and Table 8 respectively for phase 2. Plots of significant results are shown in Figure 28 and Figure 29. Plots that show all non-significant results are shown in Appendix B. AMSA responded linearly to changes in chest compression duty cycle and MS responded linearly to changes in chest compression rate. Median

slope values responded as a decreasing linear trend in contrast to a positive linear trend seen in Phase 1. Bars in these graphs are standard deviation.

**Table 7: P values in phase 2, QECG values taken at minute end**

| Simple Linear Regression P value - Phase 2 | | | | | |
|---|---|---|---|---|---|
| QECG (at Minute End) | AMSA | MS | CF | LAC | DFA |
| Depth Changes | 0.881 | 0.537 | 0.944 | 0.831 | 0.741 |
| Rate Changes | 0.137 | 0.046 | 0.647 | 0.583 | 0.455 |
| Duty Cycle Changes | 0.016 | 0.798 | 0.826 | 0.962 | 0.716 |

**Table 8: R squared values in phase 2, QECG taken at minute end**

| Simple Linear Regreesion R2 Value - Phase 2 | | | | | |
|---|---|---|---|---|---|
| QECG (at Minute End) | AMSA | MS | CF | LAC | DFA |
| Depth Changes | 0.014 | 0.214 | 0.003 | 0.029 | 0.060 |
| Rate Changes | 0.744 | 0.911 | 0.124 | 0.174 | 0.040 |
| Duty Cycle Changes | 0.969 | 0.041 | 0.030 | 0.001 | 0.088 |

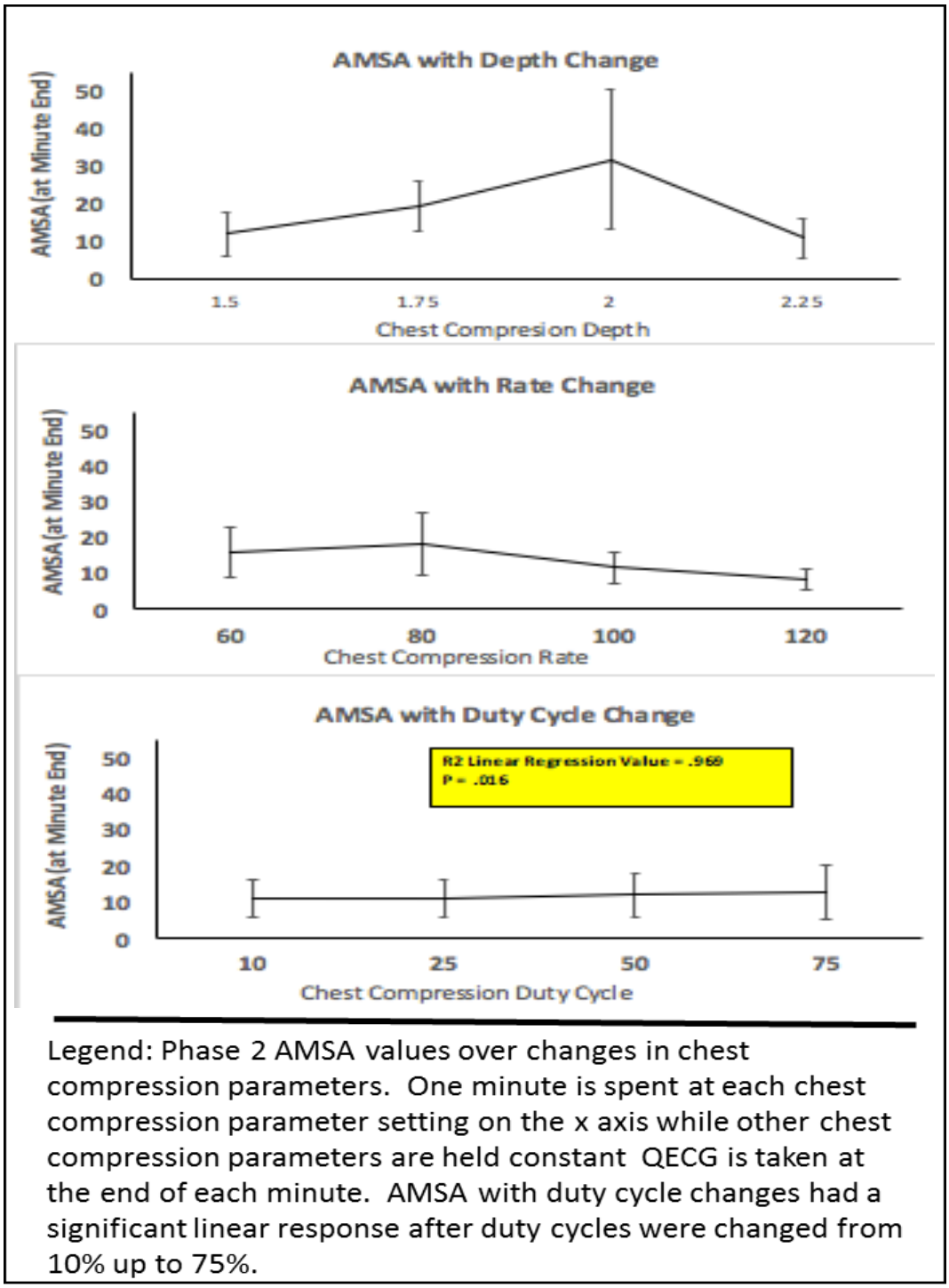


Legend: Phase 2 AMSA values over changes in chest compression parameters. One minute is spent at each chest compression parameter setting on the x axis while other chest compression parameters are held constant QECG is taken at the end of each minute. AMSA with duty cycle changes had a significant linear response after duty cycles were changed from 10% up to 75%.

**Figure 28: AMSA response to CC changes in phase 2 (Analysis Approach A)**

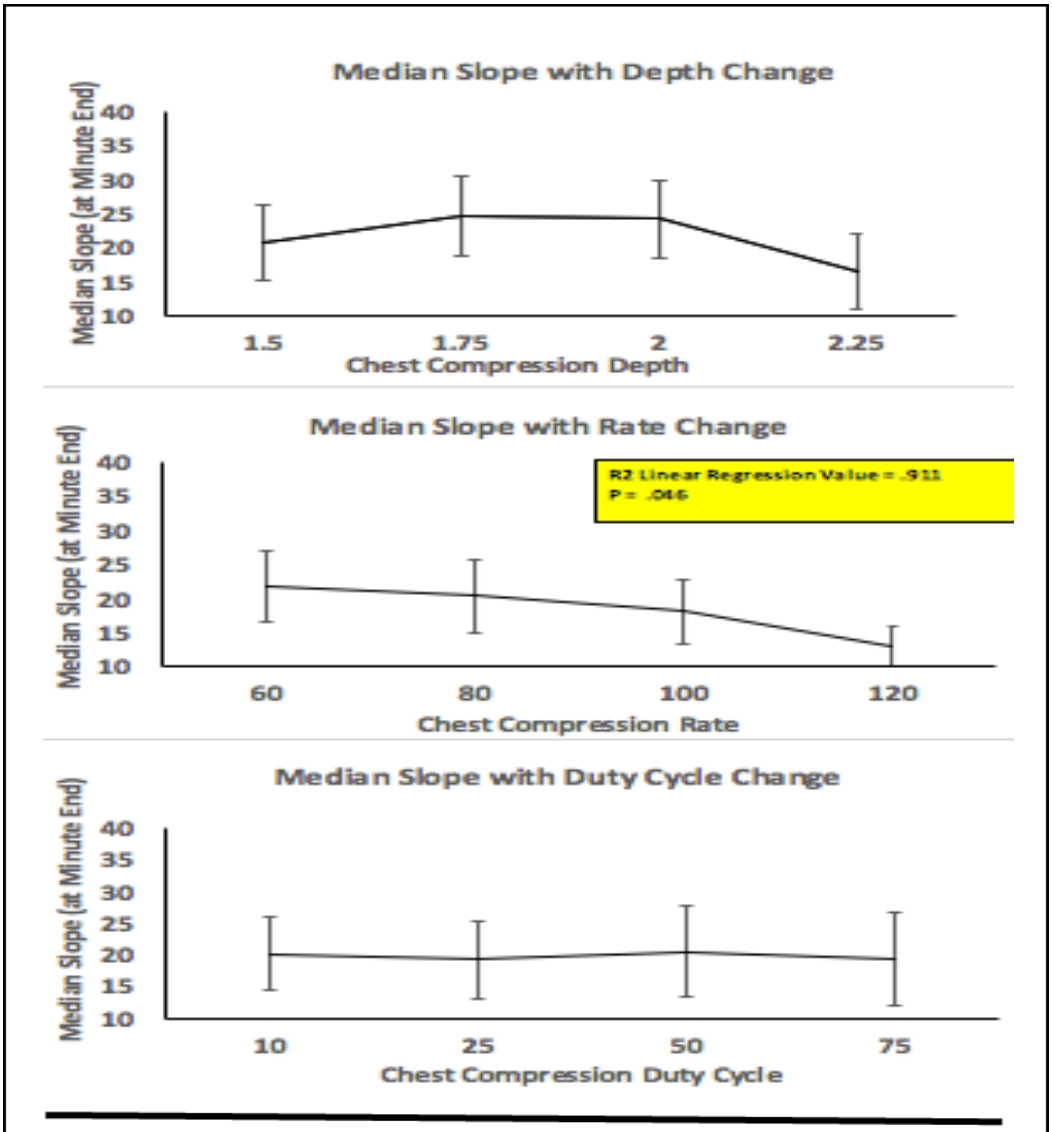


**Figure 29: Median slope response to CC changes in Phase 2 (Analysis Approach A)**

In the Phase 2 analysis for QECG values taken as change over minute (Analysis Approach B), no QECG metric exhibited a linear response to changing chest compression parameters identical to the results observed in Phase 1. These findings are displayed in Table 9 and Table 10.

In summary of the Phase 2 findings, AMSA exhibited a positive linear response to duty cycle changes and MS exhibited a negative linear response to chest compression rate changes. These significant findings were found using the QECG values observed at the end of each minute of chest compression parameter change (Analysis Approach A).

**Table 9: R squared values in phase 2, QECG values taken as change over minute**

| Simple Linear Regreesion R2 Value - Phase 2 | | | | | |
|---|---|---|---|---|---|
| dQECG (over minute) | AMSA | MS | CF | LAC | DFA |
| Depth Changes | 0.106 | 0.002 | 0.761 | 0.449 | 0.084 |
| Rate Changes | 0.586 | 0.842 | 0.002 | 0.189 | 0.108 |
| Duty Cycle Changes | 0.171 | 0.324 | 0.251 | 0.482 | 0.107 |

**Table 10: P values in phase 2, QECG values taken as change over minute (no significance)**

| Simple Linear Regression P value - Phase 2 | | | | | |
|---|---|---|---|---|---|
| dQECG (over minute) | AMSA | MS | CF | LAC | DFA |
| Depth Changes | 0.674 | 0.955 | 0.127 | 0.330 | 0.268 |
| Rate Changes | 0.234 | 0.082 | 0.957 | 0.566 | 0.737 |
| Duty Cycle Changes | 0.586 | 0.431 | 0.499 | 0.306 | 0.324 |

There is no clear indication whether the 'change over minute' approach (Analysis Approach B) or the QECG value taken 'at minute end' (Analysis Approach A) is more appropriate for this analysis. Both were reported and analyzed in an effort to study QECG responses as thoroughly as possible.

There are some limitations in approaching the data with linear regression analysis. While we hypothesize there is likely a 'dose response' in QECG generated by changes in chest

compression parameters, for example increasing chest compression rates would cause a 'dosed' increase in QECG, we are assuming that a dosed response is linear. The reasoning behind this assumption is based on existing evidence from the AHA that recommend a chest compression rate between 100 and 120 compressions per minute for adults, an increase in chest compression rates from 80 to 110 should theoretically produce a positive response in QECG[1]. The reasoning behind a dosed linear response of QECG to chest compression changes is also based on reasoning that extreme values of chest compression parameters such as a chest compression rate of 20 or a chest compression rate of 200 would be the driving contributor to any non-linear response. Extreme values of chest compression parameters were left out of these experiments. The same assumption is made in this analysis for chest compression depths that range from 1.50-2.25 inches and duty cycle values from 10% - 75%.

Analysis of Variance (ANOVA) would be a more appropriate response if non-linearity was assumed and this approach was tested as well. The ANOVA approach to the QECG/chest compression parameter relationships did not produce any significant associations across all QECG and chest compression parameters in both phase 1 and phase 2. Future experiments would likely require studies with greater sample size to increase the power to detect potential differences.

These animal data demonstrate some linear dependence for chest compression rate and select QECG values, whereas this association was not seen for depth and duty cycle. These data are in contrast to the initial simulation data that showed depth was the most influential chest compression variable in a simulated variable population. However, it is noted that the swine used in these studies were similar in size.

Both simulation data and animal data have limitations. The simulation is a simplified model of the circulatory system and may not reflect more complex physiologic responses to

changes in chest compression. Direct comparisons of the results in simulation and animal studies may not be appropriate as different biosignals were measured. The simulation data explored cardiac output response to adaptive CPR whereas the animal model primarily investigated QECG. The decision to investigate QECG in the animal model was influenced by its feasibility of use in an out-of-hospital setting where invasive measures are unavailable.

These initial feasibility, simulation, and animal data provided us with evidence that an adaptive approach to chest compressions in CPR was feasible, and that chest compression rate may influence QECG changes early in cardiac arrest based on the phase 1 animal trial results. The computational model also provided evidence that chest compression depth plays an important role in generating cardiac output in a simulated variable population. Our next goal was to understand the relationship between chest compression changes and QECG in human clinical data.

# 3.0 AIM 2 – TRANSLATION OF FINDINGS TO CLINICAL DATA

The focus of Aim 2 was to translate the findings from Aim 1 collected on computational and animal data to human clinical data. We hypothesized that QECG metrics would be predictive of defibrillation outcome and chest compression parameter rate and depth would be predictive of survival outcomes. We also hypothesized that the change in QECG value before and after durations of chest compression bouts would be linearly dependent on the chest compression parameters within that bout.

## 3.1 CLINICAL DATA FROM ROC TRIALS

The work discussed in Aim 2 of this dissertation is derived from data collected from human cardiac arrest clinical trials. The source of cardiac arrest signal data was the Resuscitation Outcomes Consortium (ROC), a multi-site project that sought to address epidemiologic and clinical questions involving cardiac arrest with the use of randomized controlled clinical trials (Morrison 2008). The ROC Epistry was designed with 11 geographical sites within the US and Canada, which included the Pittsburgh Regional Clinical Center.

Of these 11 sites, the ROC network consisted of 36,000 EMS professionals within 260 EMS systems. This network covered an estimated 24 million people from urban, suburban, and rural communities, and transported patients to 287 different hospitals. (Davis 2007) The ROC provided us with comprehensive patient data that includes such variables as witnessed status, chest compression depth, and hospital discharge outcomes.

For patients to be eligible to be included in the ROC Epistry, they needed to be 18 years or older and have sustained non-traumatic cardiac arrest. The ROC Epistry collected many variables from each cardiac arrest patient, both physiologic and demographic.

## 3.2 SPAIN (SIGNAL PARSING AND INTEGRATION)

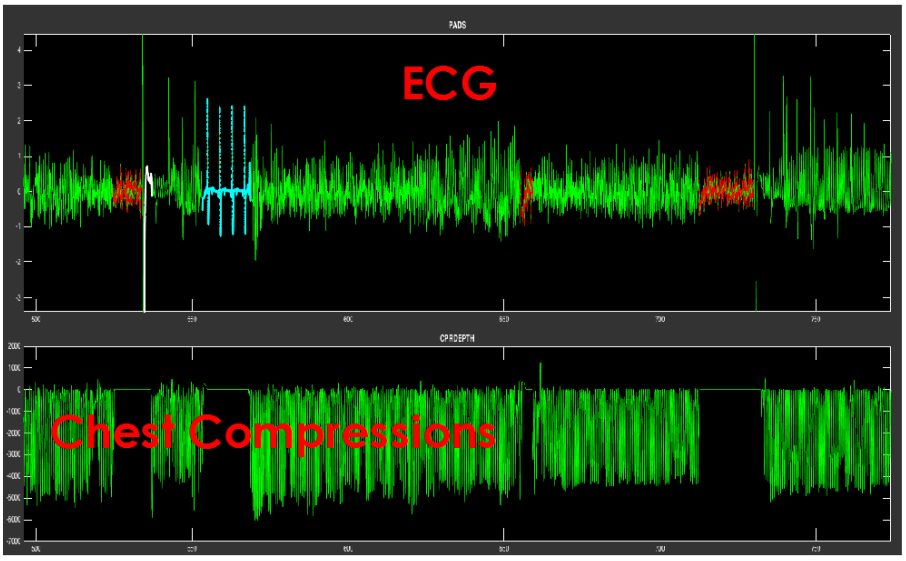


Legend: Custom built graphical user interface capable of displaying both the ECG signal trace and the compression signal trace on the same timescale. The ECG trace is on the top plot where VF segments with compression-free artifact are highlighted in red and PEA segments with compression-free artifact highlighted in blue. The lower plot displays the chest compression signal on a voltage scale convertible to inches.

**Figure 30: Custom graphical user interface**

To better organize the cardiac arrest cases and the type of signals involved, a graphical user interface (GUI) was developed in MATLAB to easily facilitate storage of thousands of hours of

CPR data. This database GUI was developed originally by Dr. David Salcido and named Signal Parser and Integration (SPAIN). A sample screenshot of the SPAIN can be seen in Figure 30.

In SPAIN, each cardiac arrest case integrates observable time-dependent signals that the user can scroll through and search for treatment specific events such as timing and gaps of chest compressions and defibrillation times.

The organization of SPAIN also standardized multiple ECG sources into one continuous signal. This is important in the ECG analyses conducted in the study as it can concatenate ECG data received from different sources (AED or EMS monitor) that are used on the same case. This commonly occurs between the 'hand-off' between the Fire crew that often arrive to the patient first, and the EMS crew who arrive second.

## 3.3 CLINICAL DATA – QECG, CPR, AND OUTCOMES

Following the build-up of the graphical user interface to allow for easy compiling of ROC cases in the shock studies discussed in this work, case data from non-traumatic EMS-treated cardiac arrests from 2011 to 2015, enrolled in the Continuous Chest Compression (CCC) trial conducted by the Resuscitation Outcomes Consortium (ROC), were used and obtained from 7 ROC sites.

The CCC trial compared uninterrupted chest compressions against the historically used 30:2 compression to ventilation ratio approach. Patients in the trial were randomized through an emergency medical services (EMS) agency-level cluster randomization design to receive either 30:2 or CCC CPR.

We sought to first characterize the distribution of QECG and CPR parameters in the clinical dataset, next show traditional relationships of QECG values and CPR parameters to outcomes, then to establish any predictive relationship between QECG and CPR parameters. We hypothesized that some of the QECG metrics would more effectively predict successful shock defibrillation and that specific chest compression parameter values within a cardiac arrest would predict survival outcomes. Successful defibrillation in this study was defined as return of organized rhythm (ROOR). ROOR was determined by visual inspection of the ECG signal directly following the shock attempt. A positive ROOR finding was determined if the morphology of the ECG in the post shock period resembled an organized rhythm capable of perfusion.

### 3.3.1 QECG and CPR Relationship to Outcomes

The first step in analyzing clinical QECG and CPR parameters in the second aim of the work was to establish relationships between preshock QECG and shock outcome as well as chest compression parameter values and survival. These relationships have been described in past literature from separate clinical trials, but not in our dataset. It was hypothesized that QECG values would have a predictive relationship with shock outcome. It was also hypothesized the rate and depth chest compression parameters would be predictive of survival outcome.

We examined cardiac arrest cases from the ROC Continuous Chest Compression trial (CCC) to establish relationships between QECG metrics directly before every shock. All ECG data were obtained from prehospital EMS-treated cardiac arrests from 2011 to 2015 that were enrolled in the CCC trial. These data were obtained from 7 ROC sites. Data were downloaded from monitors using manufacturer software. Signal data were then extracted from the downloaded files using a custom MATLAB program (Mathworks Inc, Natick, MA).

These next sections discuss prediction models for two sub-analyses within the CCC dataset. In the first sub-analysis, QECG available before a shock as well as available demographic data are assessed for their ability to predict ROOR. The other sub-analysis characterized chest compression parameters within a cardiac arrest case and its ability, along with demographic data, to predict survival.

#### 3.3.1.1 Methods

ECG and CPR process waveforms were extracted from electronic defibrillator files through a custom-built MATLAB (Mathworks Inc., Natick, MA) program. The preshock interval for each shock was automatically isolated for analysis from all identified shocks of the cases that had complete ECG records. An example of one such preshock pause is shown in the left side of Figure 25 before the ECG spike due to defibrillation. Pre-shock QECG measures, including AMSA, MS, CF, LAC, and DFA were calculated in all available 3 second segments preceding defibrillation and averaged, excluding segments with compression artifact. Compression artifact was assessed in the preshock ECG both by visual inspection, and by exclusion of non-physiologic AMSA values within the ECG (AMSA values greater than 100). To ascertain whether there was successful defibrillation, ROOR was assessed by visual inspection of the ECG during the largest compression gap in a three-minute period post defibrillation. If there were no gaps in chest compressions for three minutes post shock, ROOR was assessed to be unsuccessful.

QECG metrics were calculated as the mean of all available consecutive 3 second ECG segments that were free of compression artifact. All available, artifact free ECG was used by analyzing the last compression before the shock. If there were no compressions before the shock, the last available 5 seconds were used for analysis. Metrics included in all shock studies included

AMSA, MS, CF, DFA, and LAC. All QECG metrics were calculated identically to those in the swine studies in Aim 1 according to Figures 5-9.

CPR parameters were calculated using MATLAB code to automate extraction of bouts of CPR. Parameters collected included chest compression rate, chest compression depth, chest compression duty cycle, duration of the chest compression bout, and chest compression fraction.

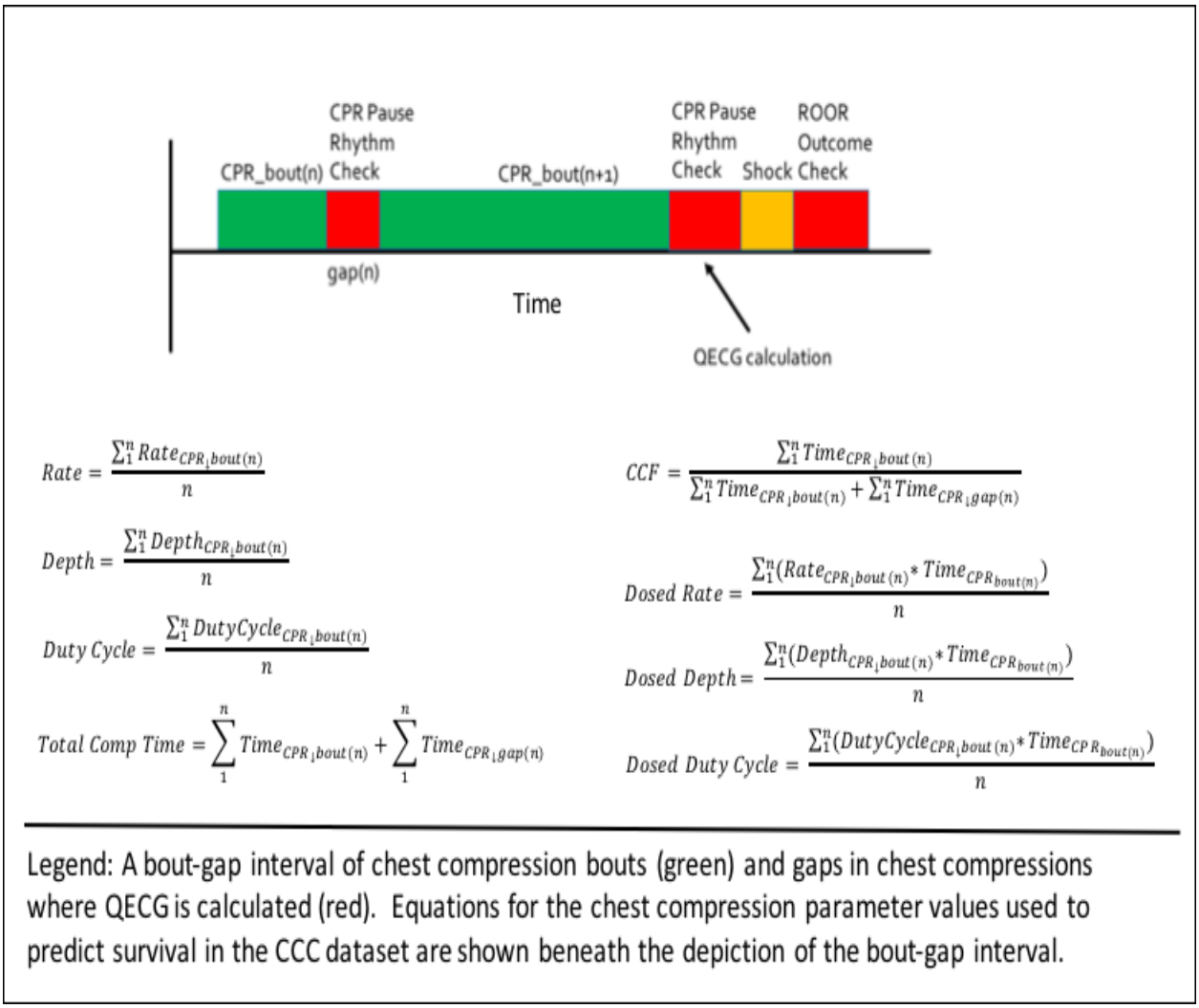


**Figure 31: Equations for chest compression parameters**

A ‘dosed’ version of rate, depth, and duty cycle was also calculated by multiplying the rate, depth, or duty cycle of a bout, by its respective bout duration. We felt that this ‘dosed version’ would account for any time dependency not explained by rate, depth, or duty cycle independent of themselves. Equations of how each parameter was calculated as well as visual representations of what they characterize can be seen in Figure 31. The chest compression parameter used in the prediction model for survival, was the average parameter across the entire case. For example, chest compression depth when used as a predictor in the survival model was average chest compression depth during resuscitation. Time dependent chest compression variables such as chest compression rate excluded gaps in compressions greater than 2 seconds as well as pauses for defibrillation attempts.

Survival to hospital discharge was ascertained by data extractors reviewing prehospital and hospital records for each case. Cases were excluded from survival calculations if outcomes were missing. Logistic regressions were performed with STATA (StataCorp LP, College Station, TX). Mixed effect univariate logistic regression was performed on QECG data to predict shock outcome (ROOR). A multivariate mixed-effect model was performed as well for QECG and ROOR outcome. Both univariate and multivariate logistic regressions were performed for CPR parameters and survival outcome.

Receiver operator curves (ROC) were generated for QECG prediction of ROOR as well as QECG prediction of survival. The first available QECG value was used for survival prediction. DeLong's comparison test was used to test the null hypothesis that the area beneath the curve (AUC) among the five QECG predictors would be the same. DeLong's test was used both for ROOR prediction and survival prediction. [77]

After AUC similarity across all QECG predictors were tested Delong's test was performed again for the metrics that performed the best in the initial analysis that contained all five QECG predictors. This secondary analysis was used in both QECG prediction of ROOR and first available QECG prediction of survival.

### 3.3.1.2 Results

4,297 total shocks were found in 1,573 unique OHCA cases. ROOR rate per shock was 20.9% and overall survival was 12.99%. Survival data were available in 1,255 cases and depth data were available in 257 cases containing 787 individual shocks. Histogram distributions of the

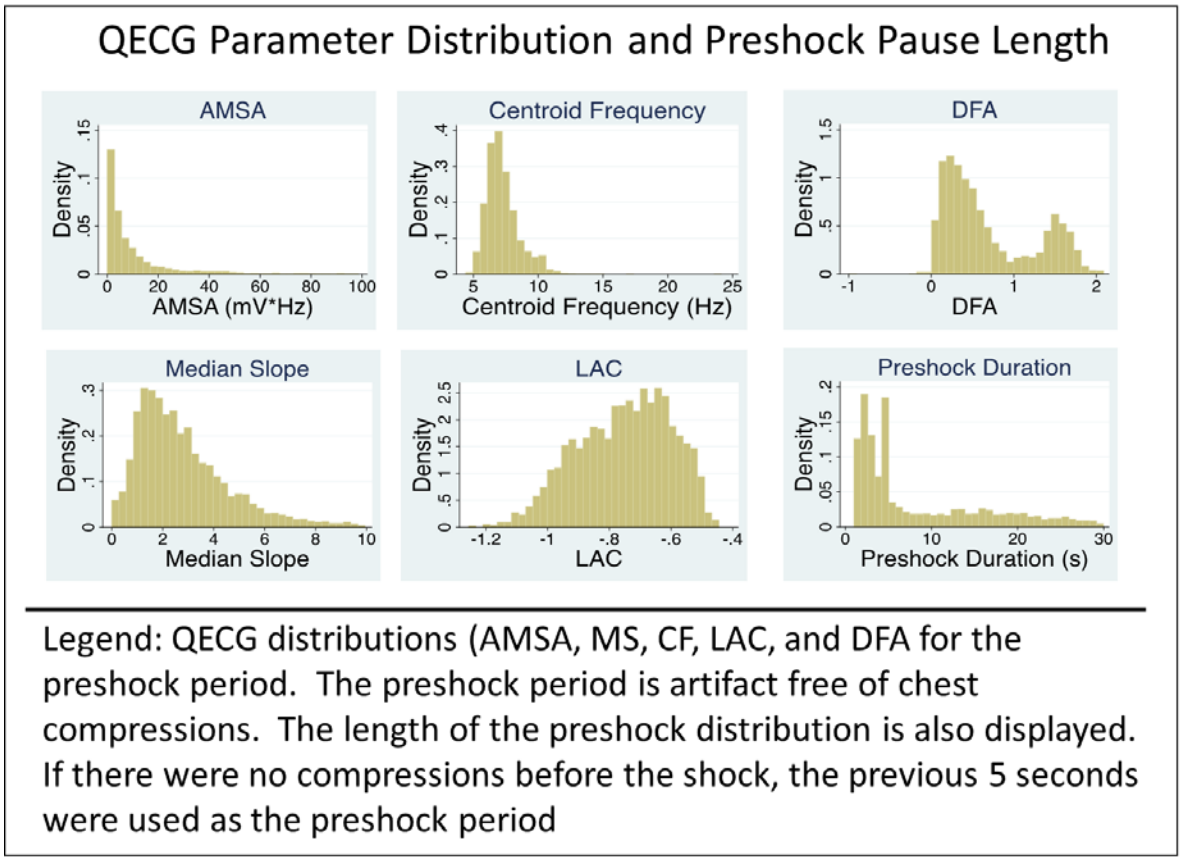


**Figure 32: QECG parameter distribution**

QECG parameter distribution data and chest compression parameter distribution can be seen in Figure 32 and Figure 33 respectively.

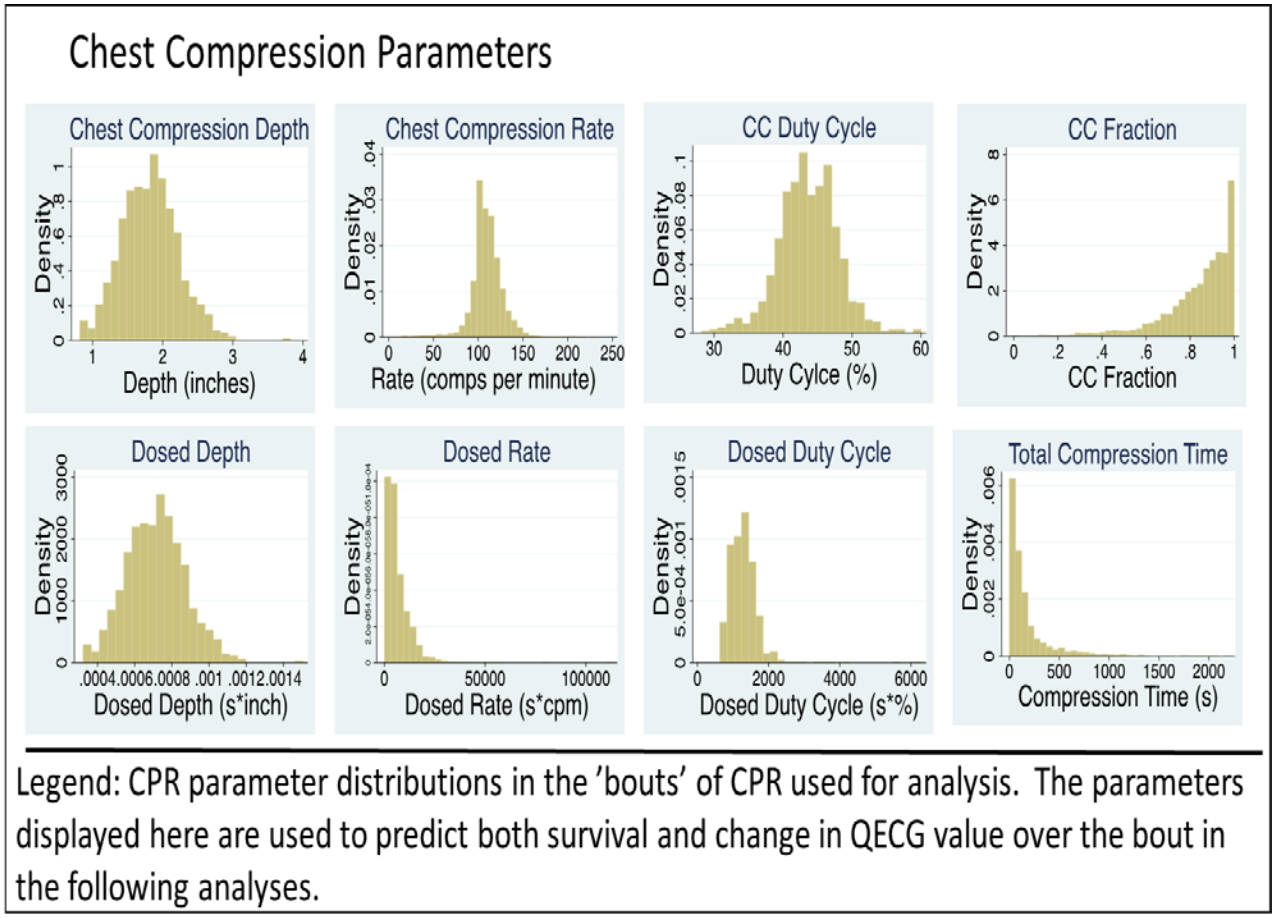


**Figure 33: Chest compression parameter distribution**

Demographic data were first assessed in the QECG-ROOR dataset to test their predictive ability independent of QECG predictors. It was hypothesized that a positive witnessed status and younger age would be associated with ROOR. Mixed effect logistic regression model was used and results are displayed in Table 11. Age and the first rhythm being a shockable VF or VT were the only significant predictors of ROOR. Interestingly, an older age was associated with a higher likelihood of ROOR.

**Table 11: Demographic logistic regression for ROOR in CCC cases with shocks**

| Mixed Effect Logistic Regression ROOR Outcome - Demographic Univariate Analysis | | | | | |
|---|---|---|---|---|---|
| Variable in Model | z value | Odds Ratio | CI Lower Bound 95% | CI Upper Bound 95% | P value |
| Bystander Witnessed | 0.3900 | 1.5080 | 1.2920 | 1.7610 | 0.694 |
| Age | 2.6100 | 1.0120 | 1.0020 | 1.0200 | 0.009 |
| Sex | -1.9400 | 0.7530 | 0.5650 | 1.0020 | 0.052 |
| Bystander CPR | 1.0800 | 1.1403 | -0.1075 | 0.3701 | 0.281 |
| First rhythm VF/VT | 5.4670 | 3.4620 | 2.2180 | 5.4030 | p<.0001 |

Legend: Demographic data was used to predict ROOR using a univariate mixed effect logistic regression. The mixed effect approach controlled for multiple shocks within the same patient. The strongest predictor of ROOR was VF/VT status. A slightly higher age was predictive of ROOR however in further analyses, a higher age was predictive of decreased survival as expected.

Next, univariate mixed logistic models were performed for all five QECG predictors for ROOR. These regression analyses were performed on the first CCC dataset sub-analysis described above that includes preshock QECG values paired with its subsequent ROOR assessment. To confirm agreement with evidence from past QECG studies and literature which described associations between QECG value and shock outcome, we hypothesized that all five QECG predictors would be significantly predictive of ROOR. We used a mixed effect logistic regression

approach that controlled for multiple shock attempts and ROOR outcomes within the same cardiac arrest case. Demographic data were left out of these initial QECG univariate models in order to observe QECG prediction of ROOR solely based on the quantifiable VF properties. The results of the univariate analyses are shown in Table 12. All five QECG metrics were significantly predictive of ROOR. Collinear analysis conducted in STATA showed that the the greatest correlation coefficient among the QECG predictors as .5425. We therefore treated each QECG metric independently.

**Table 12: Mixed-effect univariate logistic regression for ROOR based on QECG value**

| Mixed Effect Logistic Regression ROOR Outcome - Univariate Analysis | | | | | |
|---|---|---|---|---|---|
| QECG Predictor Variable | z value | Odds Ratio | CI Lower Bound 95% | CI Upper Bound 95% | P value |
| AMSA | 5.9500 | 1.0170 | 1.0120 | 1.0240 | p<.0001 |
| MS | 9.6900 | 1.3140 | 1.2440 | 1.3890 | p<.000 |
| Centroid Frequency | -3.4100 | 0.8670 | 0.7980 | 0.9410 | 0.001 |
| LAC | -5.4100 | 0.1400 | 0.0690 | 0.2860 | p<.0001 |
| DFA | -4.2900 | 0.5460 | 0.4150 | 0.7210 | p<.0001 |

Legend: Univariate mixed effect logistic regression was used to predict ROOR using QECG metrics. The mixed effect approach controlled for multiple shocks within the same patient. All five QECG metrics demonstrated strong predictive abilities for ROOR as expected.

To follow up on the univariate models of ROOR prediction by QECG metrics, a multivariate logistic regression was performed that combined all five QECG metrics. It was hypothesized that some of the QECG metrics in the univariate analysis would drop out or become insignificant when included in the multivariate model. The multivariate model results are shown in Table 13.

Inclusion of variables into multivariate models was defined at a significance level of p <.15. In the multivariate model, centroid frequency dropped out of the model with a p value of .713. Possible contributing factors for the inferiority of the centroid frequency QECG predictor in the multivariate model include the absence of an amplitude component in the centroid frequency metric.

**Table 13: Mixed-effect multivariate logistic regression for ROOR based on QECG value**

| Mixed Effect Logistic Regression ROOR Outcome - Multivariate Analysis | | | | |
|---|---|---|---|---|
| Variable in Model | z value | CI Lower Bound 95% | CI Upper Bound 95% | P value |
| AMSA | 2.1000 | 0.0073 | 0.0217 | 0.036 |
| MS | 5.7000 | 0.1912 | 0.3919 | p < .0001 |
| Centroid Frequency | -0.3700 | -0.1465 | 0.1002 | 0.713 |
| LAC | -1.8000 | -2.0950 | 0.0919 | 0.073 |
| DFA | -3.8000 | -0.9661 | -0.3086 | p < .0001 |

Legend: Multivariate mixed effect logistic regression was used to predict ROOR using QECG metrics. The mixed effect approach controlled for multiple shocks within the same patient. AMSA, MS, and DFA were the strongest predictors of ROOR in the multivariate model. LAC was near significant and CF dropped out of the model after being significant in the univariate model. Possible reasons for CF losing significance could include its absence of an amplitude component, however this is unclear.

After analyzing the first CCC subanalyses concerning QECG prediction of ROOR, the following regression models were performed using the second CCC data subanalyses which covered chest compression parameter values averaged over the course of an entire cardiac arrest case and matched to each case's survival outcome. Univariate logistic regression analysis was again performed for chest compression parameters and their predictive ability of survival. Past literature suggested evidence that demographic data, witnessed status, and chest compression rate

and depth would influence survival outcome.[1] We hypothesized that both these chest compression parameters would be predictive of survival. Demographic predictors are first shown in Table 14 independent of chest compression parameter predictors.

**Table 14: Demographic logistic regression for survival**

| Logistic Regression Survival Outcome - Demographic Univariate Analysis | | | | | |
|---|---|---|---|---|---|
| Variable in Model | z value | Odds Ratio | CI Lower Bound 95% | CI Upper Bound 95% | P value |
| Bystander Witnessed | 2.4900 | 1.2490 | 1.0490 | 1.4870 | 0.013 |
| Age | -4.8900 | 0.9830 | 0.9771 | 0.9901 | p<.0001 |
| Sex | 0.4400 | 1.0530 | 0.8380 | 1.3230 | 0.657 |
| Bystander CPR | 1.3600 | 1.1330 | 0.9466 | 1.3560 | 0.173 |
| First rhythm VF/VT | 9.2300 | 8.1601 | 5.2260 | 12.7410 | p<.0001 |

Legend: Demographic data was used to predict survival using a univariate logistic regression. The strongest predictors of survival was VF/VT status and decreased age. Being witnessed by a bystander also increased the odds for survival.

The demographic analysis showed that increasing age significantly decreased the likelihood of survival when controlled for bystander witness status and sex. This finding was in contrast to the QECG-ROOR data subset that showed that increasing age increased the likelihood of ROOR. A confirmed bystander witness status was significantly associated with an increased likelihood of survival when controlled for age and sex. Sex was not significantly predictive of survival. Having a first rhythm that was shockable was also predictive of survival.

Following the analysis using solely demographic data to predict survival, univariate logistic regression models for all chest compression parameters and their predictive ability of survival were assessed. The results of the univariate models of chest compression parameter prediction of survival are shown in Table 15.

**Table 15: Univariate logistic regression for survival outcome based on CPR parameters**

| Logistic Regression Survival Outcome - Univariate Analysis | | | | | |
|---|---|---|---|---|---|
| CPR Predictor Variable | z value | Odds Ratio | CI Lower Bound 95% | CI Upper Bound 95% | P value |
| CC Rate | -2.3900 | 0.9868 | 0.9762 | 0.9976 | 0.0170 |
| CC Depth | 0.4600 | 1.0001 | 0.9997 | 1.0006 | 0.6450 |
| CC Duty Cycle | 1.0500 | 1.0700 | 0.9426 | 1.2148 | 0.2950 |
| CC Fraction | 1.2100 | 2.2924 | 0.5976 | 8.7941 | 0.2270 |
| CC Bout Duration | -6.5300 | 0.9979 | 0.9973 | 0.9985 | p<.0001 |
| CC Rate Dose | -1.3900 | 0.9999 | 0.9999 | 1.0000 | 0.1650 |
| CC Depth Dose | 0.7100 | 1.0000 | 0.9999 | 1.0000 | 0.4810 |
| CC Duty Cycle Dose | 0.0000 | 1.0000 | 0.9984 | 1.0016 | 0.9970 |

Legend: Univariate logistic regression was used to predict ROOR using chest compression metrics. Only average chest compression rate and average chest compression bout duration were significantly predictive of survival. No multivariate model was performed after only two significant univariate predictors were found in the univariate models.

Compression rate and average chest compression bout duration were predictive of survival. Older age also was found to lower the likelihood of survival. These data align with previous findings in the literature that show that chest compression rate is an important predictor of outcomes[31]. Chest compression depth however was not significantly predictive of survival in our models.

In the final model, both CC parameter and demographic data were used in a multivarariate logistic approach to predict survival. Only variables that were significant in the univariate models ($p<.05$) were used in the multivariate model. These results are shown in Table 16. The results demonstrate that when controlling for demographic data, chest compression rate drops out of the predictive model leaving only chest compression bout duration as a significant predictor of

survival. The large effect of VF/VT status at first rhythm seemed to have largely blunted any effect CC rate had on survival outcomes.

**Table 16: Multivariate logistic model for survival using CC parameter and demographic data**

| Logistic Regression Survival Outcome - CC Parameter and Demographic Multivariate Analysis | | | | | |
|---|---|---|---|---|---|
| Variable in Model | z value | Odds Ratio | CI Lower Bound 95% | CI Upper Bound 95% | P value |
| CC rate | -1.3400 | 0.9926 | 0.9819 | 1.0030 | 0.180 |
| CC Bout Duration | -3.7200 | 0.9975 | 0.9962 | 0.9988 | p<.0001 |
| First Rhythm VF/VT | 5.8100 | 5.4750 | 3.0840 | 9.7203 | p<.0001 |
| Age | -3.4900 | 0.9790 | 0.9680 | 0.9910 | p<.0001 |
| Bystander Witnessed | ommitted for collinearity | | | | |

Legend: Multivariate logistic regression model that included both demographic data and chest compression parameter data that were significant in the univariate models of survival prediction. After controlling for demographic data CC rate dropped out of the predictive model leaving only CC Bout Duration as a significant CC parameter predictor of survival

A ROC curve was generated for the multivariate model that incorporated both chest compression predictor variables and demographic predictor variables. This curve is shown in Figure 34. The multivariate model produced an area under the curve (AUC) value of .7488. The multivariate logistic regression and ROC curve demonstrate that survival can be predicted using both demographic and chest compression parameter data.

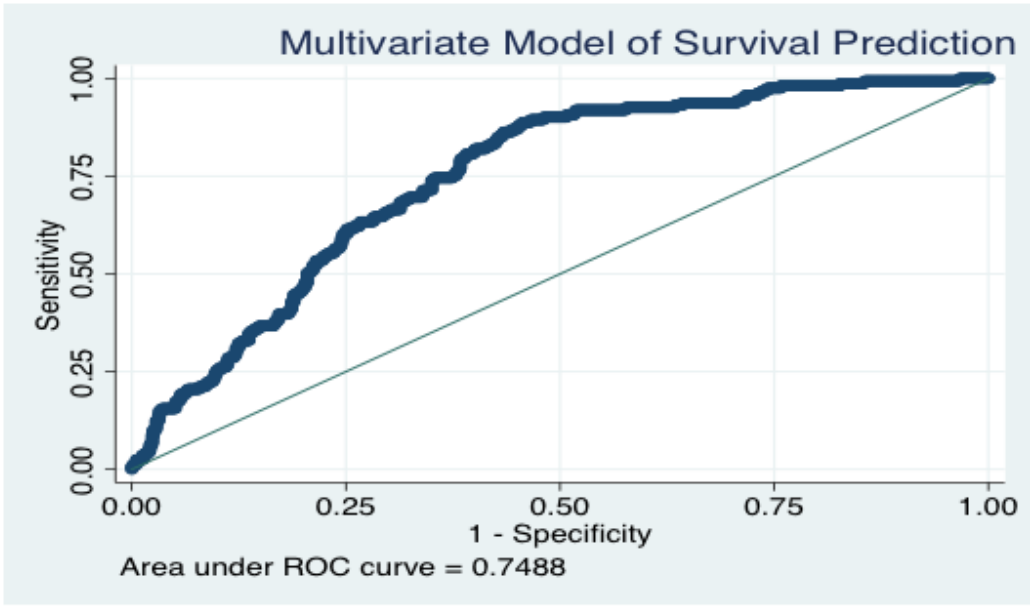


Legend: ROC curve for the multivariate logistic regression model that included both demographic data and chest compression parameter data that were significant in the univariate models of survival prediction. Predictor variables in the model includes chest compression rate, chest compression bout duration, VF/VT status, and age.

**Figure 34: ROC curve for multivariate model of survival prediction**

To visualize the QECG metrics' ability to predict outcomes ROC curves were constructed for QECG prediction of ROOR as well as first QECG assessed in the cardiac arrest case and its prediction of survival. Delong's comparison test was performed to assess similarity among area under the curve (AUC) values[77]. A large value of AUC indicates a strong predictive ability in reference to sensitivity and specificity properties. These results and plots are shown in Figure 35 and Figure 36 respectively.

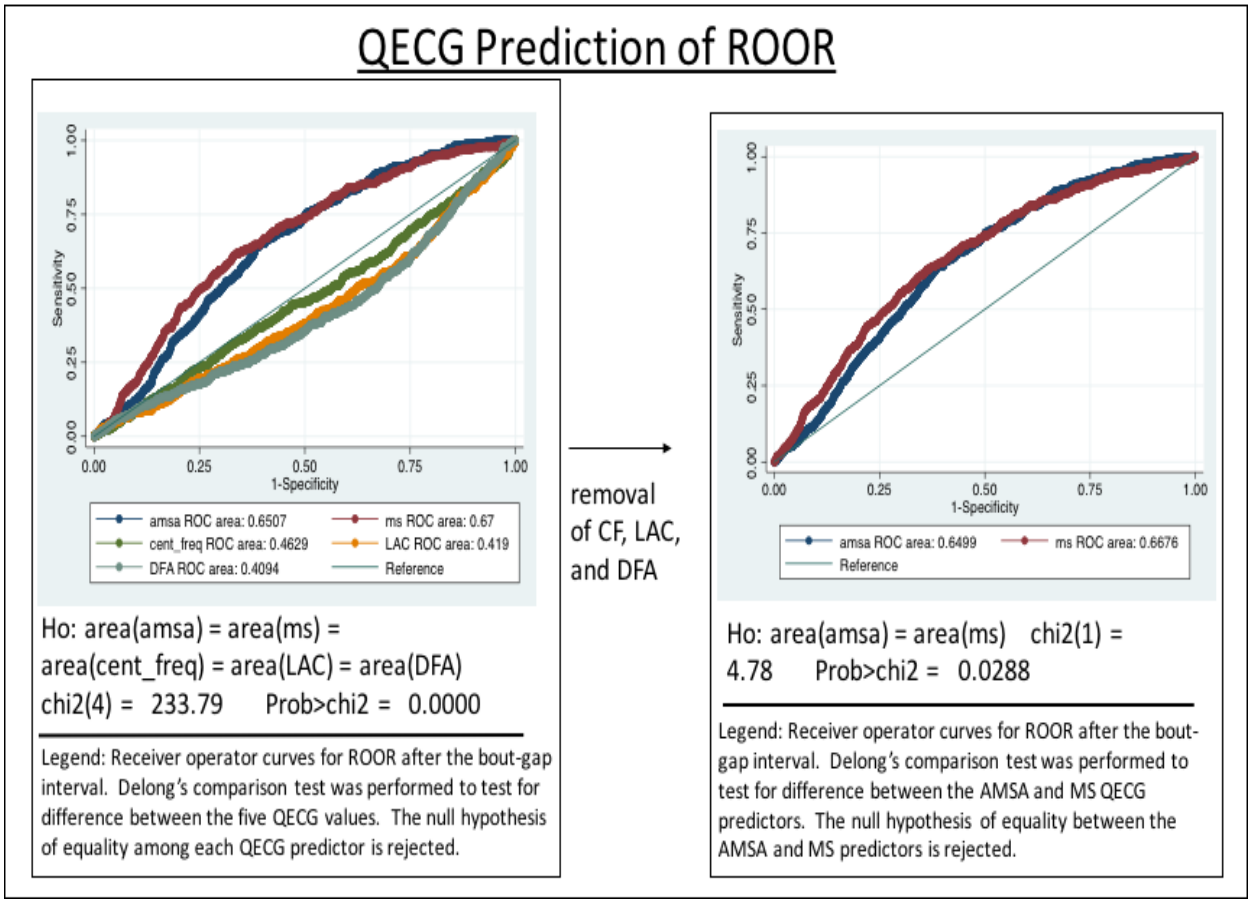


**Figure 35: QECG prediction of ROOR**

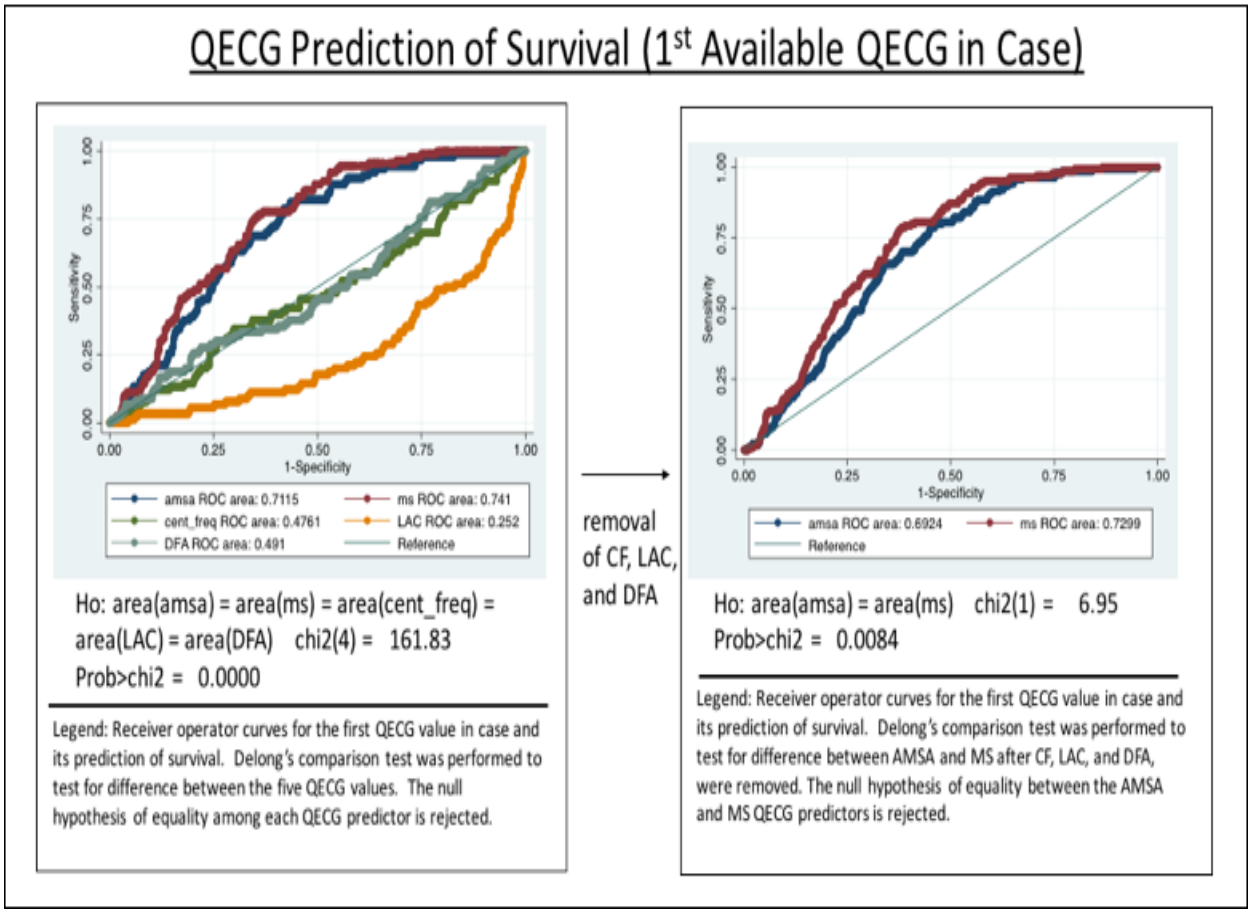


**Figure 36: First QECG prediction of survival**

#### 3.3.1.3 Discussion of ROOR and Survival Prediction Results

The outcome measurements of ROOR and survival paired with logistic regression models performed demonstrate the predictive ability of QECG metrics for ROOR and chest compression variables for survival. All QECG values were strongly predictive of ROOR, however only chest compression rate and bout duration time were predictive of survival.

The receiver operator curve analysis demonstrates that the AMSA and MS QECG metrics were the strongest predictors of ROOR. The AUC of CF, LAC, and DFA when compared to the AUC of AMSA and MS were lower in the initial ROC analysis. In the secondary ROC analysis in which the CF, LAC, and DFA metrics were removed, there was no significant difference in ROOR predictive ability of AMSA and MS. The cause of the inferiority of CF, LAC, and DFA in these predictions when compared to AMSA and MS is unclear. A possible reason for their underperformance in prediction may involve the composition of VF characteristics each metric encompasses. The AMSA and MS metrics may more comprehensively capture the relevant VF changes that reflect coronary perfusion, prediction of ROOR, and prediction of survival.

These initial studies involving QECG prediction of ROOR and chest compression parameter prediction of survival studies are limited in a number of ways. Our use of ROOR to characterize successful cardioversion of VF is disadvantaged in that it has the possibility of classifying ROOR as PEA. In this scenario ROOR is classified as a favorable outcome but is actually non-pulsatile and unfavorable. Return of spontaneous circulation (ROSC) would be the most desirable shock outcome, but we could not decisively determine ROSC status without verbal confirmation of a pulse being palpated by the medics. We did not have any available audio records, therefore we used ROOR as our shock outcome variable. Another limitation in the study is the

lack of available long term survival status. We are also limited in the number of cases that did not have depth data.

### 3.3.2 Change in QECG (dQECG) in Response to CPR Parameters

After demonstrating the predictive ability of QECG for shock outcomes and CPR parameters for survival outcomes, we sought to next establish relationships between the QECG and chest compressions parameters. This would help 'complete the loop' of feedback between biosignals (QECG) and CPR parameters that our adaptive CPR device is based on.

The hypothesis in these analyses was that changes in QECG metrics over bouts of chest compressions would respond to specific chest compression parameter values such as chest compression rate, chest compression depth, or chest compression duty cycle. Cumulative factors of these parameters were also considered by using 'dosed' versions of the chest compression metrics that took into account the time length of each bout in addition to its average parameter value across the bout. Both univariate and multivariate models containing chest compression parameters as well as demographic data were used in models to predict change in QECG values

#### 3.3.2.1 Methods

To translate the QECG and chest compression parameter findings from the animal lab to our clinical data, an analysis was conducted again on the CCC trial clinical data. We hypothesized that some chest compression variables would be predictive of change in QECG (dQECG) values over periods of CPR.

Case data from the CCC trial were included in this analysis only if chest compression data were available, allowing us to look at rate, depth, and duty cycle parameters. 1,099 cases from the

CCC trial met these criteria, producing 25,210 bout-gap intervals. A representative example of a bout-gap interval is shown in Figure 37.

We defined each dQECG using available bout-gap intervals in the CCC case data. Bout-gap intervals were defined as time periods of CPR, uninterrupted by shock attempts, that included time intervals of CPR, 'bouts', and time intervals of breaks in CPR greater than two seconds, 'gaps'. An example bout-gap interval can be seen in Figure 37. Gaps in this dataset had to be at least two seconds long. Each dQECG represented the difference between the QECG value in a 2 second window immediately after the CPR bout and a QECG value in a 2 second window immediately before the CPR bout.

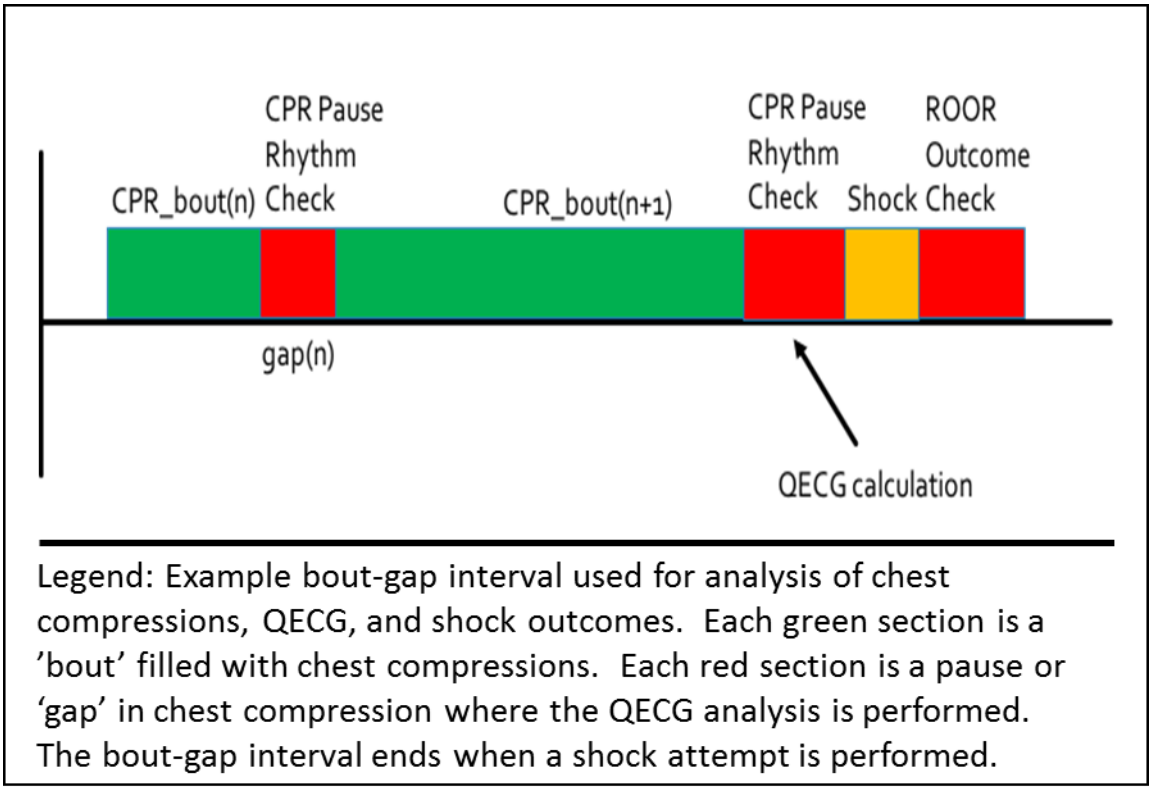


Legend: Example bout-gap interval used for analysis of chest compressions, QECG, and shock outcomes. Each green section is a 'bout' filled with chest compressions. Each red section is a pause or 'gap' in chest compression where the QECG analysis is performed. The bout-gap interval ends when a shock attempt is performed.

**Figure 37: Example bout-gap interval**

Chest compression parameters were again calculated according to the equations in Figure 31, and QECG values were calculated according to the equations in Figures 5-9, identical to methods used in previous analyses described in this work.

In order to automate the process of extracting bout gap-intervals, an algorithm that distinguished VF ECG signals from other signals such as asystole, PEA or noise was needed. In collaboration with Dr. David Salcido, an algorithm was developed that uses logistic regression based on coefficients derived from a variety of ECG signal characteristics. To validate the algorithm, a test set of gaps in the ECG clinical data containing visually confirmed VF (visual confirmation being the 'gold standard') was used and it was found that the algorithm correctly identified the visually confirmed VF segments 98% of the time.

### 3.3.2.2 Models and Results

Using data obtained from 25,210 bout-gap intervals, univariate linear regression mixed models were used for each change in QECG metric (dAMSA, dMS, dCF, dLAC, and dDFA). The results of these models are shown in Table 17 where the coefficient is displayed along with its significance p value. A significance threshold was set to $p < .15$ and highlighted as yellow.

**Table 17: dQECG univariate analysis results (yellow shade p <.15)**

| dQECG Outcome - Univariate Analysis - Linear Mixed Model - Coeff (p value) | | | | | |
|---|---|---|---|---|---|
| CPR parameter | dAMSA | dMS | dCF | dLAC | dDFA |
| CC Rate | .034 (.072) | 5.15 (.116) | 2.72e-3 (.245) | -1.34e-4 (.525) | 7.11e-7 (.940) |
| CC Depth | -.180 (.700) | 39.16 (.622) | -.033 (.559) | -4.77e-7 (.999) | -.023 (.227) |
| CC Duty Cycle | .008 (.822) | -1.15 (.846) | 7.44e-3 (.081) | -1.88e-4 (.625) | 1.06e-9 (.843) |
| CC Bout Length | -.008 (.145) | -1.38 (.126) | -5.59e-4 (.387) | -3.85e-5 (.508) | 8.34e-5 (.704) |
| CC Rate Dosed | -1.82e-6 (.099) | -2.23e-4 (.226) | -1.15e-7 (.386) | -6.70e-9 (.574) | -8.80e-9 (.843) |
| CC Depth Dosed | -6.88e-5 (.170) | -.013 (.1209) | -4.74e-6 (.434) | -4.36e-7 (.422) | 7.12e-7 (.726) |
| CC Duty Cycle Dosed | -1.80e-4 (.143) | -.031 (.136) | -1.10e-5 (.461) | -1.07e-6 (.426) | 1.06e-6 (.833) |
| CC CCF | 2.03 (.105) | -151.4 (.477) | .151 (.324) | 6.03e-4 (.965) | -.061 (.234) |
| Time from CC Start | 3.49e-8 (.794) | -4.97e-6 (.827) | -3.32e-9 (.839) | -1.55e-10 (.916) | 3.04e-9 (.579) |
| Age | -1.47e-4 (.921) | -.222 (.929) | 1.04e-3 (.564) | -1.63e-4 (.313) | 5.58e-4 (.355) |
| Sex | .121 (.788) | 53.11 (.489) | -.055 (.321) | -2.80e-3 (.571) | 8.89e-4 (.630) |

Legend: Univariate linear mixed models reported as predictor coefficient and p value for each dQECG outcome (dAMSA, dMS, dCF, dLAC, and dDFA). In each model, the patient variable is held as a random effect contributor to account for clustering of shocks within one patient. Univariate predictors shaded yellow are significant with a cutoff of $p < .15$. The most clinically significant predictors are CC rate for dMS (for every unit change in CC rate, dMS will increase 5.15) and CC CCF for dAMSA (for every unit increase in CC CCF, dAMSA will increase by 2.03). These results are limited by their assumption of linearity in the relationship between chest compression parameter and change in QECG over a bout-interval.

The univariate models give evidence that the dQECG responses of dAMSA and dMS appear to respond linearly to a larger number of chest compression variables. The other QECG predictors dCF, dLAC, and dDFA did not produce such a robust response to chest compression parameter changes over bout-gaps. The only chest compression parameter that induced a linear

response in dCF was chest compression duty cycle, while dLAC and dDFA did not respond linearly to any chest compression parameter.

It appears from the univariate logistic models that dMS in response to chest compression rate changes may have the most clinically meaningful response. The coefficient in this model informs that for every unit increase in chest compression rate, dMS will increase by 5.15 units.

The univariate models are limited in their assumption that the dQECG response to any chest compression parameter change is linear. Extreme chest compression values may exhibit a parabolic response in dQECG. To account for this a parabolic mixed effect logistic model was then fit to the bout-gap data. The results of this parabolic model are shown in Table 18. Chest compression rate was tested as this chest compression parameter appeared to be most parabolic in nature from past literature by the work of Idris et al. (Section B in Figure 2). In this model, neither the linear predictor rate, nor the parabolic predictor rate squared, were significantly predictive of any dQECG metric.

**Table 18: Parabolic mixed model with CC rate as predictor for dQECG**

| dQECG Outcome - Rate Parabolic Mixed Model - Coeff (p value) | | | | | |
|---|---|---|---|---|---|
| CPR parameter | dAMSA | dMS | dCF | dLAC | dDFA |
| CC Rate | -.033 (.867) | 10.99 (.746) | -5.58e-3 (.819) | -8.89 (.685) | -5.48e-3 (.501) |
| CC Rate^2 | 3.30e-4 (.967) | -.029 (.862) | 4.05e-5 (.732) | 3.68e-6 (.729) | 2.70e-4 (.495) |

Legend: Parabolic mixed model with CC rate as a predictor variable for each dQECG outcome (dAMSA, dMS, dCF, dLAC, and dDFA) No linear or parabolic predictors were significant for any dQECG outcome. Parabolic prediction models were not conducted for other chest compression variables after non-significance was found for CC rate.

Next, to account for the fact that chest compression bouts that take place late in resuscitation may have a different response when compared to chest compression bouts that occur

in the early part of resuscitation, a time interaction was included in the parabolic mixed model. These results are shown in Table 19. The time interaction was non significant.

**Table 19: Parabolic mixed model including a time interaction**

| dQECG Outcome - Rate Parabolic Mixed Model with Time Interaction - Coeff (p value) | | | | | |
|---|---|---|---|---|---|
| CPR parameter | dAMSA | dMS | dCF | dLAC | dDFA |
| CC Rate | .076 (.825) | 30.5 (.601) | -.027 (.524) | 9.15e-4 (.808) | -.013 (.343) |
| CC Rate^2 | -5.5e-4 (.973) | -.111 (.699) | 1.37e-4 (.494) | -7.15e-6 (.691) | 6.11e-5 (.363 |
| Time | 8.00e-6 (.639) | 1.2e-3 (.660) | -1.30e-6 (.526) | 8.40e-8 (.640) | -5.00e-7 (.471) |
| Time*Rate | 1.00e-8 (.709) | 1.00e-8 (0.689) | 1.00e-8 (.538) | -2.00e-7 (.535) | 1.00e-8 (.502) |
| Time*Rate^2 | 1.00e-8 (.789) | 1.00e-8 (.722) | 1.00e-8 (.553) | 1.00e-8 (.432) | 1.00e-8 (.544) |

Legend: Parabolic mixed model with CC rate as a predictor variable for each dQECG outcome (dAMSA, dMS, dCF, dLAC, and dDFA). Time (the amount of time elapsed when the bout-gap interval occured from the start of the case) was included as an interaction term in this model. No linear predictors, parabolic predictors, or interaction terms were significant for any dQECG outcome. Prediction models with time interaction terms were not conducted for other chest compression variables after non-significance was found for CC rate.

Multivariate models that used chest compression parameters as predictors of dQECG over a chest compression bout were then performed using linear mixed models. After observing that dAMSA, dMS, and dCF were the dQECG predictors that primarily responded in the univariate models, only these outcome variables were used in the multivariate analysis. Predictor variables that had univariate significance of $p < .15$ were included as predictors in the initial multivariate model. Age and sex variables were included in each model iteration regardless of predictive significance in previous models.

**Table 20: Multivariate model prediction of dAMSA and multivariate model prediction of dMS**

| dAMSA - Multivariate Model | |
|---|---|
| CPR parameter | Coeff (p value) |
| CC Rate | .032 (.094) |
| CC Bout Length | 7.24e-3 (.836) |
| CC Duty Cycle Dosed | 4.50e-7 (.995) |
| CC CCF | -1.73 (.173) |
| Age | -1.35e-3 (.927) |
| Sex | -.099 (.825) |

Cutoff: $p < .15$

| dAMSA - Multivariate Model - Reduced | |
|---|---|
| CPR parameter | Coeff (p value) |
| CC Rate | .035 (.070) |
| Age | -5.95e-5 (.968) |
| Sex | -.137 (.762) |

Legend: CC parameter prediction of dAMSA multivariate model. CC parameters were used in initial model if they had a univariate prediction model with significance of $p < .15$. Additional reduction of model predictors was conducted again with a significance cutoff of $p < .15$

| dMS - Multivariate Model | |
|---|---|
| CPR parameter | Coeff (p value) |
| CC Rate | 8.91 (.033) |
| CC Bout Length | 11.5 (.271) |
| CC Depth Dosed | -.127 (.126) |
| CC Duty Cycle Dosed | .016 (.906) |
| Age | -.304 (.904) |
| Sex | 52.8 (.492) |

Cutoff: $p < .15$

| dMS - Multivariate Model - Reduced | |
|---|---|
| CPR parameter | Coeff (p value) |
| CC Rate | 5.35 (.103) |
| CC Depth Dosed | -.014 (.108) |
| Age | -.231 (.927) |
| Sex | 53.0 (.491) |

Legend: CC parameter prediction of dMS multivariate model. CC parameters were used in initial model if they had a univariate prediction model with significance of $p < .15$. Additional reduction of model predictors was conducted again with a significance cutoff of $p < .15$

**Table 21: Multivariate model prediction of dC**

| dCF - Multivariate Model | |
|---|---|
| CPR parameter | Coeff (p value) |
| CC Duty Cycle | 7.52e-3 (.079) |
| Age | -1.11e-3 (.538) |
| Sex | .050 (.369) |

Legend: CC parameter prediction of dCF in a multivariate model. CC parameters were used in initial model if they had a univariate prediction model with significance of $p < .15$.

The results of the multivariate model for dAMSA prediction is shown in the left side of Table 20. The chest compression variables that had a significant univariate predictive value were CC rate, CC bout length, CC duty cyele dosed, CC CCF, age and sex. In the first iteration of the multivariate dAMSA model,,only CC rate was significant. After eliminating predictors for the second iteration with a cutoff of $p < .15$, CC bout length was removed from the model due to non-significance.

The right side of Table 20 displays the same approach for a multivariate dMS model. In this model only CC rate and CC bout lenght was predictive of dMS in the first and second iterations of the model when using a cutoff of $p < .15$ for the second iteration. Age and sex predictors were left in the model for all iterations.

Table 21 displays the only multivariate iteration for dCF. In this model only CC duty cycle was significantly predictive of dCF. Age and sex predictors were left in the model for all iterations.

dLAC and dDFA were not attempted as neither dQECG metric were predictive in the univariate analyses

These multivariate models demonstrate that dAMSA and dMS may be the most robust response metrics to changing chest compression parameter values. They also demonstrate that dMS response to CC rate may be the most promising signal to guide an adaptive approach to chest compressions.

To further visualize the relationship between dQECG and chest compression parameters, and to address the possibility of an interaction between compression rate and depth, 3D surface plots were generated for dAMSA, dMS, and dCF for all chest compression values observed in the CCC dataset. dLAC and dDFA were excluded from this analysis as none of the linear regression analysis proved significant for these dQECG metrics. The 3D surface plots are shown in Figure 38, Figure 39, and Figure 40 respectively.

The plots demonstrate that there are separate maxima and minima for each dQECG metric. dAMSA is maximized at a chest compression depth of 2.0 inches and a chest compression rate of 107 compressions per minute. dAMSA is minimized at chest compression depth of 2 inches and a chest compression rate 95.2 compressions per minute.

dMS is maximized at a chest compression depth of 1.1 inches and a chest compression rate of 117.5 compressions per minute. dMS is minimized at a chest compression depth of 1.3 inches and a chest compression rate of 97.8 compressions per minute.

dCF is maximized at a chest compression depth of 1.5 inches and a chest compression rate of 91.3 compressions per minute. dCF is minimized at chest compression depth of 2.5 inches and a chest compression rate 96.1 compressions per minute.

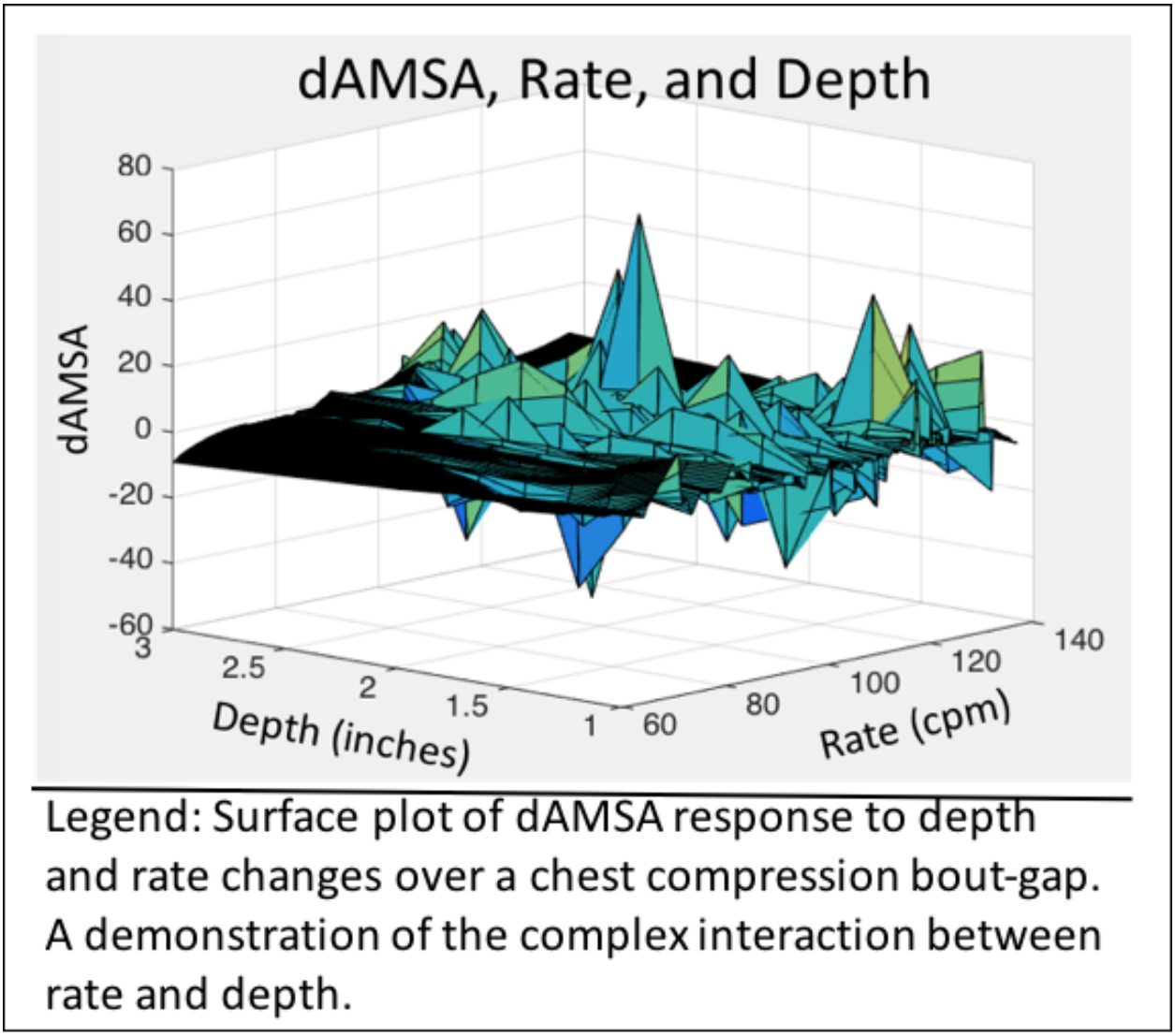


**Figure 38: 3D surface plot of dAMSA, Rate, and Depth**

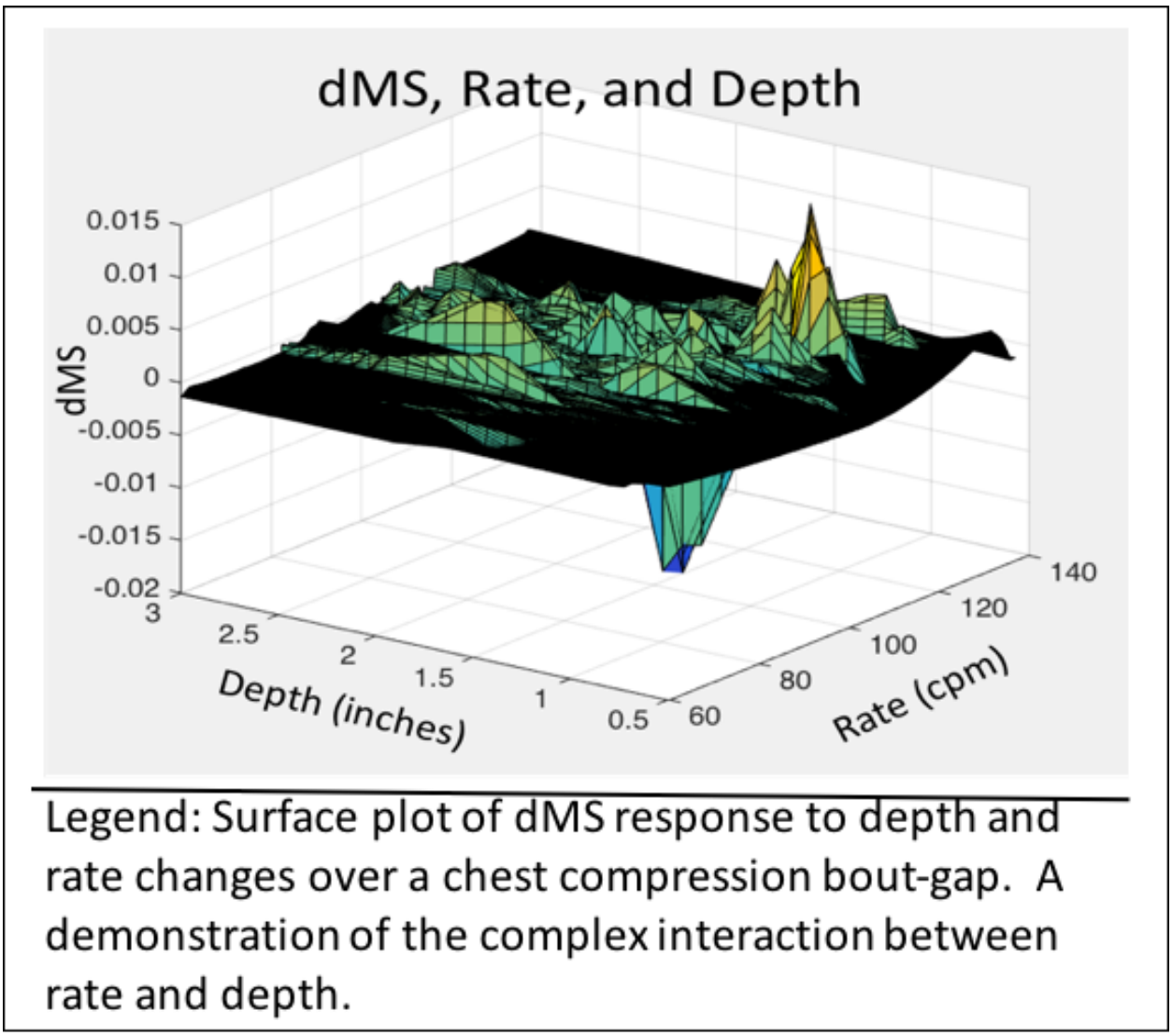


Legend: Surface plot of dMS response to depth and rate changes over a chest compression bout-gap. A demonstration of the complex interaction between rate and depth.

**Figure 39: 3D surface plot of dMS, Rate and Depth**

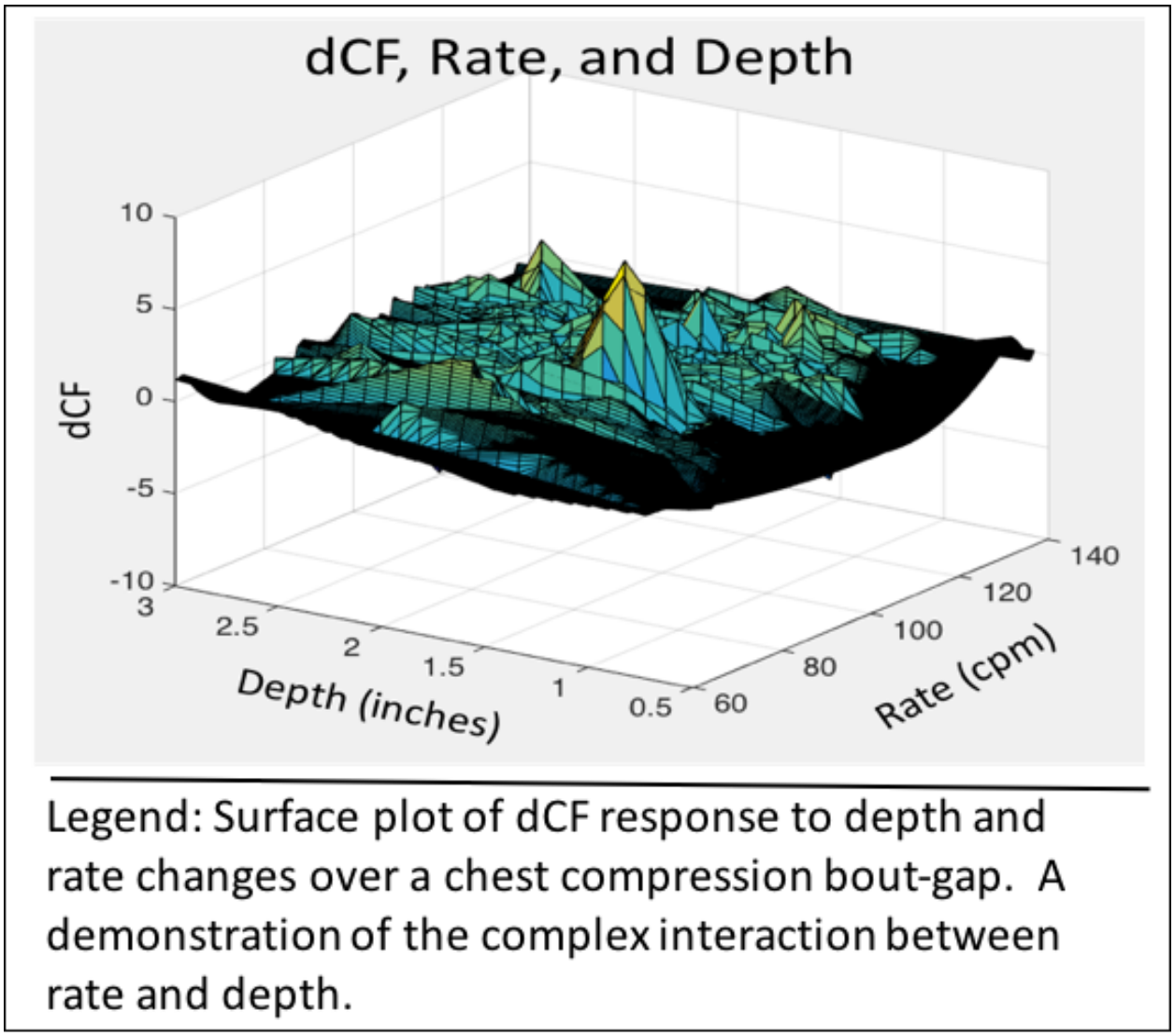


**Figure 40: 3D surface plot of dCF, Rate, and Depth**

The 3D plot assessment shows that there are pronounced peaks and troughs in the relationship between dQECG with chest compression rate and chest compression depth. Each dQECG metric plotted against the rate and depth chest compression parameters informs us that not only do each dQECG metric respond uniquely to changes in chest compression rate and chest compression depth, but that there is interaction between chest compression rate and chest compression depth. This phenomenon would complicate usage of multiple dQECG metrics in any chest compression feedback algorithm that is developed. While one dQECG metric could be optimized on the 'rate-depth' response surface, another dQECG metric could respond negatively for its complement's optimization. Further work is required to identify not only which dQECG metric would take preference in such an optimization scheme, but which metrics could be afforded to deteriorate for the optimization of another. This optimization scheme could have a time dependence as well.

#### 3.3.2.3 Conclusion to clinical data results

Change in the QECG metric median slope (dAMSA) appeared to be responsive to changes in chest compression rates when controlled for all other chest compression parameters, age, and sex in the second iteration of the multivariate linear model. Change in the QECG metric median slope (dMS) appeared to be responsive to changes in chest compression rates and dosed chest compression depths when controlled for all other chest compression parameters, age, and sex in the second iteration of the multivariate linear model. Change in the dQECG metric median slope (dCF) appeared to be responsive to changes in chest compression duty cycle when controlled for all other chest compression parameters and age and sex in the first iteration of the multivariate model. The significance cutoff for inclusion in this multivariate model was $p < .15$.

The findings from the dQECG plots suggest that a simple linear regression may not be the most optimal way of describing relationships between biosignals such as dQECG and basic chest compression parameters such as chest compression rate and chest compression depth. This was observed in the complex nature of the 3D surface plots of dQECG, chest compression rate, and chest compression depth. In these plots there appeared to be an interaction between chest compression rate ad chest compression depth. There were distinct minima and maxima across the response of all dQECG responses.

# 4.0 DISCUSSION AND FUTURE DIRECTIONS

## 4.1 FEASIBILITY OF ADAPTIVE CPR

Our initial animal studies showed that a chest compression device can appropriately respond to biosignals it receives to tailor chest compressions based on those biosignals. The initial feasibility study described in Aim 1 demonstrated that an adaptive chest compression device could not only be engineered and constructed, but proven to respond to real time biosignals generated by an animal model. Real-time sensing of biosignals in an ambulance setting would therefore be feasible and next steps would involve miniaturizing the prototype device as well as establishing wireless connections between the chest compression device and the clinical monitor measuring the biosignals. Establishment of such a wireless connection and increasing usability by miniaturizing would be essential in translating our prototype to clinical practice.

Additional animal studies described in this work demonstrated that QECG is a potential non-invasive biosignal capable of driving changes in chest compressions. The QECG metrics MS, CF, and LAC showed potential to respond to rate changes in the animal experiments described in Aim 1. Results found in Aim 2 demonstrated that change in some QECG metrics (dQECG) responded to chest compression changes such as rate. These results demonstrate initial feasibility and translation to human clinical data from the initial animal results.

## 4.2 WHEN IS CPR MOST EFFECTIVE

The treatment of cardiac arrest remains a 'black box' in terms of providing optimized care for patients. Patients may have different chest sizes, different cardiac arrest etiology, and may respond to chest compressions and drug treatment in different ways. The variable nature of patients necessitates an adaptive approach to CPR.

CPR is most effective when it is done immediately after cardiac and when it is done well. The work described in this dissertation adds an additional qualifier to measuring CPR quality; In addition to maintaining standards for chest compression rate and depth, chest compressions should factor in the patient, and how that patient responds to the chest compressions he or she receives. This feedback approach to chest compressions has the potential to improve perfusion during CPR, and increase the likelihood of favorable outcomes, because it optimizes care based on the patient.

Any adaptive approach very much depends on how accurately the adaptive device is able to acquire and interpret biosignals, and in turn relate those biosignals to the quality of perfusion generated by the CCs. In a prehospital setting however, it would be required that these biosignals are non-invasively measured. QECG metrics that have been used in the swine studies described here are non-invasive, readily available, and are derived from the ECG, which is ubiquitously recorded in ambulances for every cardiac arrest patient. A link could therefore be established between existing defibrillator monitors and a biosignal driven CPR device.

Our findings provide preliminary evidence that a beneficial increase in perfusion may be achieved in cardiac arrest patients by linking the delivery of CPR to invasive and non-invasive biosignals (especially QECG). With more optimal CPR given to patients, patient survival outcomes could be improved. While we have focused on using biosignals to modify the chest

compressions provided by a mechanical CPR device, this feedback could also be given verbally to EMS personnel providing manual compressions.

## 4.3 MECHANICAL CHEST COMPRESSION DEVICES

The work conducted here shows preliminary evidence that a feedback based approach to CPR may provide better outcomes for cardiac arrest patients. But even with strong evidence that this approach is effective, its eventual adoption by the EMS community is dependent on the wide use of mechanical chest compression devices. It may be possible to give audio biosignal feedback to a human provider, for example a device could signal the provider to press deeper and/or faster in response to a suboptimal QECG metric the EMS monitor is measuring, but mechanical devices have the precision to adjust chest compressions in a much more nuanced and finite way when compared to a human provider.

## 4.4 CHEST COMPRESSION GUIDANCE

The studies presented in this work sought to elucidate how to best deliver adaptive chest compressions based on biosignals received from a patient. The primary gaps in knowledge discussed in the beginning of this dissertation were characterized by three questions. These questions involved which biosignals to measure, which chest compression parameters to adjust, and how much and when to adjust the chest compression parameter.

These questions that surround the development of a biosignal driven chest compression algorithm include many variables. Potential biosignal variables taken into consideration for the feedback algorithm included invasive pressure in animal models as well as multiple QECG metrics in clinical data. Chest compression parameter variables taken into consideration for the feedback algorithm included variables such as chest compression rate, and chest compression depth, and chest compression duty cycle. Additional variables that applied to the approach of biosignal driven chest compressions included the development of threshold values for biosignals used in the algorithm as well as the time interval of analysis between chest compression adjustments.

To answer the first question concerning which biosignal to measure, the work described here gives preliminary evidence that some non-invasive QECG signals respond to changing chest compression parameters. During the animal tests described in Aim 1, the QECG metric median slope (MS) appeared to be most responsive to changes in chest compression parameters in a controlled setting. In the clinical data discussed in Aim 2, change in MS (dMS) responded linearly over bouts of chest compressions to the chest compression parameter predictors rate and dosed depth.

To answer the second question of which chest compression parameter to adjust, contrasting results were found in separate experiments described in this work. In the simulation model of cardiac arrest in Aim 1, an adaptive approach to chest compressions was applied to a variant population with different chest sizes and anatomy along with a fixed approach to chest compressions. A final cardiac output in the adaptive model was compared to its respective final cardiac output in the 'fixed' model and it was found that the final settings of chest compression parameters in the adaptive model involved only chest compression depth changes. These initial

findings demonstrate the potential utility in relying mostly on depth to influence cardiac output and chest compression effectiveness.

Cardiac output however is difficult to measure non-invasively in the out-of-hospital environment. Therefore, in the subsequent experiments we relied on QECG signals to guide chest compression changes. After the initial feasibility animal test, we again sought to answer the second question posed in the introduction of which chest compression parameter to adjust. Here we found that chest compression rate changes, when applied to similar sized animals and controlled for other chest compression parameters, produced the strongest linear response in QECG.

An explanation for the difference in conclusions between the simulation data showing chest compression depth as most relevant and clinical data showing chest compression rate as most relevant is unclear. The simulation data is based on a simplified model of the circulatory system and is limited in its relevance to animal and human clinical data. The simulation data helps us guide initial algorithm development, however it is ultimately clinical data that will form the evidence to base the chest compression parameter priority in the final algorithm feedback loop. After examining the clinical findings, we believe chest compression rate may be the best candidate to first adjust in future developed chest compression algorithms.

To answer the third question posed in the introduction concerning how much to adjust chest compressions and when to adjust them, the work described in this dissertation provides precursory evidence for this component of adaptive chest compressions, but much remains still to be answered. In the feasibility study, increments of chest compression parameter changes were arbitrarily set to clinically relevant increments such as depth adjustments of .5 inches. The time intervals of analysis between each change was also set only based on observations in past studies

in our lab that showed thirty seconds may be a reasonable amount of time to wait for biosignal response to chest compression changes.

Future work would involve experiments that varied the amount of change in chest compression depth, rate, and duty cycle in separate groups and compared those groups to 'fixed' chest compression that did not adjust. Additional experiments would also vary the time interval of analysis between adjustments; the time interval of thirty seconds used in the feasibility study and the time interval of one minute used in the animal study may not be optimal.

Future additions to the scope of biosignal driven feedback CPR include the addition of medication dosage and timing to the treatment algorithm, synchronization of the chest compression device the the QRS complexes of a PEA rhythm., and non-invasive biosignals to supplement QECG metrics such as doppler ultrasound detection of a patient's pulse. These additions are actively being explored in the lab.

## 4.5 DOSED MEASURES OF CPR

Multiple metrics were used in this work to describe the process and reaction to chest compression during CPR. Process metrics such as chest compression depth, rate, and duty cycle characterize the delivery of chest compressions and reaction metrics such as dQECG describe how the quantifiable components of the VF waveform respond and change due to the chest compression process. Dosed metrics of chest compression depth, rate, and duty cycle that incorporated the time duration of each chest compression bout were also included in the logistic models developed in Aim 2. QECG metrics including AMSA, MS, CF, LAC, and DFA were used to quantify reactions

to chest compressions with the aim that positive reactions reflecting better perfusion would both respond to and guide adjusting chest compression.

Individually these process and reaction metrics were predictive of outcomes in response to chest compressions. In the clinical data described in Aim 2, chest compression rate predicted survival and AMSA and MS were the strongest predictors of ROOR. Change in MS (dMS) across chest compression bouts (dMS) also responded linearly to chest compression rate changes described in Section 3.3.

The combination of multiple metrics into one outcome prediction model would be desirable in simplifying the characterization of chest compressions as a 'dose of CPR'. A quantifiable 'dose' would weigh both the individual process components of chest compressions and a reactionary biosignl response into a metric easily conveyed to medical providers with the purpose of optimizing outcomes. Multivariate models described in this work aim to combine these individual predictors to make a superior multi-parameter characterization of chest compression effectiveness. However only select multivariate models were successful in combining multiple individual predictors.

In the case of chest compression parameter prediction of dQECG discussed over bouts of CPR in Section 3.3.2, only chest compression rate was predictive of dAMSA, only chest compression rate and dosed chest compression depth were predictive of dMS, and only chest compression duty cycle was predictive of dCF in the final multivariate models using significance cutoffs of $p < .15$. Thus only dMS yielded a model with more than one significant chest compression predictor variable. From this work dMS appears to be the most viable dQECG candidate to be used as a biosignal to drive changes in chest compressions during CPR.

Future work would necessarily involve more complex models to factor in both chest compression parameters and QECG biosignals above the basic linear and quadratic model fits used in the work described in this dissertation.

# 5.0 CONCLUSION

The findings presented in this study establish a foundation for planned subsequent research that will involve incorporating CPR quality metrics into the models identifying associations with the way CPR is delivered with both QECG and outcome variables. Findings from this work have the potential to provide real-time CPR feedback to health care providers based on patient physiology.

In our first aim we developed the adaptive chest compression device and tested it in animal feasibility studies which demonstrated that it responded appropriately to the biosignals it received. Next, in a computational model of adaptive chest compressions, adjustments in chest compression depth yielded the largest increase in cardiac output in patients with simulated variable physiology. In follow-up animal studies, select QECG measures responded to changes in chest compression parameters which demonstrated the initial feasibility of QECG measures as a potential biosignal in this model. We found that the QECG measures of median slope, centroid frequency, and log of the absolute correlation responded to changes in chest compression rate in the early phase of chest compressions. We found that in late phases of chest compressions the QECG measure median slope responded to chest compression rate changes and the QECG measure AMSA responded to chest compression duty cycle changes.

In our second aim, all QECG metrics that we tested in the clinical data set was predictive of shock outcome and chest compression rate along with chest compression bout duration were predictive of survival. However, when controlled for the presenting first rhythm status and demographic variables, only chest compression bout duration was predictive of survival. In addition to the predictive value of chest compression parameters and QECG measures, associations

were found between varying chest compression parameters averaged across bouts of compressions with change in QECG values (dQECG) in the clinical data. Chest compression rate was found to be predictive of the dQECG metric median slope (dMS) and the dQECG metric (dAMSA). Dosed compression rate was found to be predictive of the dQECG metric dMS as well. dCF responded to changes in chest compression duty cycle. These findings provide a foundation for delivering adaptive chest compressions with the potential of improving survival outcomes to cardiac arrest. These studies help us push the boundaries of optimizing perfusion generated from chest compressions in both the in-hospital and out-of-hospital setting.

# APPENDIX A

## ADDITIONAL FIGURES

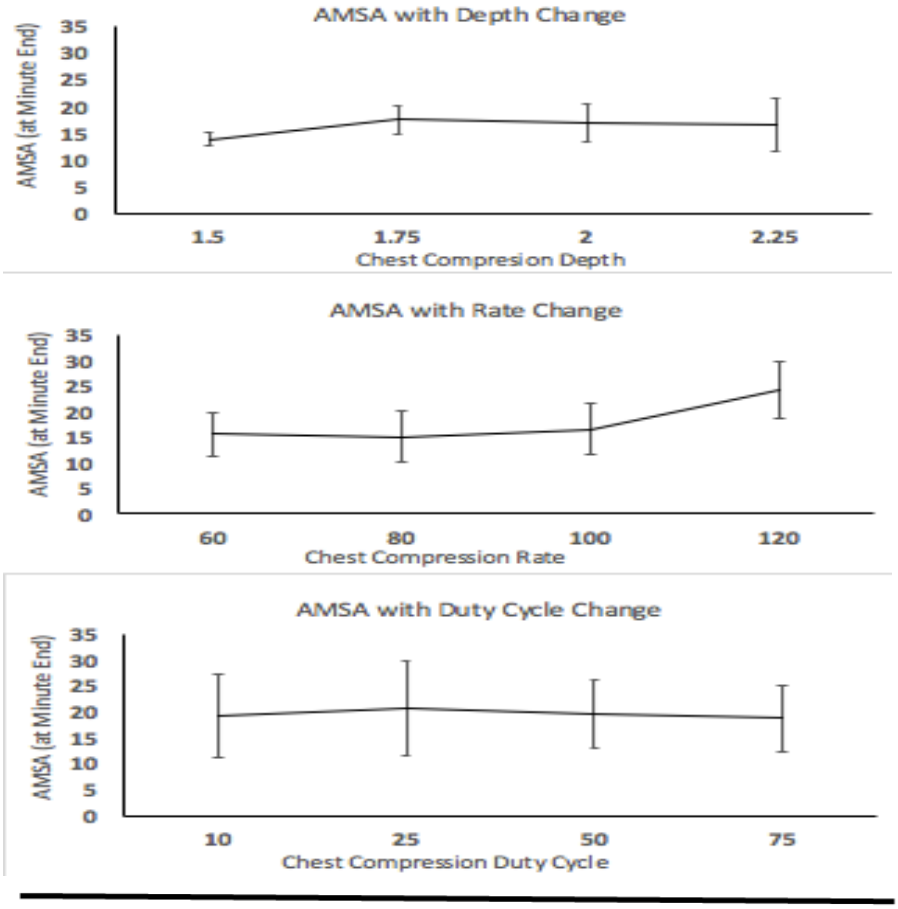


Legend: Phase 1 AMSA values over changes in chest compression parameters. One minute is spent at each chest compression parameter setting on the x axis while other chest compression parameters are held constant QECG is taken at the end of each minute. No AMSA response had a significant linear response.

**Figure 41: Phase 1 AMSA response to CC parameter changes (Analysis Approach A)**

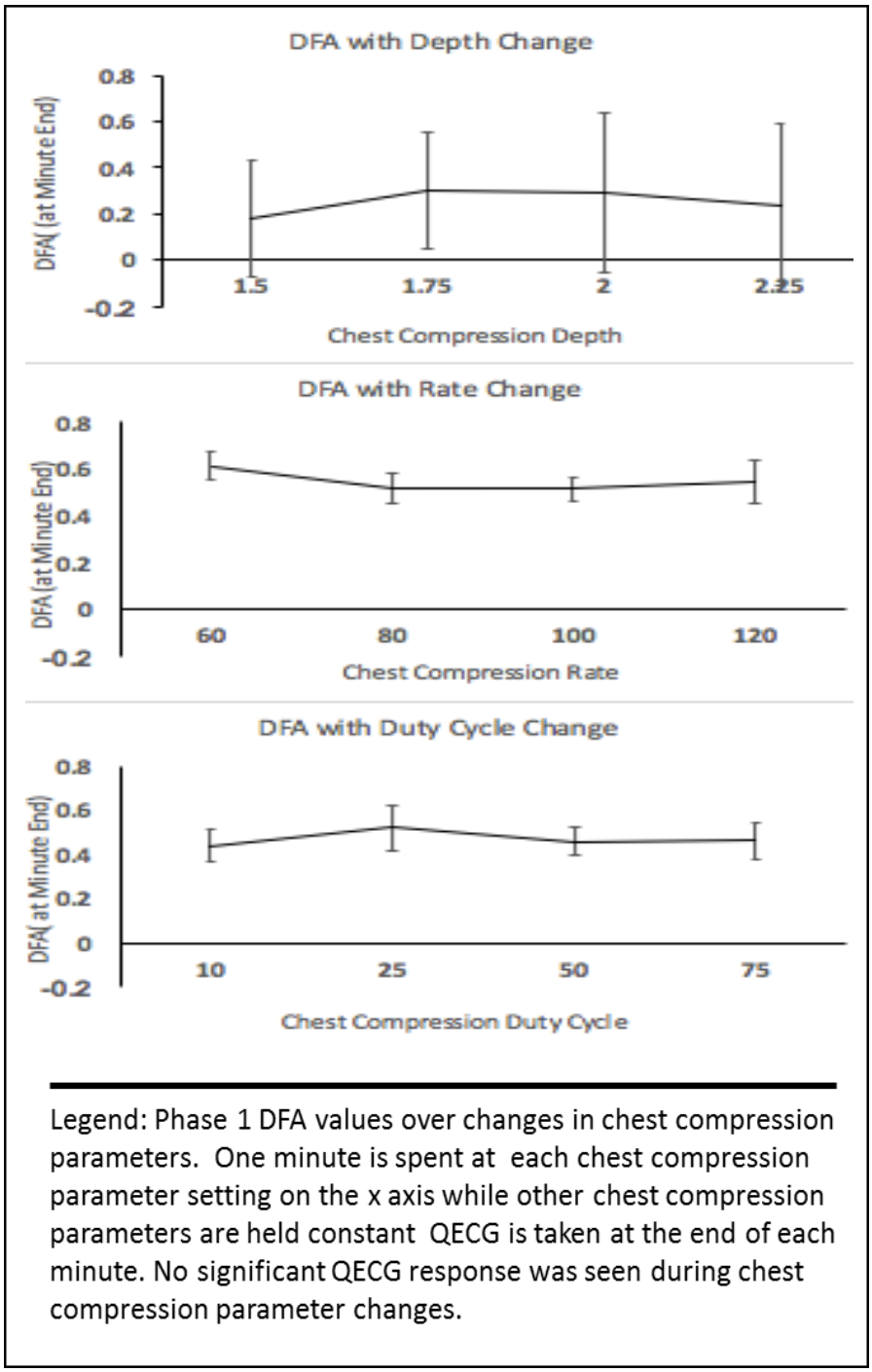


**Figure 42: Phase 1 DFA response to CC changes (Analysis Approach A)**

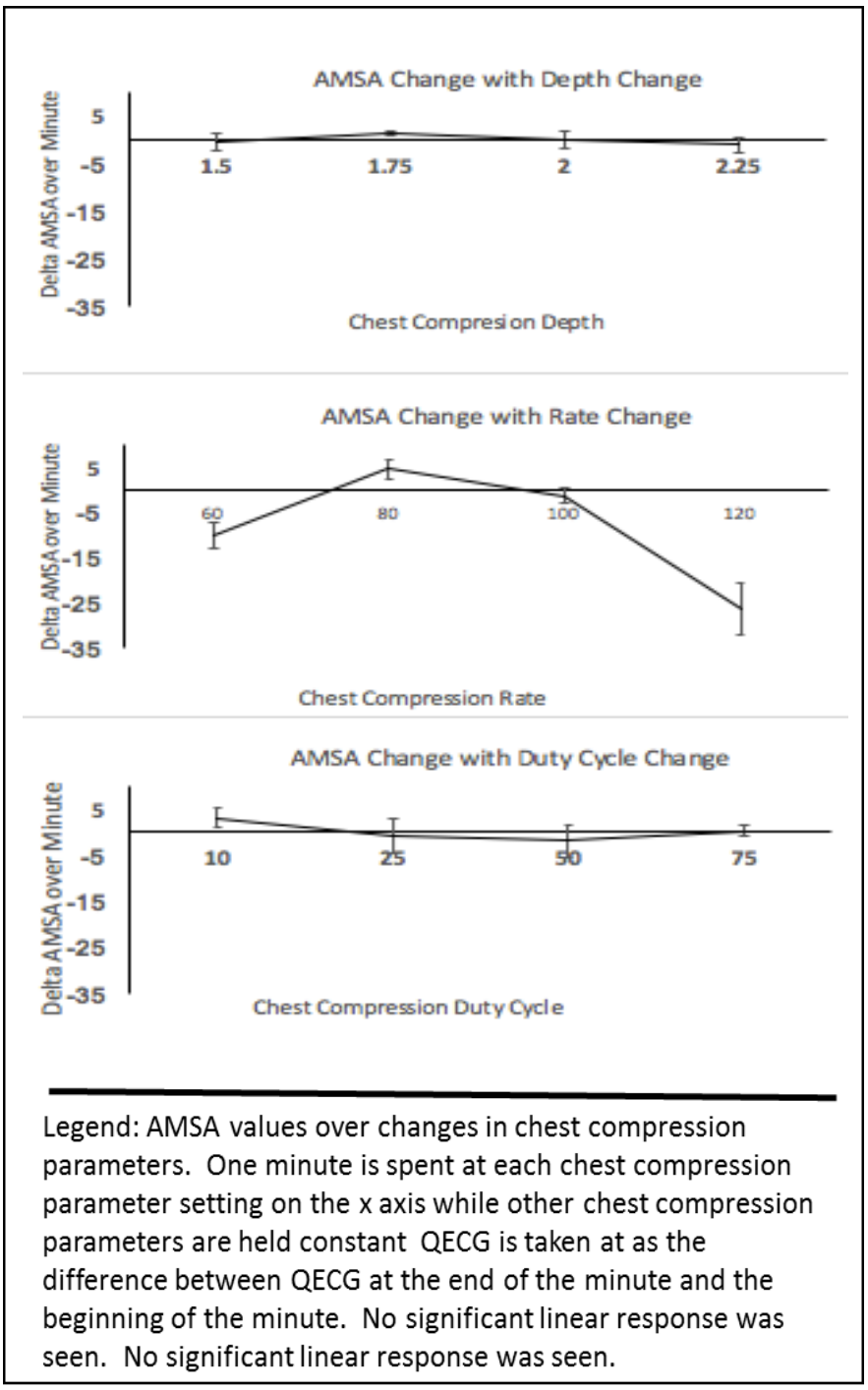


**Figure 43: Phase 1 AMSA response to CC parameter changes (Analysis Approach B)**

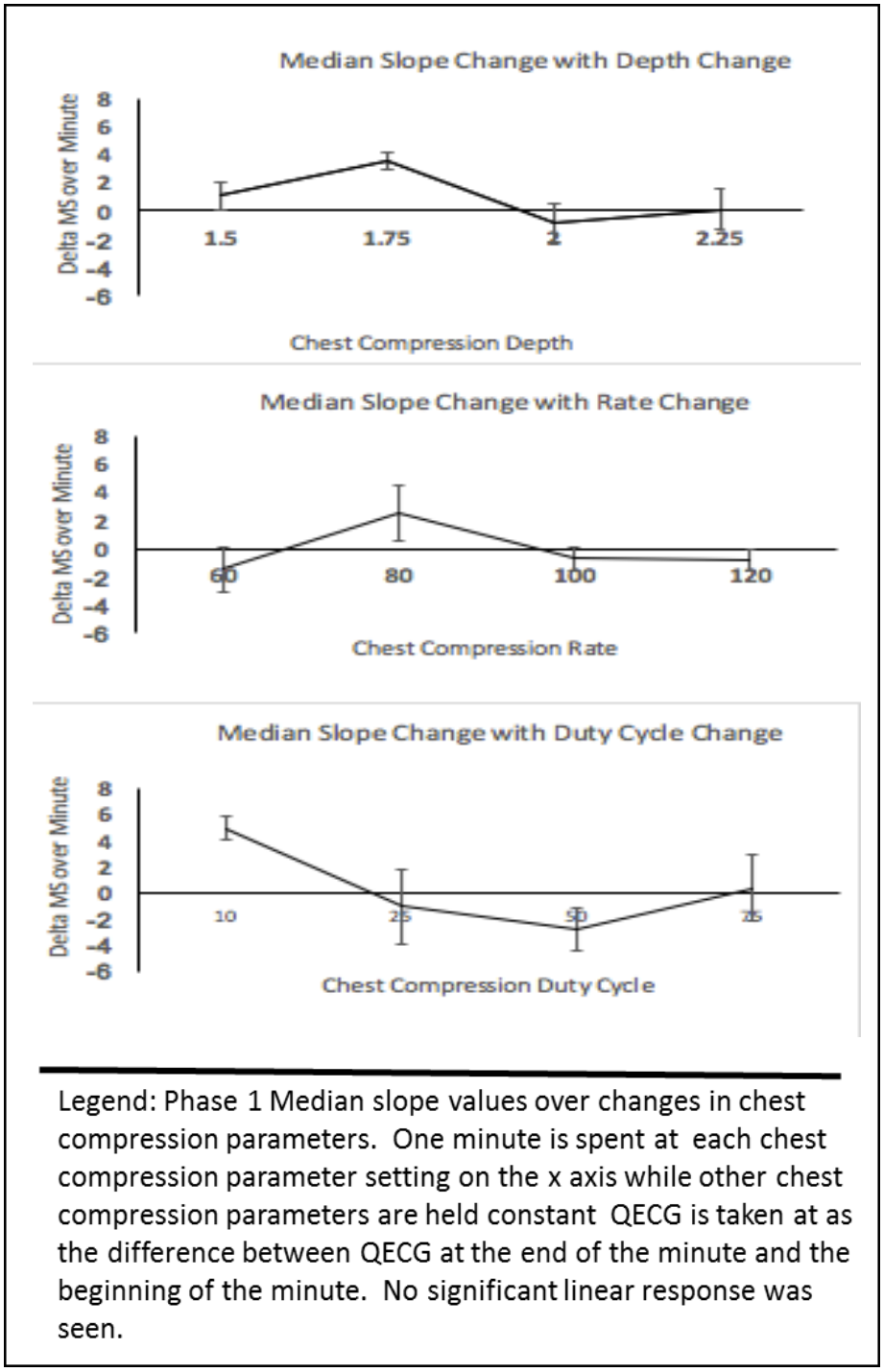


**Figure 44: Phase 1 MS response to CC parameter changes (Analysis Approach B)**

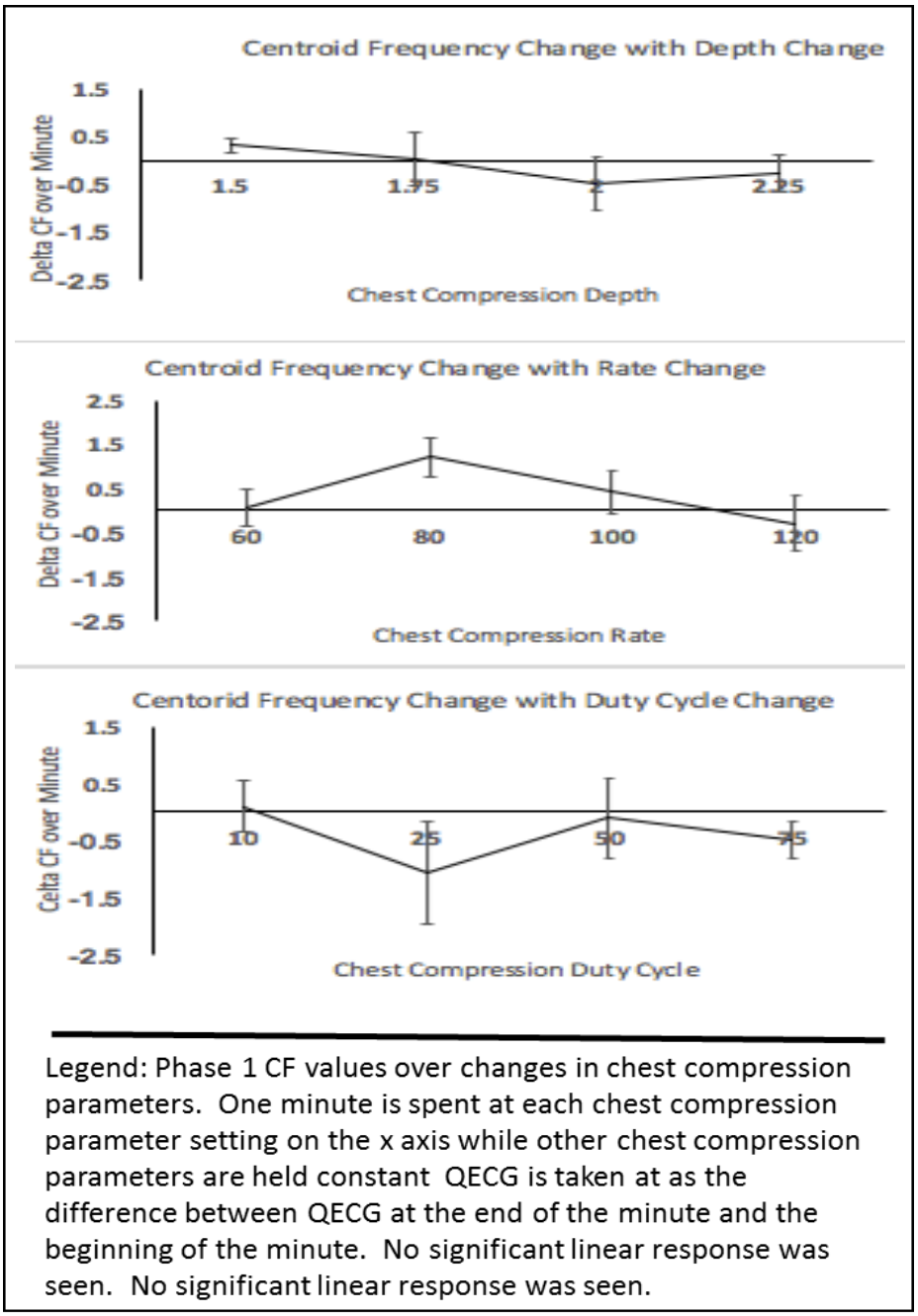


**Figure 45: Phase 1 CF response to CC parameter changes (Analysis Approach B)**

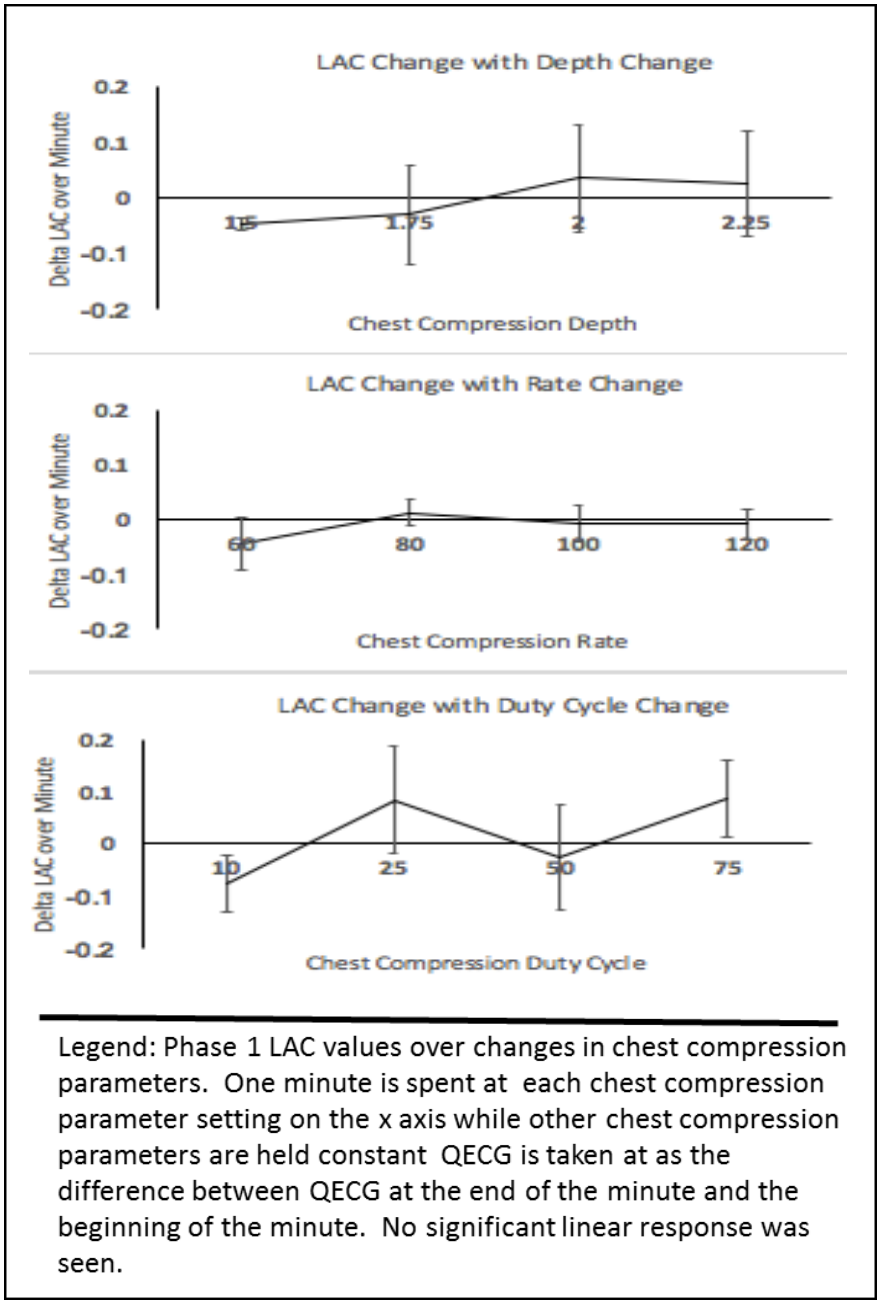


**Figure 46: Phase 1 LAC response to CC parameter changes (Analysis Approach B)**

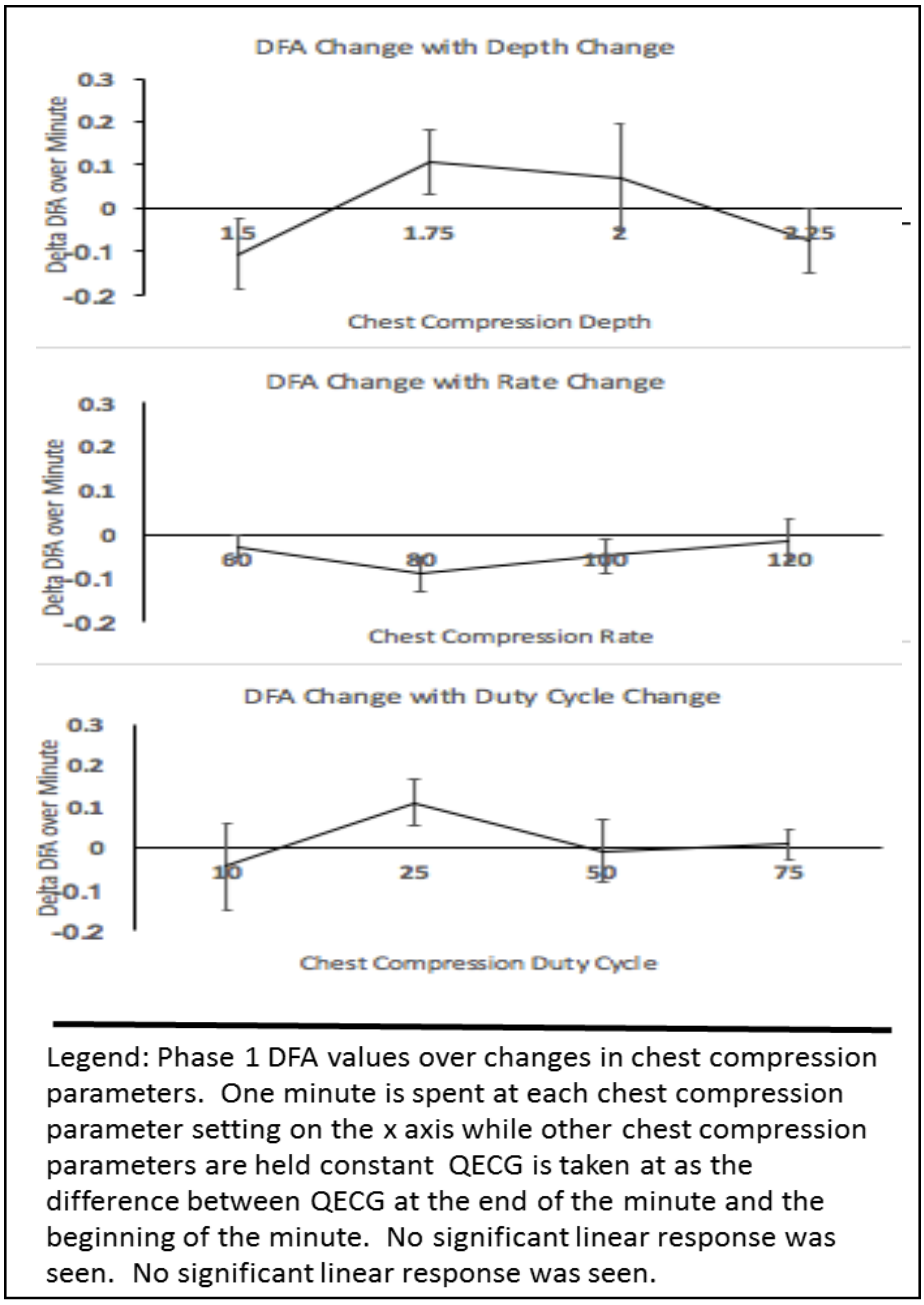


Legend: Phase 1 DFA values over changes in chest compression parameters. One minute is spent at each chest compression parameter setting on the x axis while other chest compression parameters are held constant QECG is taken at as the difference between QECG at the end of the minute and the beginning of the minute. No significant linear response was seen. No significant linear response was seen.

**Figure 47: Phase 1 DFA response to CC parameter changes (Analysis Approach B)**

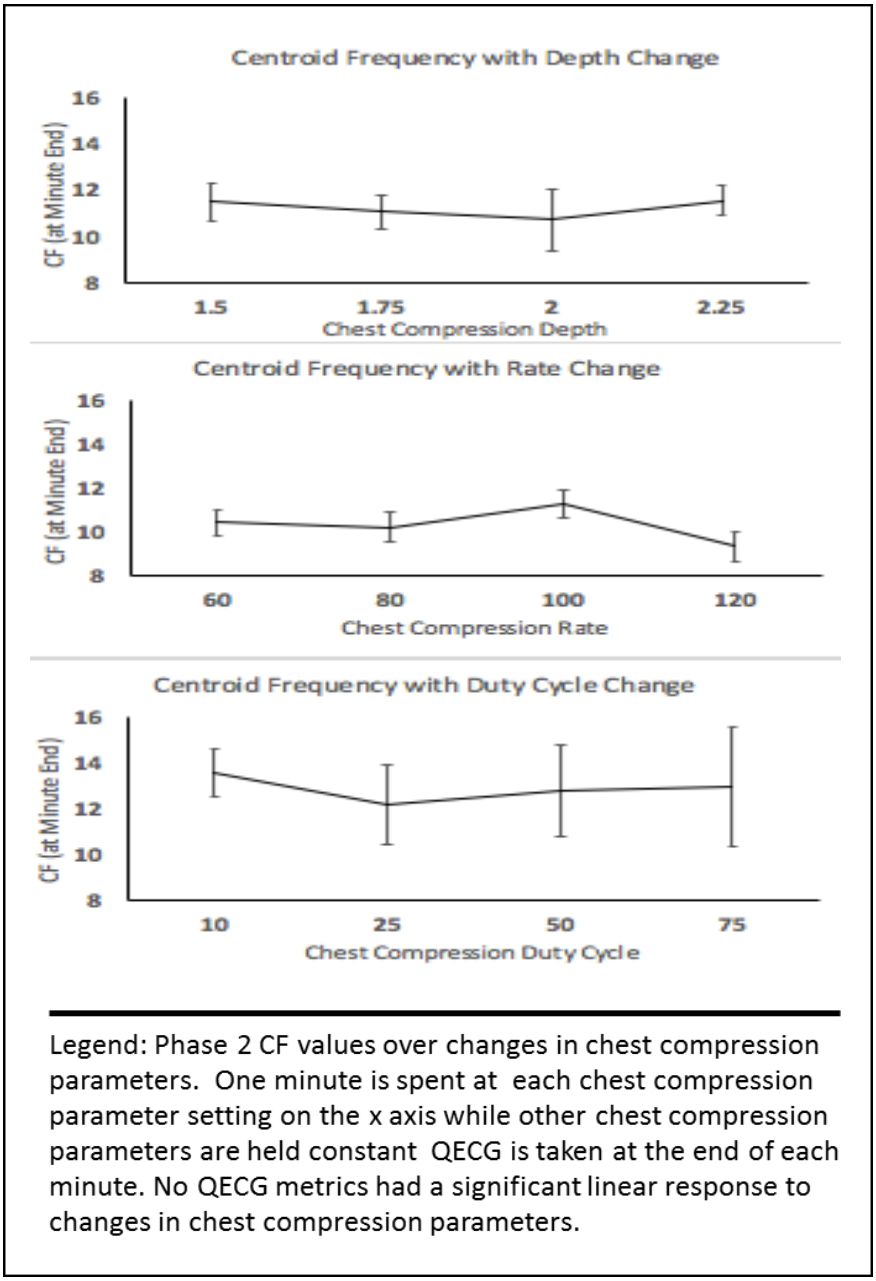


**Figure 48: Phase 2 CF response to CC parameter changes (Analysis Approach A)**

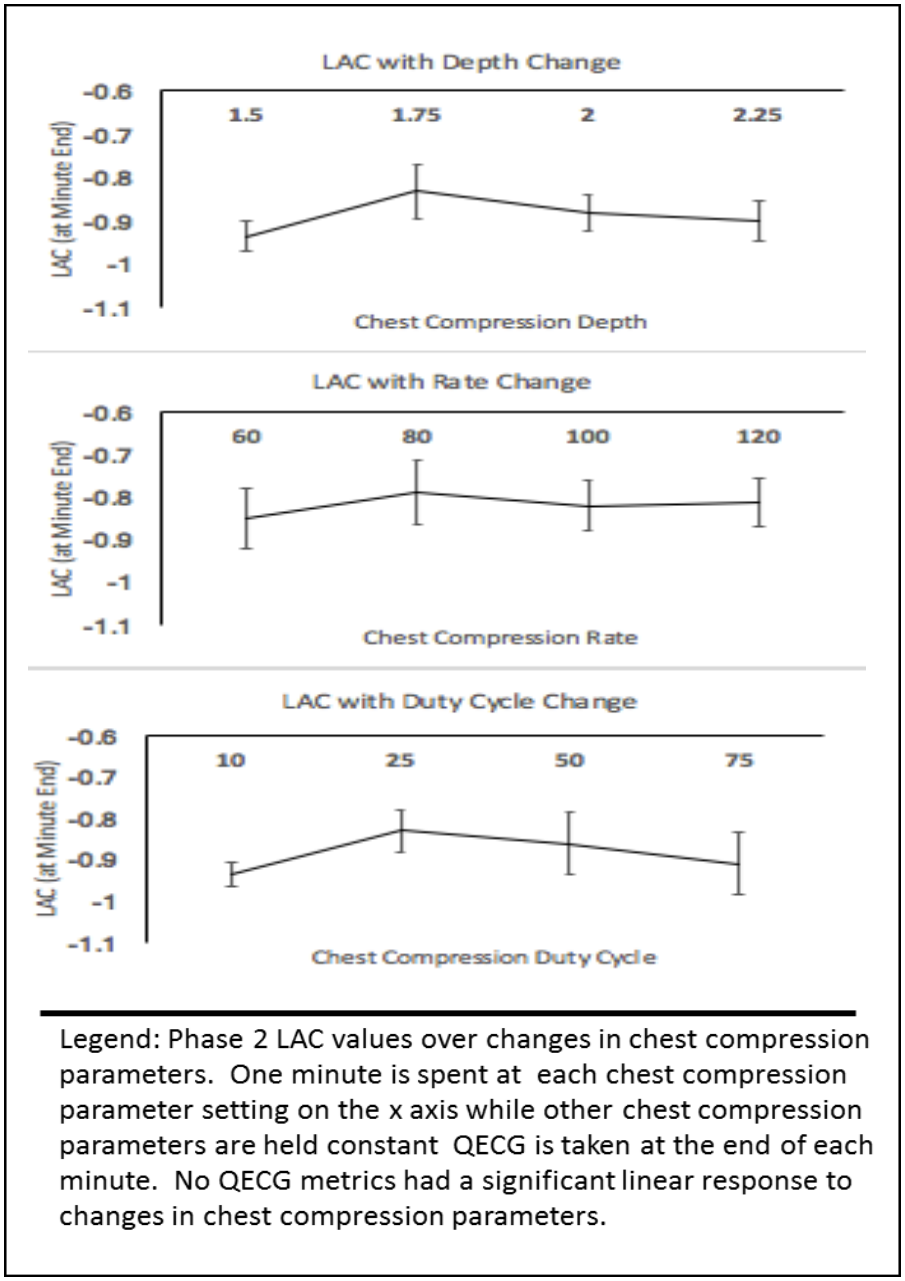


**Figure 49: Phase 2 LAC response to CC parameter changes (Analysis Approach A)**

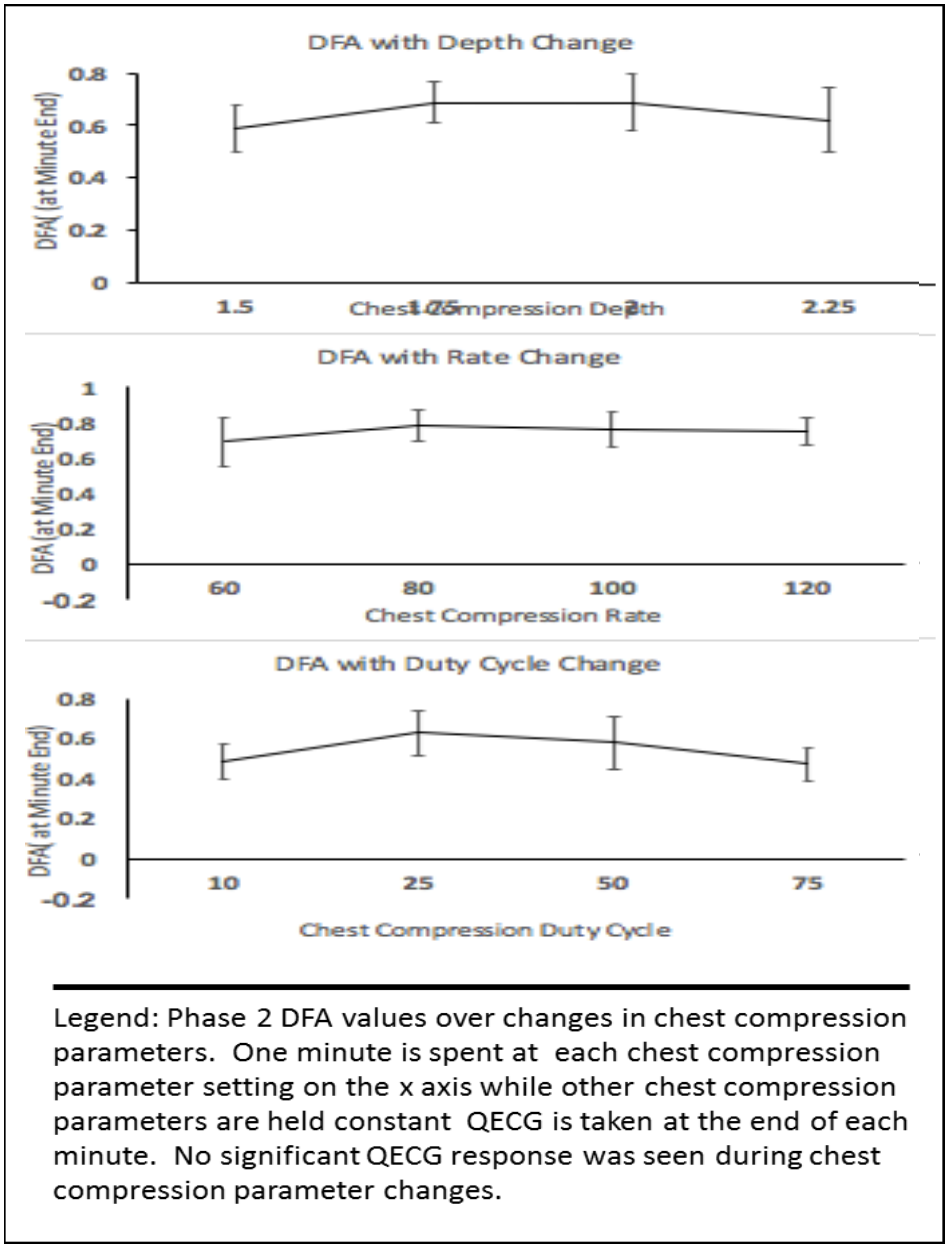


**Figure 50: Phase 2 DFA response to CC parameter changes (Analysis Approach A)**

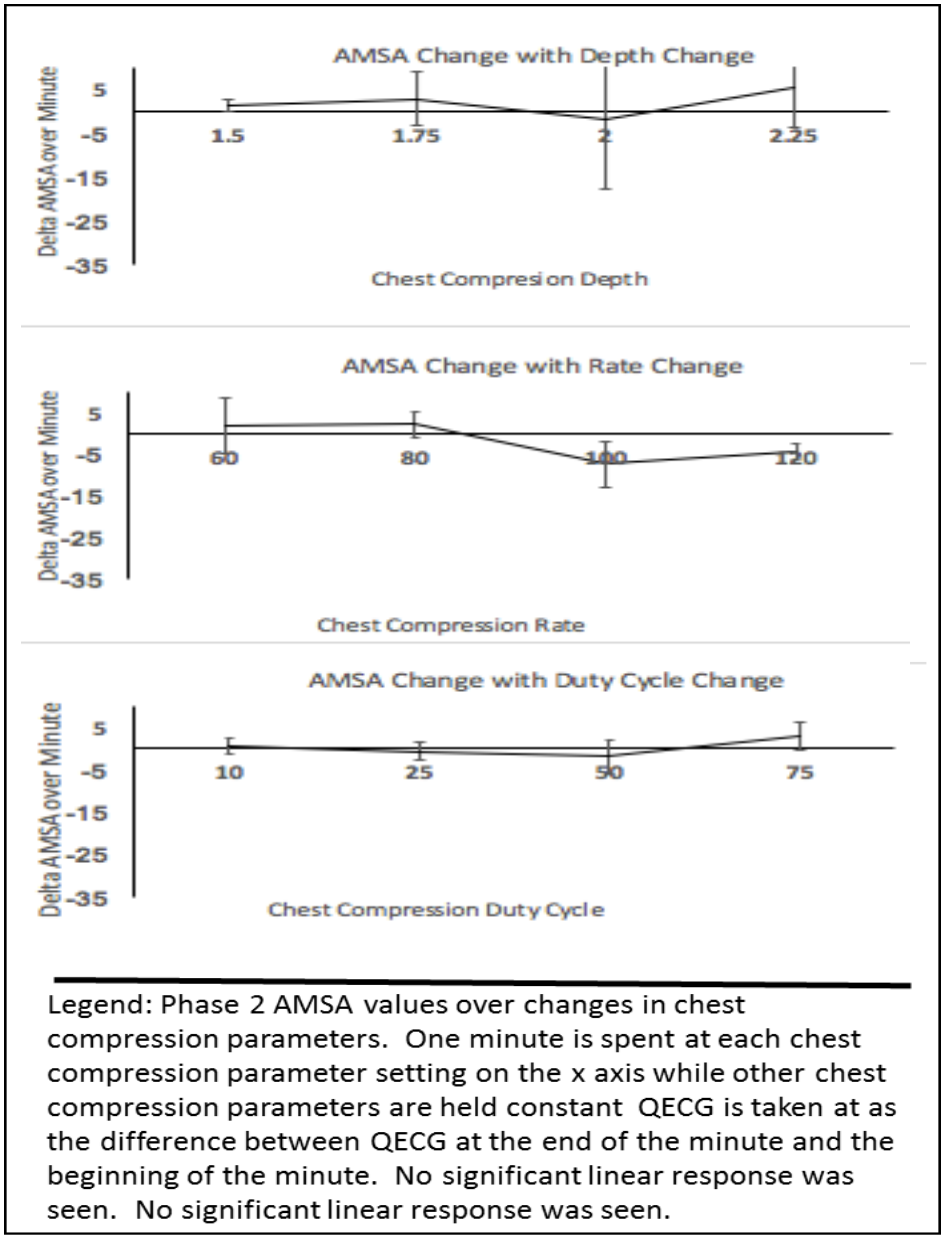


**Figure 51: Phase 2 AMSA response to CC parameter change (Analysis Approach B)**

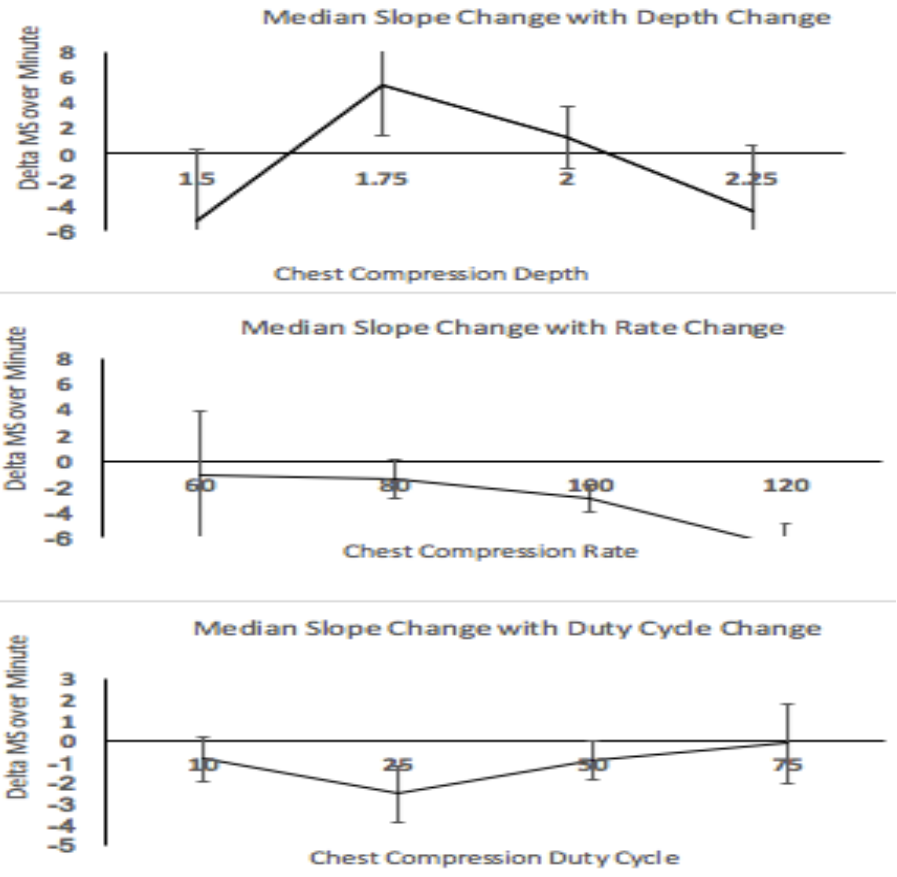


Legend: Phase 2 Median slope values over changes in chest compression parameters. One minute is spent at each chest compression parameter setting on the x axis while other chest compression parameters are held constant QECG is taken at as the difference between QECG at the end of the minute and the beginning of the minute. No significant linear response was seen.

**Figure 52: Phase 2 MS response to CC parameter change (Analysis Approach B)**

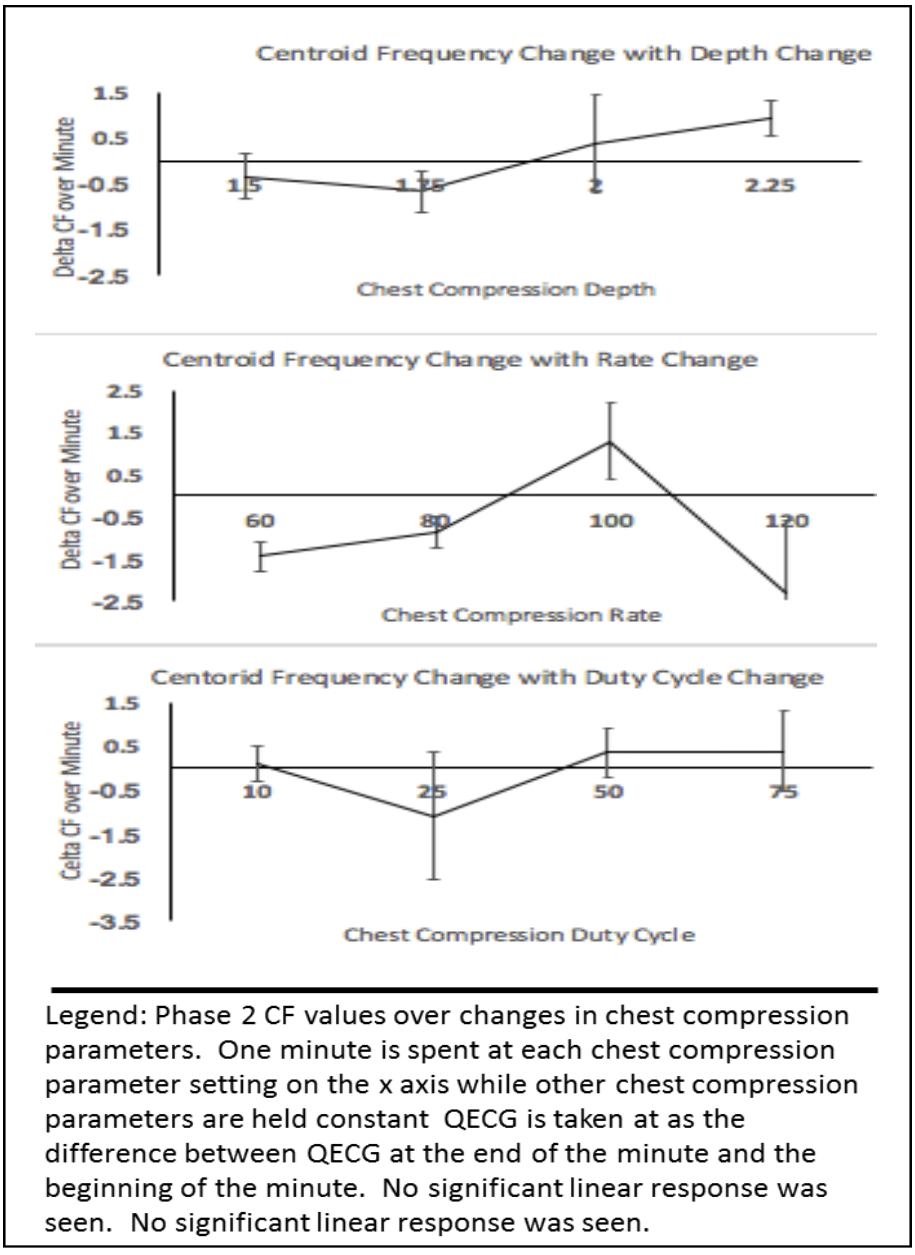


**Figure 53: Phase 2 CF response to CC parameter change (Analysis Approach B)**

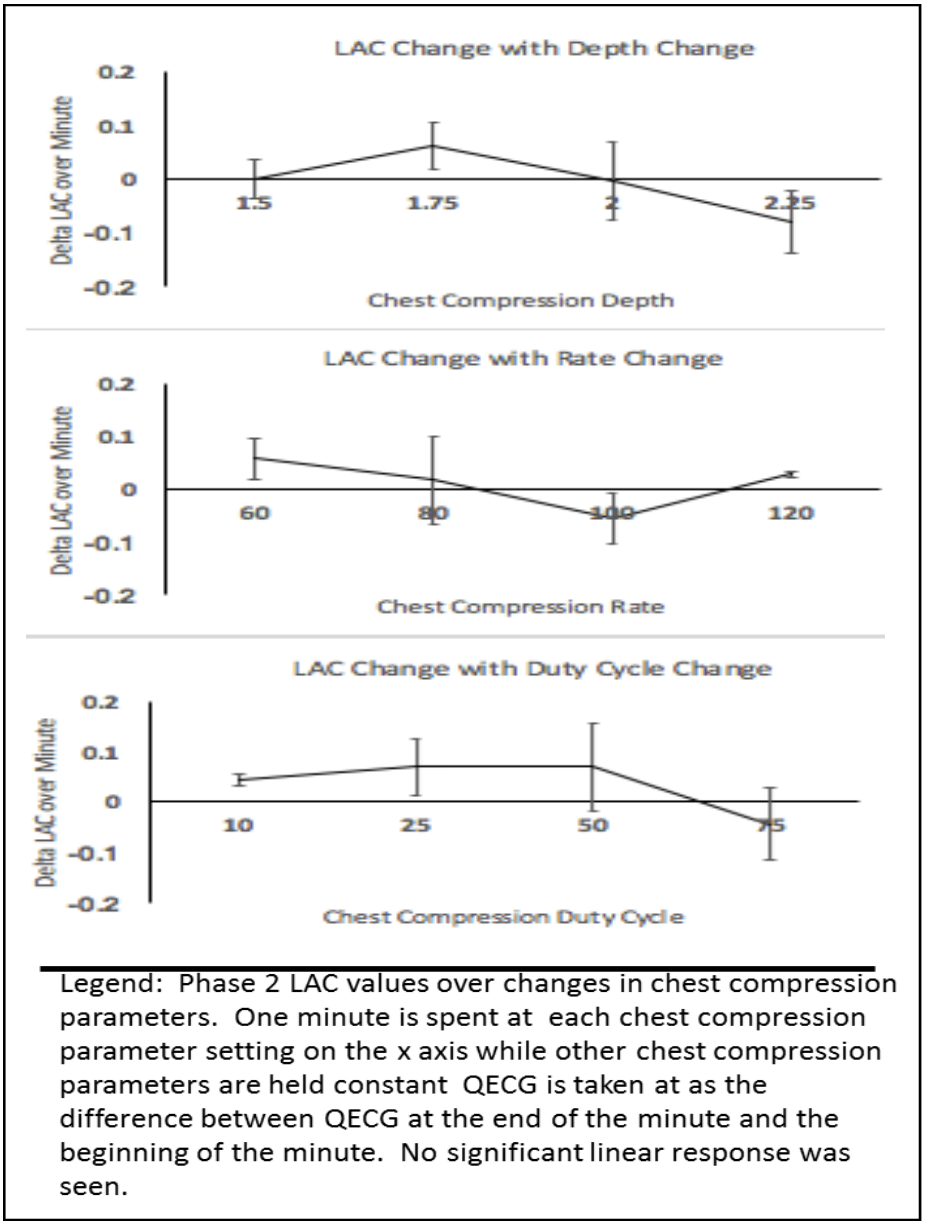


Legend: Phase 2 LAC values over changes in chest compression parameters. One minute is spent at each chest compression parameter setting on the x axis while other chest compression parameters are held constant QECG is taken at as the difference between QECG at the end of the minute and the beginning of the minute. No significant linear response was seen.

**Figure 54: Phase 2 LAC response to CC parameter changes (Analysis Approach B)**

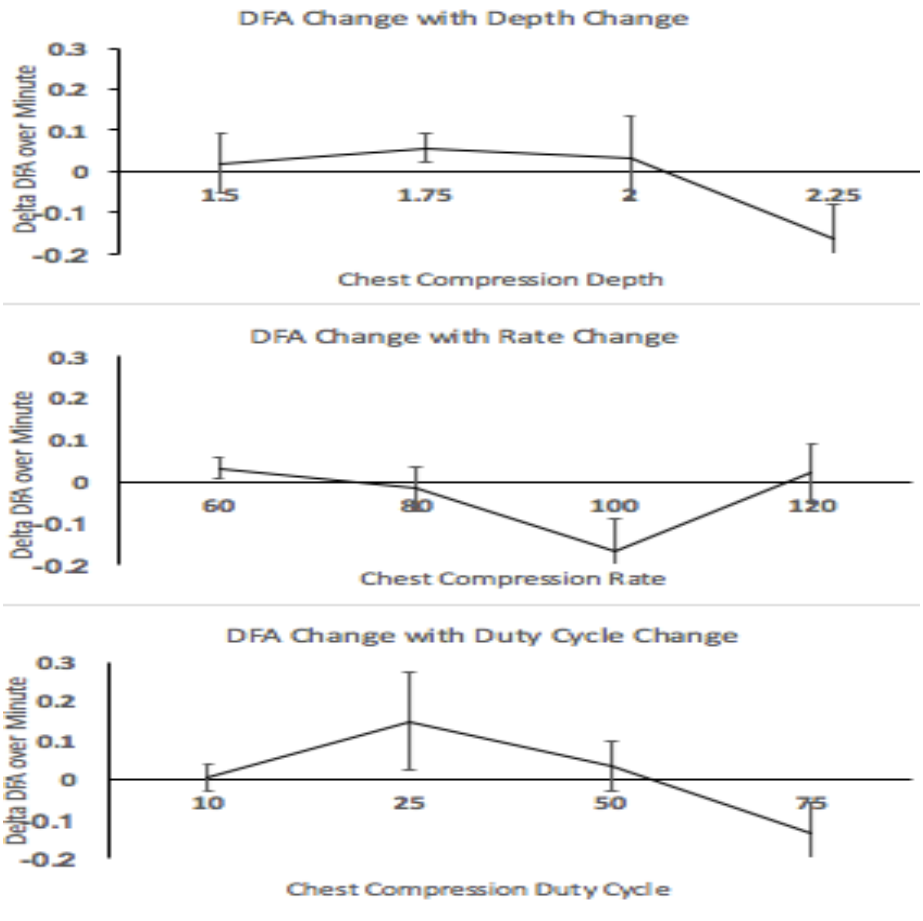


Legend: Phase 2 DFA values over changes in chest compression parameters. One minute is spent at each chest compression parameter setting on the x axis while other chest compression parameters are held constant QECG is taken at as the difference between QECG at the end of the minute and the beginning of the minute. No significant linear response was seen. No significant linear response was seen.

**Figure 55: Phase 2 DFA response to CC parameter changes (Analysis Approach B)**

## BIBLIOGRAPHY


1. Mozaffarian, D., et al., *Heart Disease and Stroke Statistics - 2015 Update.* Circulation, 2015: p. 206-214.
2. Kitamura, T., et al., *Epidemiology and outcome of adult out-of-hospital cardiac arrest of non-cardiac origin in Osaka: a population-based study.* BMJ Open, 2014. **4**.
3. Hess, E.P., R.L. Campbell, and R.D. White, *Epidemiology, trends, and outcome of out-of-hospital cardiac arrest of non-cardiac origin.* Resuscitation, 2007. **72**: p. 200-206.
4. Engdahl, J., et al., *Characteristics and outcome among patients suffering from out of hospital cardiac arrest of non-cardiac aetiology.* Resuscitation, 2003. **2002**(57).
5. Kuisma, M. and A. Alaspaa, *Out-of-hospital cardiac arrests of non-cardiac origin: Epidemiiology and outcome.* European Heart Journal, 1997. **18**(7): p. 1122-1128.
6. Low, L.S. and K.B. Kern, *Importance of Coronary Artery Disease in Sudden Cardiac Death.* J Am Heaert Assoc., 2014. **3**(5): p. 1-3.
7. Rajan, S., et al., *Incudence and survival outcome according to heart rhythm during resuscitation attempt in out-of-hospital cardiac arrest patients with presumed cardiac etiology.* Resuscitation, 2017. **114**: p. 157-163.
8. Weisfeldt, M.L. and L.B. Becker, *Resuscitation After Cardiac Arrest A 3-Phase Time-Sensitive Model.* JAMA, 2002. **288**(23): p. 3035-3038.
9. Chan, P.S., et al., *Delayed Time to Defibrillation after In-Hospital Cardiac Arrest.* NEJM, 2008. **358**(1): p. 9-17.
10. Salcido, D.D., et al., *Quantitative waveform measures of the electrocardiogram as continuous physiologic feedback during resuscitation with cardiopulmonary bypass.* Resuscitation, 2012. **83**(505-510).
11. Kouwenhoven, W.B. and J.R. Jude, *Closed-Chest Cardiac Massage.* JAMA, 1960. **173**(10): p. 1064-1067.
12. Oddo, M. and A.O. Rossetti, *Predicting neurological outcome after cardiac arrest.* Current Opinion in Critical Care, 2011. **17**(3): p. 254-259.
13. McNally, B., et al., *Out-Hospital cardiac arrest surveillance: Cardiac Arrest Registry to Enhance Survival (CARES), United States, October 1, 2005-December 31, 2010.* Morbidity and Mortality Weekly Report, 2011. **60**(8): p. 1-19.
14. Meaney, P.A. and V.M. Nadkarni, *Rhythms and outcomes of adult in-hospital cardiac arrest.* Critical Care Medicine, 2010. **38**(1): p. 101-108.

15. Jo Kramer-Johansen, D.P.E., Heidrun Losert, Klemens Kohler, Benjamin S. Abella, *Uniform reporting of measured quality of cardiopulmonary resuscitation (CPR).* Resuscitation, 2007. **74**: p. 406-417.

16. Olasveengen, T.M., L. Wik, and P.A. Steen, *Quality of cardiopulmonary resuscitation before and during transport in out-of-hospital cardiac arrest.* Resuscitation, 2008. **76**(2): p. 185-190.

17. Olasveengen, T.M., et al., *Is CPR quality improving? A retrospective study of out-of-hospital cardiac arrest.* Resuscitation, 2007. **75**(2): p. 260-266.

18. Stiell, I.G., et al., *What is the Optimal Chest Compression Depth During Out-of-Hospital Cardiac Arrest Resuscitation of Adult Patients?* Circulation, 2014. **130**(22): p. 1962-1970.

19. Idris, A., et al., *Chest Compression Rates and Survival Following Out-of-Hospital Cardiac Arrest.* Critical Care Medicine, 2015. **43**(4): p. 840-848.

20. Babbs, C.F., *New versus old theories of blood flow during CPR.* Critical Care Medicine, 1980. **8**(3): p. 191-194.

21. Rudikoff, M.T., et al., *Mechanisms of Blood Flow During Cardiopulmonary Resuscitation.* Circulation, 1980. **61**: p. 345-352.

22. Werner, J.A., et al., *Two-dimensional echocardiography during CPR in man: implications regarding the mechanism of blood flow.* Critical Care Medicine, 1981. **9**(5): p. 275-376.

23. Niemann, J.T., et al., *Documentation of systemic perfusion in man and in an experimental model: a "window" to the mechanism of blood flow in external CPR.* Critical Care Medicine, 1980. **8**(3).

24. Paradis, N.A., et al., *Simultaneous Aortic, Jugular Bulb, and Right Atrial Pressures During Cardiopulmonary Resuscitation in Humans; Insights into Mechanisms.* Circulation, 1989. **80**: p. 361-368.

25. Lampe, J.W., et al., *Developing a kinematic understanding of chest compressions: the impact of depth and release time on blood flow during cardiopulmonary resuscitation.* Biomed Eng Online, 2015. **14**(102).

26. Stiell, I.G., et al., *What is the Role of Chest Compression Depth during Out-of-Hospital Cardiac Arrest Resuscitation.* Critical Care Medicine, 2012. **40**(4): p. 1192-1198.

27. Vadeboncoeur, T., et al., *Chest compression depth and survival in out-of-hospital cardiac arrest.* Resuscitation, 2014. **85**(2): p. 182-188.

28. Edelson, D.P., et al., *Effects of compression depth and pre-shock pauses predict defibrillation failure during cardiac arrest.* Resuscitation, 2006. **71**: p. 137-145.

29. Monsieurs, K.G., et al., *Excessive chest compression rate is associated with insufficent compression depth in prehospital cardiac arrest.* Resuscitation, 2012. **83**: p. 1319-1323.

30. Field, R.A., et al., *The impact of chest compression rates on quality of chest compressions - A manikin study.* Resuscitation, 2012. **83**: p. 360-264.

31. Idris, A.H., et al., *The Relationship Between Chest Compression Rates and Outcomes from CArdiac ARrest.* Circulation, 2012. **125**(24): p. 3004-3012.

32. Abella, B.S., et al., *Chest Compression Rates During Cardiopulmonary Resuscitation are Suboptimal.* Circulation, 2004. **111**: p. 428-434.

33. Dean, J., et al., *Improved blood flow during prolonged cardiopulmonary resuscitation with 30% duty cycle in infant pigs.* Circulation, 1991. **84**: p. 896-904.

34. Johnson, B.V., et al., *Cardiopulmonary resuscitation duty cycle in out-of-hospital cardiac arrest.* Resuscitation, 2015. **87**: p. 86-90.

35. Aufderheide, T.P., et al., *Incomplete chest wall decompression: a clinical evaluation of CPR performance by EMS personnel and assessment of alternative manual chest compression-decompression techniques.* Resuscitation, 2005. **64**: p. 353-362.

36. Christenson, J., et al., *Chest compression fraction determines survival in patients with out-of-hospital ventricular fibrillation.* Circulation, 2009. **120**: p. 1241-1247.

37. Vaillancourt, C., et al., *The impact of increased chest compression fraction on return of spontaneous circulation for out-of-hospital cardiac arrest patients not in ventricular fibrillation.* Resuscitation, 2011. **82**(12): p. 1501-1507.

38. Paradis, N.A., et al., *Coronary Perfusion Pressure and the Return of Spontaneous Circulation in Human Cardiopulmonary Resuscitation.* JAMA, 1990. **263**: p. 1106-113.

39. Joshua C. Reynolds, D.S.A.C.K., Matthew L. Sundermann, Adam Frisch, Brian P. Suffoletto, James J. Menegazzi, *Tissue oximetry by near-infrared spectroscopy in a porcine model of out-of-hospital cardiac arrest and resuscitation.* Resuscitation, 2013. **84**: p. 843-847.

40. Max Harry Weil, J.B., Robert P. Trevino, Eric C. Rackow, *Cardiac output and end-tidal carbon dioxide.* Critical Care Medicine, 1985. **13**(11): p. 881-999.

41. Sheak, K.R., et al., *Quantitative relationship between end-tidal carbon dioxide and CPR quality during both in-hospital and out-of-hospital cardiac arrest.* Resuscitation, 2015. **89**: p. 149-154.

42. Brown, C.G. and R. Dzwonczyk, *Signal Analysis of the Human Electrocardiogram During Ventricular Fibrillation: Frequency and Amplitude Parameters as Predictors of Successful Countershock.* Annals of Emergency Medicine, 1996. **27**(2): p. 184-188.

43. Nadkarni, V., et al., *First documented rhythm and clinical outcome from in-hospital cardiac arrest among children and adults.* JAMA, 2006. **295**: p. 50-57.

44. Callaway, C.W. and J.J. Menegazzi, *Waveform analysis of ventricular fibrillation to predict defibrillation.* Current Opinion in Critical Care, 2005. **11**: p. 192-199.

45. Salcido, D.D., et al., *Association of intramyocardial high energy phosphate concentrations with quantitative measures of the ventricular fibrillation electrocardiogram waveform.* Resuscitation, 2009. **80**: p. 946-950.

46. Niemann, J.T., et al., *Is all ventricular fibrillation the same? A comparison of ischemically induced with electrically induced ventricular fibrillation in a porcine cardiac arrest and resuscitation model.* Critical Care Medicine, 2007. **35**(5): p. 1356-1361.

47. RE, I., R. J, and H. J, *Types of ventricular fibrillation: 1,2,4,5, or 3000,000?* Jornal of Cardiovascular Electrophysiology, 2004. **15**(12): p. 1441-1443.

48. ML, R., K. ML, and G. RF, *Electrical Restitution and Spatiotemporal Organization During Ventricular Fibrillation.* Circulation, 1999. **84**: p. 955-963.

49. FX, W., et al., *Spatiotemporal evolution of ventricular fibrillation.* Nature, 1998. **392**: p. 78-82.

50. Indik, J.H., et al., *Predictors of resuscitation in a swine model of ischemic and nonischemic ventricular fibrillation cardiac arrest: Superiority of amplitude spectral area and slope to predict a return of spontaneous circulation when resuscitation efforts are prolonged.* Critical Care Medicine, 2010. **38**(12): p. 2352-2357.

51. Shanmugasundaram, M., et al., *Analysis of amplitude spectral area and slope to predict defibrillation in out of hospital cardiac arrest due to ventricular fibrillation (VF) according to VF type: Recurrent versus shock-resistant.* Resuscitation, 2012. **83**: p. 1242-1247.

52. He, M., et al., *Combining multiple ECG features does not improve prediction of defibrillation outcome compared to single features in a large population of out-of-hospital cardiac arrests.* Critical Care, 2015. **19**(425).

53. Nakagawa, Y., et al., *Novel CPR system that predicts return of spontaneous circulation from amplitude spectral area before electric shock in ventricular fibrillation.* Resuscitation, 2017. **113**: p. 8-12.

54. Ristagno, G., et al., *Amplitude Spectrum Area to Guide Defibrillation: A Validation on 1617 Ventricular Fibrillation Patients.* Circulation, 2014. **135**(16): p. AHA.114.010989.

55. Ristagno, G., et al., *Amplitude spectrum area to guide resuscitation — A retrospective analysis during out-of-hospital cardiopulmonary resuscitation in 609 patients with ventricular fibrillation cardiac arrest.* Resuscitation, 2013. **84**(12): p. 2013.

56. Eftestol, T., et al., *Predicting Outcome of Defibrillation by Spectral Characterization and Nonparametric Classification of Ventricular Fibrillation in Patients With Out-of-Hospital Cardiac Arrest.* Circulation, 2000. **102**: p. 1523-1529.

57. Sherman, L.D., et al., *Logarithm of the Absolute Correlations of the ECG Waveform Estimates Duration of Ventricular Fibrillation and Predicts Successful Defibrillation.* Resuscitation, 2008. **78**(3): p. 346-354.

58. Lin, L.-Y., et al., *Detrended fluctuation analysis predicts successful defibrillation for out-of-hospital ventricular fibrillation cardiac arrest.* Resuscitation, 2010. **81**: p. 297-301.

59. Neurater, A., et al., *Prediction of countershock success using single features from multiple ventricular fibrillation frequency bands and feature combinations using neural networks.* Resuscitation, 2007. **73**: p. 253-263.

60. Firoozabadi, R., et al., *Predicting defibrillation success in sudden cardiac arrest patients.* Journal of Electrocardiology, 2013. **46**: p. 473-479.

61. Clifton W. Callaway, L.D.S., Vincent N. Mosesso Jr, Thomas J. Dietrich, Eric Holt, M. Christopher Clarkson, *Scaling Exponent Predicts Defibrillation Success for Out-of-Hospital Ventricular Fibrillation Cardiac Arrest.* Circulation, 2001. **103**: p. 1656-1661.

62. Amann, A., et al., *Reduction of CPR artifacts in the ventricular fibrillation ECG by coherent line removal.* BioMedical Engineering OnLine, 2010. **9**(2): p. 1-15.

63. Werther, T., et al., *CPR Artifact Removal in Ventricular Fibrillation ECG Signals Using Gabor Multipliers.* IEEE Transactions on Biomdical Engineering, 2009. **56**(2): p. 320-327.

64. Berger, R.D., J. Palazzolo, and H. Halperin, *Rhythm discrimination during uninterrupted CPR using motion artifact reduction system.* Resuscitation, 2007. **75**: p. 145-152.

65. Morgan, R.W., et al., *A hemodynamic-directed approach to pediatric cardiopulmonary resuscitation (HD-CPR) improves survival.* Resuscitation, 2017. **111**: p. 41-47.

66. Sutton, R.M., et al., *Patient-centric blood pressure-targeted cardiopulmonary resuscitation improves survival from cardiac arrest.* Am J Respir Crit Care Med, 2014. **190**(11): p. 1255-1262.

67. Sutton, R.M., et al., *Hemodynamic Directed CPR Improves Short-term Survival from Asphyxia-Associated Cardiac Arrest.* Resuscitation, 2013. **84**(5): p. 696-701.

68. Friess, S.H., et al., *Hemodynamic directed CPR improves cerebral perfusion pressure and brain tissue oxygenation.* Resuscitation, 2014. **85**: p. 1298-1303.

69. Vognsen, M., et al., *Contemporary animal models of cardiac arrest: A systematic review.* Resuscitation, 2017. **113**: p. 115-123.

70. Sutton, R.M., et al., *Physiologic monitoring of CPR quality during adult cardiac arrest: A propensity-matched cohort study.* Resuscitation, 2016. **106**(76-82).

71. Sundermann, M.L., et al., *Feasibility of Biosignal-guided Chest Compression During Cardiopulmonary Resuscitation: A Prof of Concept.* Academic Emergency Medicine, 2015. **23**(1): p. 93-97.

72. Chang, M.W., et al., *Active Compression-Decompresison CPR Improves Vital Organ Perfusion in a Dog Model of Ventricular Fibrillation.* Chest, 1994. **106**(4): p. 1250-1259.

73. Steen, S., et al., *Evaluation of LUCAS, a new device for automatic mechanical compresison and active decompression resuscitation.* Resuscitation, 2002. **55**: p. 285-299.

74. Babbs, C.F., et al., *Cardiac, thoracic, and abdominal pump mechanisms in cardiopulmonary resuscitation: Studies in an electrical model of the circulation.* The American Journal of Emergency Medicine, 1984. **2**(4): p. 299-308.

75. Babbs, C.F., *CPR Techniques That Combine Chest and Abdominal Compression and Decompression; Hemodynamic Insights From a Spreadsheet Model.* Circulation, 1999. **100**: p. 2146-2152.

76. Charles F. Babbs, A.E.K., Weilun Quan, Gary Freeman, *A new paradigm for human resuscitation research using intelligent devices.* Resuscitation, 2008. **77**: p. 306-315.

77. Delong, E., D. Delong, and D. Clarke-Pearson, *Comparing the areas under two or more correlated receiver operating characteristic curves: a nonparametric approach.* Biometrics. **44**(3): p. 837-845.